ROBUST MULTIVARIABLE CONTROLLER DESIGN FOR AN ACTIVATED SLUDGE PROCESS

Ph.D Thesis

Submitted in partial fulfillment of the requirements for the degree of

DOCTOR OF PHILOSOPHY

by

SANJITH S. ANCHAN

Under the guidance of

Dr. CHINTA SANKAR RAO

DEPARTMENT OF CHEMICAL ENGINEERING

NATIONAL INSTITUTE OF TECHNOLOGY KARNATAKA

SURATHKAL, MANGALORE - 575025

July, 2023

Dedicated to my Parents, Family and Friends

DECLARATION

(By the Ph.D. Research Scholar)

I hereby declare that the Research Thesis entitled "**Robust Multivariable Controller Design for an Activated Sludge Process"** is being submitted to the National Institute of Technology Karnataka, Surathkal in partial fulfilment of the requirements for the award of the Degree of **Doctor of Philosophy** in Chemical Engineering is a *bonafide report of the research work carried out by me*. The material contained in this Research Thesis has not been submitted to any University or Institution for the award of any degree.

Place: NITK, Surathkal.
Date: 14th July 2023

Sanjith S. Anchan
Reg. No.: 187CH005
Department of Chemical Engineering

CERTIFICATE

This is to *certify* that the Research Thesis entitled **Robust Multivariable Controller Design for an Activated Sludge Process** submitted by **Sanjith S. Anchan**, (Reg. No.: 187CH005) as the record of the research work carried out by him, is *accepted as the Research Thesis submission* in partial fulfillment of the requirements for the award of the degree of **Doctor of Philosophy**.

CSRG 14/7/23

(Dr. Chinta Sankar Rao)

Research Supervisor

Assistant Professor

Department of Chemical Engineering, NITK

Chairman - DRPC

Dr. P. E. Jagadeeshbabu

Head of the Department

Chemical Engineering, NITK

Head of the Department
विभागाध्यक्ष
Department of Chemical Engineering
रासायनिक अभियांत्रिकी विभाग
National Institute of Technology Karnataka - Surathkal
राष्ट्रीय प्रौद्योगिकी संस्थान कर्नाटक, सुरत्कल
PO Srinivasnagar, Mangalore - 575025 Karnataka

Date: 14th July, 2023

ACKNOWLEDGMENT

I would like to take this opportunity to thank all those people who have made this thesis possible.

I owe my deep gratitude to my advisor Dr. Chinta Sankar Rao, for the continuous support of my Ph.D study and related research, and for his patience, motivation, and immense knowledge. His overwhelming attitude toward helping students, his dedication, and his keen interest in research had been mainly responsible for completing my research work. His meticulous scrutiny, scholarly advice, and scientific approach have propelled me to accomplish my task to a great extent.

I am highly obliged to the Director, NITK, Surathkal, and Head of the Department, Chemical Engineering, NITK Surathkal for providing all the facilities, help, and encouragement for carrying out the research work.

I am extremely grateful to Dr. Hari Prasad Dasari Sir and Dr. Beneesh P. B. Sir, for their invaluable guidance and suggestions throughout my research.

It is a great pleasure for me to acknowledge the valuable suggestions, help, and ideas of all my Ph.D batchmates (Atmuri Shourya, Sedevino Sofia, and Sahana Vijay Kumar).

I thank Bangalore Water Supply and Sewerage Board officials and Chief Engineers for permitting me to visit the Bangalore Hebbal plant and for sharing the online WWTP data.

I would like to sincerely thank Mr. Dinesh Poojary (plumber), Ph.D. groupmate Mr. Ramesh Potnuri, and my M.Tech group mates (Mr. Gaurav Yadav, Uday Kiran, and Prabhu Teja) for their assistance during my study especially in setting up the pilot-scale ASP plant.

I express my heartfelt gratitude to Mrs. Bhavya Suvarna, Mrs. Sandhya, Mrs. Vijetha, Mrs. Thrithila Shetty, Mr. Mahadeva, Mr. Suresh, Mr. Harish, Mr. Ramesh, Mr. Sukesh, Mr. Jyaneshwar for all the assistance and support.

I take this opportunity to thank my friends and colleagues Mr. Sathish Kolluru, Dr. Kishore Kumar, Dr. Pragadeesh K., Dr. Lister Herington, Mr. Sai Teja, Mrs. Sunaina Patil, Mr. Arpan Gupta, Mr. Arun Kumar, Mr. Banu Prakash, Mr. Rakesh Reddy, and Mr. Mahindra Kotturi for providing a fun-filled work environment during my tenure in NITK.

I am deeply thankful to all non-teaching staff of the Academic section, Finance section, Library section, and Establishment section of NITK, security personnel, and mess staff for all the timely help they have rendered.

Last, but not least, I would like to thank my family: my Parents Mr. Sridhar K., Mrs. Jayanthi J. S., and Mrs. Padmavathi S. for their unconditional love, constant support, and motivation throughout this project and my life. You have let go of your dreams and sacrificed a ton so that I can achieve mine. I cannot say enough thanks to you in this lifetime for your contribution to my life.

Above all, I am indebted and grateful to the Almighty for giving me the opportunity, strength, and knowledge to successfully complete this endeavor.

Place: NITK, Surathkal **Sanjith S. Anchan**

Date: 14^{th} July, 2023

Sanskrit Shloka

अज्ञानतिमिरान्धस्य ज्ञानाञ्जनशालाकया ।
चक्षुरुन्मीलितं येन तस्मै श्रीगुरवे नमः॥

Transliteration

ajñānatimirāndhasya jñānāñjanaśālākayā ।
cakṣurunmīlitaṁ yena tasmai śrīgurave namaḥ ॥

Transcription

ajnanatimirandhasya jnananjanashalakaya |
chakshurunmilitam yena tasmai shrigurave namah||

Hindi meaning

ज्ञान के प्रकाश को दीप्तिमान करके हमारे भीतर की अंधी आंखों से अज्ञान के अंधेरे को दूर करने वाले गुरु को नमस्कार,
उन गुरु को नमस्कार, जिनके द्वारा हमारे भीतर ज्ञान की आंखें खुलती हैं।

English meaning

Salutations to the Guru Who Removes the Darkness of Ignorance from our Blind Eyes by applying the Collyrium of the Light of Knowledge.
Obeisance to that sri-guru by whom the eyes have been opened.

ABSTRACT

The importance of freshwater supply and safely treated wastewater return cannot be overemphasized. The human race is still a long way from the most efficient, economical, and reliable ways to ensure our cities with a properly equipped treatment system. It demands the treatment of polluted/used water without discharging it to receiving water bodies. Principally, a sudden drop of dissolved oxygen concentration is observed in receiving water bodies when the organic pollutants are discharged along with the untreated wastewater. This reduces the self-purification character of the water body, which involves the breakdown of complex organic molecules similar to biological treatment systems. The organic effluent generally contains a large quantity of suspended and settleable solids that will obstruct sunlight to reach the bottom surface of water bodies which then gives rise to water pollution causing eutrophication. Particularly, this can be solved by optimizing the aeration rate for better treatment, which intern reduces energy consumption and any additional chemical dosage in biological Wastewater Treatment plants (WWTP). One tool that has been successfully implemented to achieve such goals is the WWTP process model. Model development is necessary for simulating a system's behavior, and optimizing or controlling its performance. The main motive behind controlling any WWTP is, primarily to abide by the effluent discharge standards and secondarily to maintain the operational costs as low as possible. The robust controller designs are plant-specific, but the principle and goal remain the same.

Hence in this research, a mathematical model is identified using two approaches namely the system identification technique and the Process Reaction curve method for an Activated Sludge Process (ASP). By keeping this as a benchmark, the controllers are designed that aimed to control effluent dissolved oxygen or biomass concentration and substrate concentration by manipulating the aeration rate and recycle sludge flowrate. Two types of controllers are designed to govern the ASP system: Centralized and Decentralized controllers. Each type has its respective pros and cons which are discussed in the upcoming chapters. To overcome the challenge of the grey box model for the ASP system, a data-driven approach was selected to fit a model class for the ASP

unit. This technique will reduce the effort, complex tasks, and time for the process and control engineer to develop a mathematical model of the plant. Subsequently, it is then utilized to design a centralized control system for an ASP unit.

Contents

List of Figures

List of Tables

List of Acronyms /Abbreviations

ADP	Adaptive Dynamic Programming
ANN	Artificial Neural Network
ART	Average Residence Time
ASM	Activated Sludge Model
ASP	Activated Sludge Process
CbT	Correlation based Tuning
COD	Chemical Oxygen Demand
DNN	Deep Neural Network
DO	Dissolved Oxygen
DRGA	Dynamic Relative Gain Array
EOTF	Effective Open-loop Transfer Function
ETF	Effective Transfer Function
FOPTD	First Order Plus Time Delay
FPM	First Principle Modeling
GP	Gaussian Process
HSC	Half-saturation Coefficient
IAE	Integral Absolute Error
IFT	Iterative Feedback Tuning
ISE	Integral Square Error
ITAE	Integral Time weighted Absolute Error
ITSE	Integral Time weighted Square Error
LAM	Linear regression-based Model
MIMO	Multi Input Multi Output
MINPL	Mixed-Integer Non-Linear Programming
MISO	Multi Input Single Output
MLSS	Mixed Liquor Suspended Solid

List of Acronyms /Abbreviations

MPC	Model Predictive Control
MVC	Minimum Variance Control
N	Nitrogen
NGA	Normalized Gain Array
NMPC	Nonlinear Model Predictive Control
NRM	Nonlinear Regression-based Model
P	Phosphorous
PEM	Predictive Error Method
PI	Proportional Integral
PID	Proportional Integral Derivative
RART	Relative Average Residence Time
RARTA	Relative Average Residence Time Array
RGA	Relative Gain Array
RHOC	Receding Horizon Optimal Control
RNGA	Relative Normalized Gain Array
RTO	Real Rime Optimization
SCADA	Supervisory Control and Data Acquisition
SISO	Single Input Single Output
SRT	Solids Retention Time
TIE	Time Integral Error
TITO	Two Input Two Output
TV	Total Variance
VRFT	Virtual Reference Feedback Tuning
WWTP	Waste Water Treatment Plant

List of Symbols and Notations

W	Aeration rate
K_s	Affinity constant
K_{NH}	Ammonia Hsc. for autotrophs
k_a	Ammonification rate
b_A	Autotrophic decay rate
$\hat{\mu}_A$	Autotrophic max. specific growth rate
Y_A	Autotrophic yield
X	Biomass concentration
K_c	Controller gain
S_s	Concentration of readily biodegradable COD in ASM1 model
η_h	Correction factor for anoxic hydrolysis
η_g	Correction factor for anoxic growth of heterotrophs
τ_D	Derivative time constant
g_{c1} g_{c2}	Decentralized controllers
K_d	Derivative gain
D	Dilution rate
C	Dissolved oxygen concentration
S_o	Dissolved oxygen concentration in ASM1 model
$\hat{\theta}_{ij}$	Effective dead time
g^*_{11}, g^*_{22}	Effective open-loop transfer function
$\hat{k}_{p_{ij}}$	Effective process gain
$\hat{\tau}_{ij}$	Effective process time constant
e	Error between measured output and set point
f_P	Fraction of biomass yielding particulate products

List of Symbols and Notations

$\odot$	Hadamard division
$\otimes$	Hadamard product
K_s	Half-saturation coefficient for heterotrophs.
$\hat{\mu}_H$	Heterotrophic max. specific growth rate
b_H	Heterotrophic decay rate
Y_H	Heterotrophic yield
K_x	Hsc. for hydrolysis of slowly biodegradable substrate
X_I	Inert suspended organic matter concentration in ASM1 model
C_{in}	Influent dissolved oxygen concentration
S_{in}	Influent substrate concentration
u_1 & u_2	Input variables
$U(s)$	Input vector
K_i	Integral gain
τ_i	Integral time constant
μ_{max}	Maximum specific growth rate
i_{XB}	Mass N/mass COD in biomass
i_{XP}	Mass N/mass COD in products from biomass
C_s	Maximum dissolved oxygen concentration
k_h	Max. Specific hydrolysis rate
K_{NO}	Nitrate Hsc. for denitrifying heterotrophs
$K_{O,H}$	Oxygen Hsc. for heterotrophs
$K_{O,A}$	Oxygen Hsc. for autotrophs
y_1 & y_2	Output variables
K_{La}	Oxygen mass transfer coefficient
$g_{11}, g_{12}, g_{21}, g_{22}$	Process transfer functions
r	Ratio of recycle flow to the influent

List of Symbols and Notations

β	Ratio of waste flow to the influent
X_r	Recycled biomass concentration
r	Recycle sludge flow-rate
$Y(s)$	Output vector
S_{NH}	Soluble ammonia nitrogen concentration in ASM1 model
X_S	Slowly biodegradable organic nitrogen concentration in ASM1 model
X_{ND}	Slowly biodegradable organic matter concentration in ASM1 model
S_{ND}	Soluble biodegradable organic nitrogen concentration in ASM1 model
S_{NI}	Soluble Inert organic nitrogen concentration in ASM1 model
S_{NO}	Soluble nitrate-nitrogen concentration in ASM1 model
y_{r1} y_{r2}	Set points of control variables y_1 and y_2
μ	Specific growth rate
S	Substrate concentration
$G(s)$	Transfer function matrix
Y	Yield cell mass

Chapter 1

INTRODUCTION

Climate change, imbalances in water supply and consumption, and a flourishing population will cause an unfavorable and dramatic change in the water cycle. There is a necessity to supply clean and potable water for society to support adverse human activities. It is clearly evident that in the 21st century, the world will face severe water scarcity resources (Day, 1996). As reported in various wastewater reuse studies, more than 80% of the water that is used is disposed of untreated, polluting rivers, lakes, and oceans. Wastewater is water that has picked up various contaminants during its utilization in domestic, commercial, and industrial applications. One of the major causes of pollution of these water resources is the direct disposal of solid waste generated from human anthropogenic activities. While other sources can be industrial effluent, pesticides, and fertilizers. The primary source for nutrient pollution in groundwater bodies is effluent from WWTPs (Jiang et al., 2019). Commonly present organic contents in this wastewater will reduce the Dissolved Oxygen (DO) level in receiving water bodies (Degs et al., 2000). In addition, some micro-pollutants in municipal wastewater can pose a serious threat to the receiving water source (Parrott and Blunt, 2005). As the scientific approach has diversified significantly, the comprehensive study of the characteristics of wastewater to analyze its health and environmental consequences has become more frequent.

The used water from municipalities and communities is collected and transported to a WWTP, where it is treated before being disposed of at the water source, on land, or reused. Generally, a WWTP consists of preliminary, primary, secondary, and tertiary treatment stages, where wastewater is treated based on the required effluent standards Figure. 1.1. Several conventional wastewater treatment techniques like chemical coagulation, adsorption, and biological treatment can be adopted to reduce the impact on the receiving environment. Nevertheless, these techniques encounter several limitations, especially uneconomical operation costs. Hence, it is necessary to develop an optimal and effective technique for treating wastewater for safe disposal or reuse.

1.1 Biological Wastewater Treatment

Most of the treatment plants across the world adopt biological treatment techniques for treating wastewater. The principal objective of any biological treatment plant is to: achieve an acceptable end product by transforming dissolved and particulate biodegradable constituents; develop floc or bio-film to capture suspended and non-settleable colloidal solids, eliminate or transmute nutrients, such as nitrogen and phosphorous (Steilos and Patrick, 2002). The key processes involve transforming dissolved and suspended contaminants into stable biomass with the release of some gases like CO_2, CH_4, N_2, and SO_2. This transformation is nothing but biological degradation that can be enhanced by providing ozonation (Abbassi et al., 2000). Typically, the biological wastewater treatment plant involves a complex ecosystem for microbial ecology studies (Holger et al., 2006).

Even industrial wastewater can be biologically treated, provided it undergoes the necessary pre-treatment since it contains toxic constituents for microorganisms. It is always desirable to have a combined industrial and domestic wastewater treatment system to fulfil economically feasible alternatives (Del Borghi et al., 2003). To remove nutrients from wastewater streams, a combination of different conditions and diverse microbial populations is always essential (Coma et al., 2012). The removal of nutrients becomes vital if the treated water has to be used for gardening or irrational applications. This is mainly because these nutrients, specifically nitrogen and phosphorous, are capable of stimulating the growth of aquatic plants. If the treated water has to be discharged to sensitive water bodies, then the nitrogen removal system has to be incorporated into the WWTP to prevent it from causing eutrophication (Shimura and Tabuchi, 1994; Rim et al., 1997; Largus et al., 2004). Generally, biological processes adopted for treating wastewater can be categorized into two main streams: suspended growth and attached growth processes. In short, if the microorganism responsible for substrate degradation is kept in liquid suspension, it is known as a suspended growth process; otherwise, in the attached growth process, the microorganisms are attached to inert packing material, also known as a biofilm.

1.1.1 Suspended Growth Process

In the suspended growth process, the microorganism responsible for wastewater treatment is kept in liquid suspension by undertaking appropriate mixing methods. During this process, microorganisms convert the organic or other substances into a stable end product (gases or cell tissues). Basically, it is a natural process where organisms break down the substrate from wastewater and improve the water quality. The most predominantly adopted suspended growth process adopts an aerobic approach. Conventionally, this process operates at positive dissolved oxygen concentrations. However, based on substantial research, some of the advancements and modifications involved keeping anaerobic (no oxygen present) stages for domestic and industrial treatment units. Although the process demands extensive area for plant set-up, due to the treatment efficiency and economical perspectives, the suspended growth process is widely accepted over other advanced techniques.

The Activated Sludge Process (ASP) is the most widely used unit because of its simplicity and smooth operation. But, its processes are very complex due to their biochemical nature and the uncertainty of the incoming waste flow and composition. Although a basic mechanistic model describing the activated sludge kinetics (Henze et al., 1987) has become available, there are still many difficulties in modelling a particular plant accurately. Perhaps, this process was investigated by Dr. Angus Smith in the early 1880s, it was first developed by Clark and Gage at the Lawrence Experiment Station in Massachusetts in 1913 (Metcalf and Eddy, 2003). ASP unit consists of a reactor with aeration and a settling unit, along with regular physical units for removing floating, suspended inert materials (Figure. 1.1). Either mechanical or diffused aerators are used to transfer oxygen into the influent stream, with an estimated contact time for microbial suspension, generally referred to as mixed liquor-suspended solids (MLSS). The portion of settled biomass is recycled back to the aerated reactor, and the rest is removed periodically as there is excess biomass generation. The formation of floc particles that can be removed using gravity settling is the key feature of ASP. A complete mix stabilization, high rate method, oxidation ditch, contact stabilization, and conventional aeration are a few advanced scientific approaches in ASP (Ashish et al., 2016).

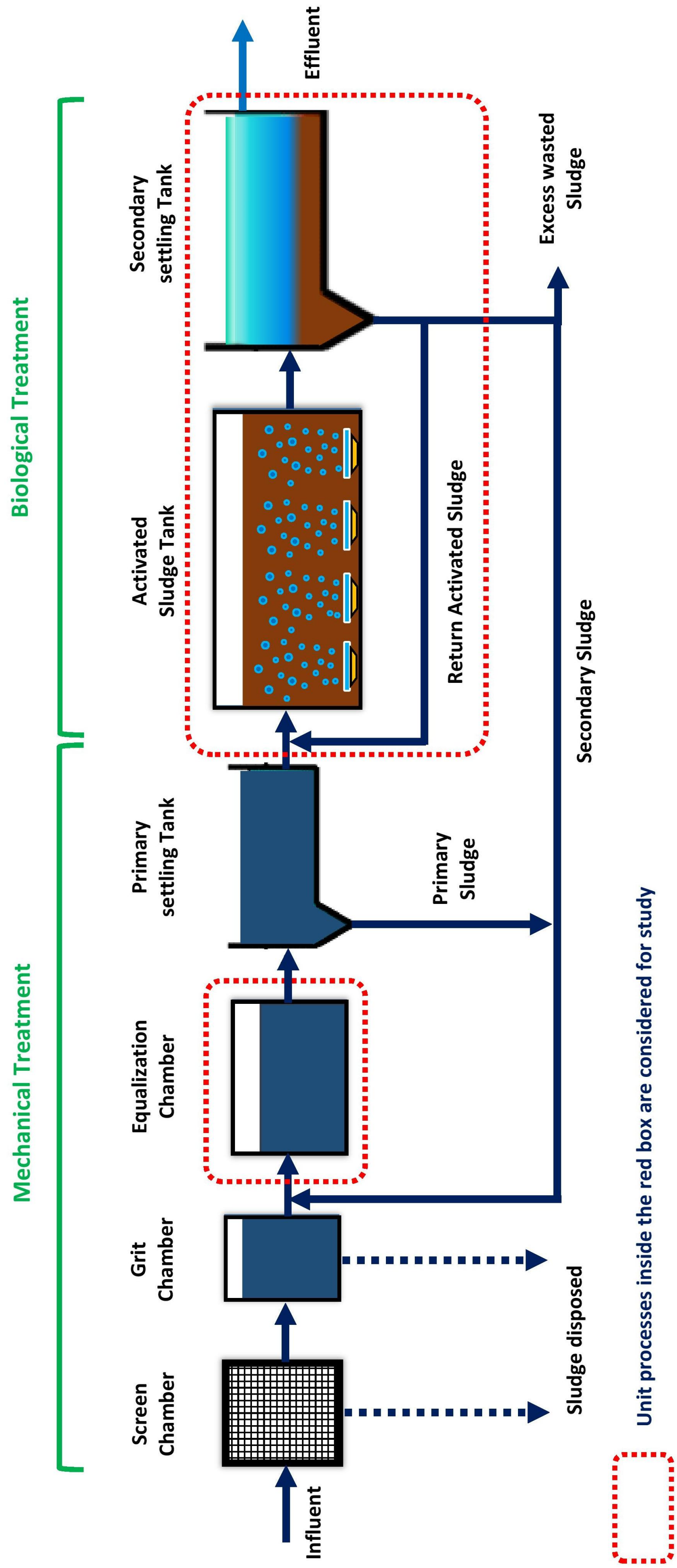

Figure 1.1 Scheme of conventional Activated Sludge Process in Wastewater Treatment Plant

1.2 Multivariable Process

Any process that has more than one input and/or more than one output variable is referred to as a Multivariable process. Most of the operations in process industries are Multi Input Multi Output (MIMO) systems with input and output parameters having a high level of interactions. Whereas, the Single Input Single Output (SISO) system has one variable to yield one output. To reduce the complexity in implementation and easy understandability, a multi-loop SISO system is considered for controlling interactions in the MIMO system.

The three major terms associated with process systems are Manipulated variables, disturbance, and control variables. For each controlled variable, there is an associated manipulated variable. The control system must adjust the manipulated variables so that the desired value or set point of the controlled variable is maintained despite any disturbances Figure. 1.2.

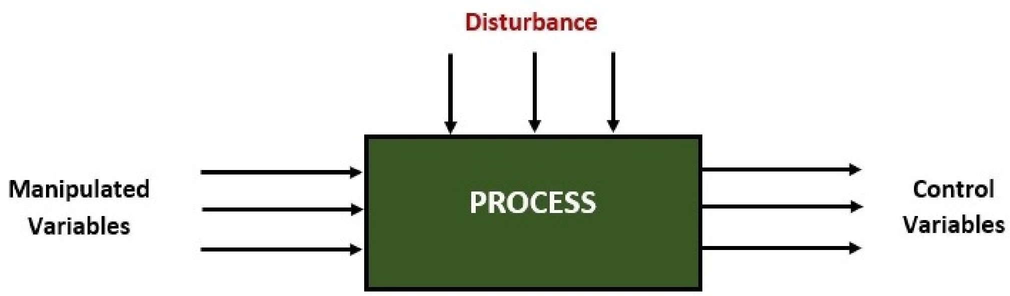

Figure 1.2 Generic process description

If there exists an equal number of inputs to an equal number of outputs, then the system is referred to as a square system, whereas different numbers of inputs and outputs are referred to as a non-square system. A set point is provided for each variable that has to be controlled. To govern these variables respective manipulated variables are chosen according to the required output. Due to the high level of interaction, the analysis of the MIMO system is an extremely complex and time-consuming process (Raviteja et al., 2016). This means a change in one set point will cause a change in each of the process variables, not only the output variable corresponding to that set point. Due to the existence of such cross-coupling among process variables, it imposes a challenging task to design a controller for a MIMO system.

1.3 Control system

A control system is a system that can provide a desired response by manipulating one or more parameters. In 1767, the first control device was invented by James Watt's Flyball governor, which controlled the speed of the engine. Later it witnessed several advancements in various fields of engineering. In recent years, the control system has contributed to the advancement of modern technologies and civilization. These days, plant alone does not fit the requirement of any industrial constraints. For precise and fast working of any plant, the controller is a must in industries. According to the specific requirement of the industries, the controllers are introduced to meet the desired specification.

A clear mathematical relationship between the input and output is the key feature of any effective control system. Based on the number of inputs and outputs, the control system is broadly classified into the SISO control system and MIMO control system. The SISO system can be easily controlled and handled conveniently. Whereas, it requires a more complex analysis to control the MIMO systems than that of the SISO system. Controlling a multivariable system is a difficult and challenging task when compared to the SISO system (Luan et al., 2015; Truong and Moonyong, 2010). A very common problem associated with multivariable control systems is the interaction among the control loops. An acceptable understanding of these interactions is very vital since it causes the manipulated variable to affect more than the control variable. However, this challenge can be rectified by selecting the most important loop and tuning it so as to give a good performance. Meanwhile detuning the other loops till the interaction with an important loop is acceptable (V. Vijay et al., 2012).

Indeed, the objective of multivariable control includes, maintaining several controlled variables at independent set points. It mainly depends on the goals of the entire plant and the design of associated equipment. Adopting a multivariable control system to the real-world system it ensures more richness and alternatives in controlling the process. Multi-loop controllers are commonly used due to their simplicity, and robustness. The fundamental basis of multivariable process control has an enormous database of literature on dynamic systems modeling, process identification, linear and multivariable feedback control, and dynamic process optimization (W. Harmon, 1983). The integrated control system has to be considered in a multivariable system study since it is not possible to analyze each manipulated-controlled variable connection individually for determining its performance.

There are various types of controllers reviewed in the literature that can be used to control multivariable systems. The controllers that are widely used are centralized controllers, decentralized controllers, and decouplers. The decentralized control system is largely favored over the centralized controller because there are only n controllers for n output variables in the control system. In the case of a centralized controller for n output variables there prevails n^2 number of controllers. If there exist two inputs variables namely u_1 and u_2 and, two outputs variables namely y_1 and y_2, then the change in input variable u_1 directly influences output y_1, meanwhile it also indirectly has an impact on output y_2, similarly change in input u_2 directly has an impact on y_2, but also has an indirect influence on output y_1. This condition prevails due to the interaction between the process variables. If the interaction between the loops is moderate or less, the decentralized control system works well however, they fail if there are more interactions between the loops. Since the decentralized system involves interaction it can be estimated by the RGA index and Niederlinski method by paring the manipulated and control variables for a stable system. By virtue of its simplicity and the potential to achieve failure tolerance, the decentralized controller has been adopted by most of the process industries (Su et al., 2006).

Wastewater Treatment in urban areas is one of the major importance nowadays and most civic authorities are forced to consider the issue seriously with urgency. Huge investment in money and time is allotted for new plant construction or improving/modifying the existing WWTP to meet the ever-increasing demand of urban sprawl. During the 1920-1960s plant operators carried out manual adjustments and observations where statistical tools like histograms and charts were utilized to control the WWTP. Expensive equipment, few control theories, and lack of expertise forced operators to use manual control operations (Olsson, 2012). Even though computers were used to deduce the first principle model in the late 1980s, because of its lack of reliability it struggles till 2000 were most of the WWTP adopted its own version of a digital control system. The most common control operation followed in WWTP is to maintain the set point using online sensor reading and feedback loop response. Based on the online measurements required operations like blower speed, pumping quantity, and dosage level can be monitored through SCADA system. For instance, this study uses an ASP system and majorly focuses on controlling Dissolved Oxygen (DO) concentration (70% of plant maintenance expenses and purification) and substrate concentration (meet effluent discharge standard) by manipulating aeration rate and recycle sludge flow rate. Because of its complexity and interactions between principle variables, it put forwards a challenging task for modeling and controller design. The primary objective of controlling any WWTP is to achieve reliable, efficient, and stable outcomes with the bare minimum cost. The major challenges that a control engineer faces while controlling a WWTP are (Katebi et al., 1998).

- To abide by strict effluent discharge standards
- Expensive and unavailability of the online parameter (BOD, COD, Biomass, Substrate, TKN, etc.) measuring instruments
- Highly nonlinear system
- Need of expertise on biological and biochemical processes
- Stochastic nature of state variables

Different methods approached from the literature include conventional PI/PID type controller, advanced strategies like optimal, adaptive, linearizing, robust, etc. (Luca et al., 2014; Brdys and Zhang, 2001) or based on artificial intelligence techniques like fuzzy, neuronal network, etc., (Ding et al., 2023; Abdul et al., 2022; Hai et al., 2021). The proposed algorithms in this report will provide more reliable, feasible, and stable feedback over the control system for respective WWTP.

1.4 Scope

The importance of freshwater supply and safely treated wastewater return cannot be overemphasized. No matter how hard we try, we are still a long way from the most efficient, economical, and reliable ways to ensure our cities are properly equipped and ready for the challenge. Accordingly, wastewater demand is growing every day with an increase in population, the standard of living, and industrial activities. In order to manage the water resource and safeguard nature without letting polluted or used water (wastewater) enter water bodies, it demands the treatment of wastewater. Thereby, wastewater treatment plants have to be designed by considering various design parameters and standards. As wastewater standards move towards stringent effluent limits, there is a greater demand for utilities to better manage their existing assets. Thus, it demands proactive planning and project management to achieve the required and anticipated levels of treatment while saving costs.

One tool that has been successfully implemented to achieve such goals is wastewater process modeling and control. Wastewater process models have been adopted successfully in planning and project development for various applications. By considering process models, it can benefit plants by avoiding pitfalls, more accurately estimating potential chemical and energy savings, and evaluating threats and benefits, impacts, and feasibility. Similarly, the purpose of any WWTP control is primarily to meet effluent discharge standards and, secondarily, to keep maintenance and operational costs as low as possible. The best controller design depends on and differs from plant to plant, but the principle and goal remain the same throughout. Hence, this study aims at identifying the activated sludge model that assists the prime objective of designing a controller.

1.5 Research gaps

1. Identification of the Activated Sludge Process Model
2. Investigation of a real-time control study targeting the aeration factor for the conventional biological suspended growth process
3. Controller tuning techniques
4. Implement the data-driven approach to design a controller

1.6 Motivation

Often due to limited resources small-scale WWTPs face various challenges to accomplish their designed functions. Generally, two main reasons are, (a) Insufficient treatment capacity, and (b) the requirement of superior treatment by upgrading the existing practice. Modeling of WWTP can be a valuable tool to overcome these issues and come up with an upgraded system without much cost and complexity. Even though there is a limitation of inadequate monitoring systems in small-scale treatment plants, this approach may be simple and logical for designing a control system. Model identification is an essential tool for simulating a system's behavior, that assists in the control and optimization study of any system. In general, models derived from first principles demand in-depth knowledge as well as involve significant time and effort. Moreover, such a model will consist of correlations for process parameters that may have consequential inaccuracies. Some of these parameters may also have to be recalibrated using plant data to keep adapting to changing plant states.

The prime objective of the process controller is to improve the stability, robustness, and performance of any system. Especially, this is important for any biological process since the risk of adapting to sudden change is extremely slow. There have been very minimal open-source reported studies on controlling the activated sludge process using decentralized, decoupler, and centralized approaches. There is a need to design an effortless technique to design a controller with the best performance with the minimal investment. Hence, this study focused on designing a controller for a MIMO system through various techniques and comprehensively compared their performance for better understanding.

As an alternative, models can also be completely derived from data. With significant advances in the techniques of model building and improvements in sensor technology that allow large volumes of data to be collected at high sampling rates, this approach is becoming increasingly attractive for industrial applications. In process control, such data-driven models have been used for the last four decades. These types of models are formulated and developed from historical data that reveal useful information about the system's dynamics. One of the major objectives of this research is to assess whether data-driven models can be used to control and optimize process performance and monitor it effectively.

1.6.1 Research Objectives

1. To identify a simplified model of an Activated Sludge Process for controller design.

2. To design a decentralized controller for a multivariable Activated Sludge Process.

3. To design a centralized controller for a multivariable Activated Sludge Process.

4. To develop/design a data-driven multivariable controller for an Activated Sludge Process.

5. To study the set point tracking and disturbance rejection of the designed controllers.

6. To study the robustness and uncertainty of the designed controllers for an Activated Sludge Process.

1.7 Outline of the Study

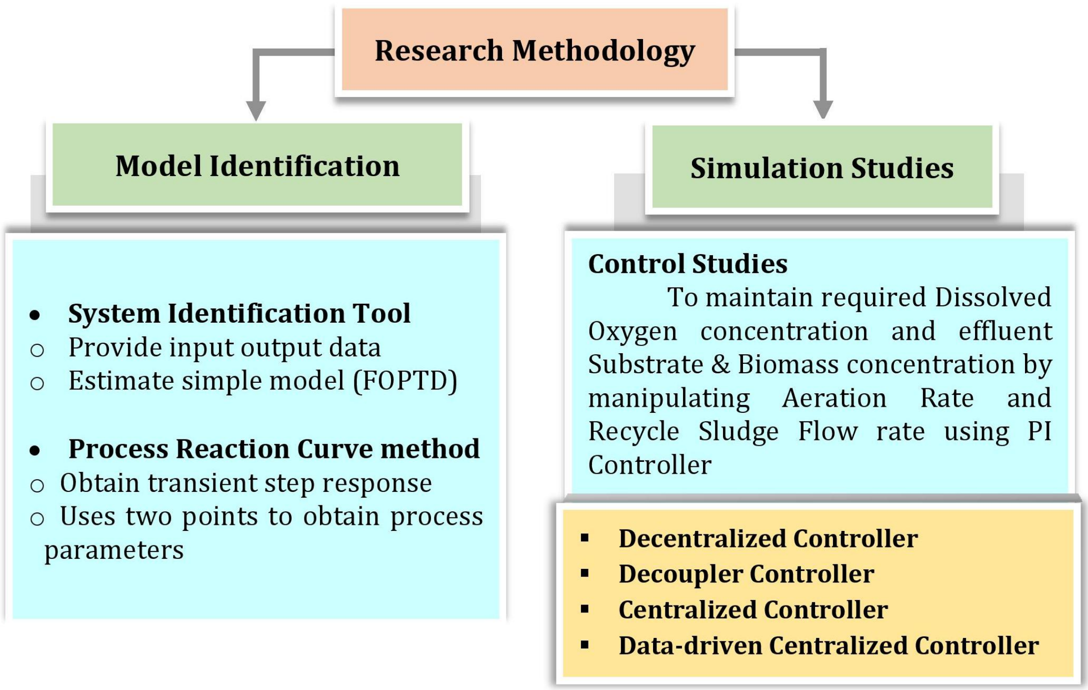

Figure 1.3 Flowchart for research outline

To accomplish the formulated research objectives, the project outline has been designed as presented in flowchart format below (Figure. 1.3). A model identification can be accomplished by undertaking a theoretical approach or/an experimental approach. Generally, the first principle is used to formulate the model equations, that considers conservation laws i.e., Mass and Component balance. Whereas measured data from existing WWTP or from pilot-scaled WWTP are utilized for the experimental approach. In this study, the methodology is broadly classified into two sections namely model identification and simulation studies for controller design. Two approaches namely system identification and process reaction curve method were adopted to identify the simplest form of activated sludge process model. Subsequently, the same is utilized to design a decentralized, decoupler, and centralized controller to govern DO or biomass and substrate concentration by manipulating the aeration rate and recycle sludge flow rate. To overcome the limitation of First Principle Modeling (FPM) a data-driven approach was also adopted for designing a centralized controller and the performance of the same is compared with the reported methods.

1.8 THESIS ORGANIZATION

The thesis is organized according to the following chapters,

Chapter 1: Introduction – The background, environmental issues related to water scarcity and management, insight on wastewater treatment and technologies, initial brief on the control system, and necessity of this study are discussed in this chapter.

Chapter 2: Review of literature – This chapter is subdivided into 4 sections to review the works of literature. Section one briefs about WWTP layout and various studies related to it, section two addresses modelling studies related to the ASP system, and section three and four summarizes studies related to the control of WWTP and data-driven control of several processes. The research gaps are highlighted followed by the scope and objectives of the current research work.

Chapter 3: System description and preliminaries – This chapter explains the ASP system in detail with the model equation and model parameters, control system prerequisites that were considered for all the studies.

Chapter 4: Decentralized controller design for an ASP – Methodology of decentralized controller design and outcome of the study.

Chapter 5: Centralized controller design for an ASP – Describes the procedure of centralized controller design, comparison of two methods, and outcome of the study.

Chapter 6: Centralized controller design for an ASP using a data-driven approach – Explains the data-driven approach for designing a centralized controller, a novel optimization technique for obtaining controller tuning parameters with results comparison with the reported method.

Chapter 7: Summary and Conclusions – This chapter consists of findings and a summary of all the above studies, scope, and future perspectives of the research work.

The final section includes references to all the referred reported works (Textbooks, Journal articles, and Conference articles.)

Chapter 2

REVIEW OF LITERATURE

This chapter summarises the previous research outcomes that have been referred to formulate the current research objective. Below pictorial representation provides a brief idea about four key topics (WWTP layout, WWTP Modeling, WWTP Control studies, and WWTP Data-driven approach) that were focused on in this survey.

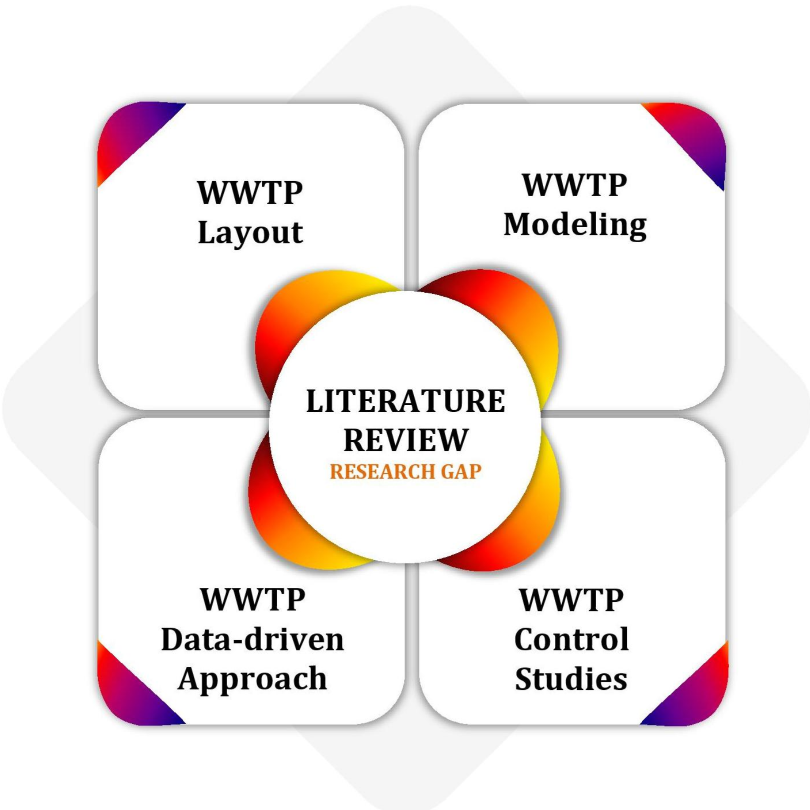

Segments of literature survey

2.1 Literature survey on Wastewater Treatment Plant Layout

Selecting the wastewater treatment plant layout is the key task which is majorly determined by aspects like the level of treatment required, economy (initial and maintenance cost), and availability of resources for existing influent wastewater. Various treatment units (Aerobic, Anoxic, and Anaerobic) have their own advantage over the nutrient removal process (O'Brien et al., 2005). To achieve biological nitrogen removal, both the aerobic stage and anoxic stage are must (Norbert and H. Johannes, 1996). Wherein, biological nitrification occurs in the aerobic unit, followed by biological denitrification in the anoxic unit (Foscoliano et al., 2016; Shen et al., 2008). Some substrate elimination studies have been reported where an anoxic chamber has been placed ahead of an aerobic chamber (Francisco et al., 2011; Jun et al., 2014). investigated This will lead to NH_4-N oxidation and NO_3-N and NO_2-N reduction to nitrogen gas (Steilos and Patrick, 2002). Better nitrogen removal was observed when an internal recycling stream was added for WWTP layout (Michela et al., 2013). However, treatment streams can also be equipped with a mixing pocket at the beginning of the primary treatment units (O'Brien et al., 2011; Cristea and Agachi, 2006). Most of the streams consider internal re-circulation from aeration units (Francisco and Vega, 2007), exceptionally few studies adopted it from anoxic chamber (Brdys et al., 2008). Conversely for phosphorous removal, the treatment plant should position the aerobic unit at the beginning, where the growth of a microorganism is supported, followed by an anoxic unit where denitrification occurs at the cost of the microorganism's decay (Vega et al., 2014). The next unit should be anaerobic, which will assist the phosphorous removal process. Table 2.1 provides us with an insight into various combinations of operating units adopted in the ASP system based upon the study objectives.

Hence, after understanding the above discussions the effluent from primary treatment stages is considered to be treated biologically where organic matter is decomposed by aerobic bacteria with the supply of oxygen. A single-stage unit consisting of an aeration chamber (biological reactor) and a sedimentation chamber is considered for the current study. Based on the objectives of the study a few assumptions in process conditions were recommended. The subsequent stage is the secondary settling unit from which, some portion of sludge is returned back to the reactor and the remaining is drawn out for further applications.

Table 2.1: Literature review on WWTP Layout

Sl. No.	Plant Layout	Remarks - Work done		Reference
1.	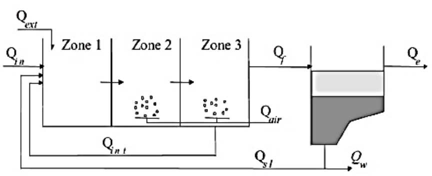	- Plant for the removal of COD and N from domestic effluents. - MPC Controller, Sampling rate of 0.16 hours.	- The DO Concentrations in anoxic zone assumed 0. - Linear state-space model was obtained	Oscar A et al., (2002)
2.	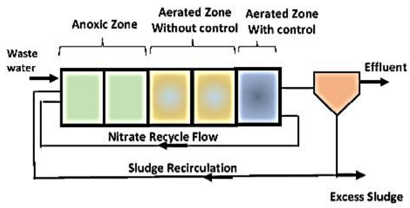	- ASM1 model. - Air flow control on the final tank for dissolved oxygen, and optional plant flow control on the second tank for nitrate.	- Considers treatment plant dynamics, that is the influent into the plant - No sewer dynamics.	M. O' Brien et al., (2005)
3.	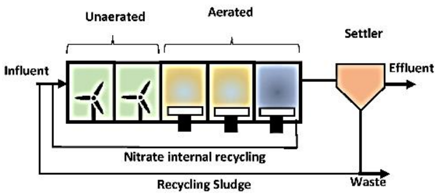	- The Benchmark European program COST-624. - Substrate, oxygen and nitrogen control. - Simplified plant for integrated design	- Basis lies in maintaining a (biomass). - A Sequential quadratic programming (SQP) method to obtain plant parameters	Mario Francisco et al., (2007)
4.	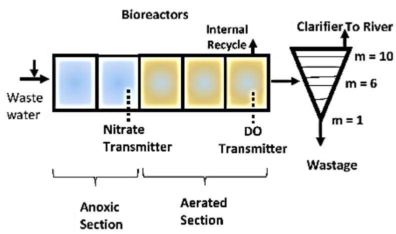	- Combines nitrification with pre-denitrification. - 5: bioreactor & a secondary settler. - Effluent composition will be sensitive to applied control Strategy (sludge load)	The efficiency of treatment influenced by an overload in a local community due to varying WW sources, chemical composition, and flowrate.	Wenhao Shen et al., (2008)
5.	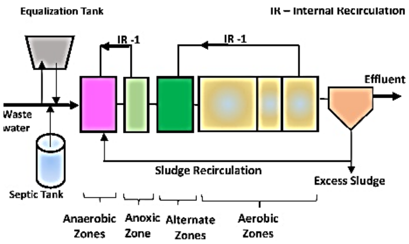	- P removal, iron sulphate (PIX) is added to aerobic zone to precipitate - Sewer network tank retention is imbedded into the equalisation tank retention.	- Complex Layout for Controlling and Modelling. - Hard constraint on the maximum flow rate in order to prevent wash out of the biological sludge.	M.A. Brdys et. al., (2008)

<table>
<tr><th>Sl. No.</th><th>Plant Layout</th><th colspan="2">Remarks - Work done</th><th>Reference</th></tr>
<tr><td>6.</td><td>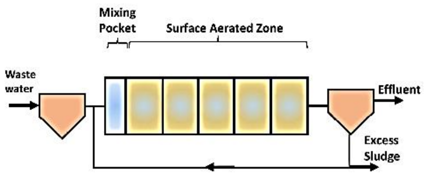</td><td>- Carbonaceous removal, as the Nitrifying Trickling Filter ensures ammonia at the Final Effluent.
- Provided aeration control by regulating the DO levels.</td><td>- The changes in influent load affect the aeration process under closed loop control.</td><td>M. O'Brien et al., (2011)</td></tr>
<tr><td>7.</td><td>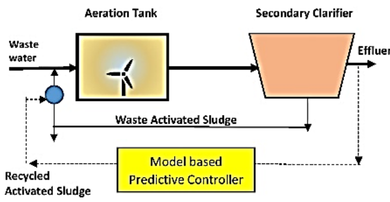</td><td>- ASP for substrate Elimination.
- Satisfy the need of readily degradable organic matter form the denitrification process the anoxic reactor.</td><td>- Assuming perfectly mixed tanks.
- Dynamic simulations are not performed.</td><td>M. Francisco et. al., (2011)</td></tr>
<tr><td>8.</td><td>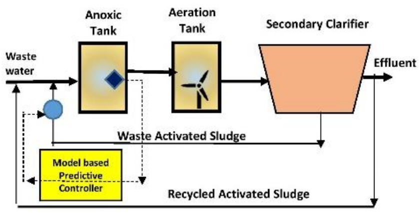</td><td>- ASP for nitrogen removal.
- Models considered are too simple to simulate.
- Improved the design procedure by using dynamical models.</td><td>- Integrated design for optimal and control system with MPC.</td><td>M. Francisco et. al., (2011)</td></tr>
<tr><td>9.</td><td>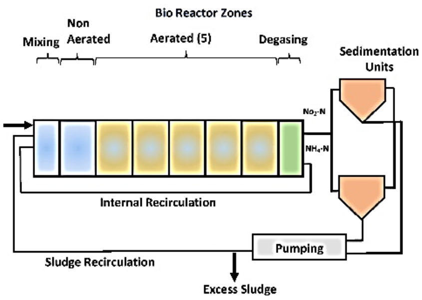</td><td>- Improving N removal while reducing the operational costs.
- 85% is domestic and 15% industrial WW.
- Biogas from sludge is used for electricity and heat production.</td><td>- Effluent nitrate removal in post-denitrification unit by dosing methanol.
- Total N removal of approximately 90%.</td><td>Michela Mulas et al., (2013)</td></tr>
<tr><td>10.</td><td>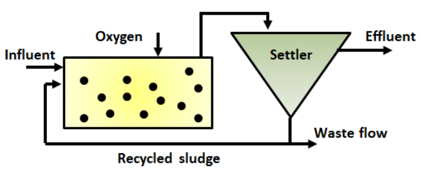</td><td>- Simplified model structure.
- Compared with exogenous input (ARX) model.</td><td>- An Activated sludge system for carbon removal (aerobic process).</td><td>Gaya et al., (2013)</td></tr>
</table>

Sl. No.	Plant Layout	Remarks - Work done		Reference
11.	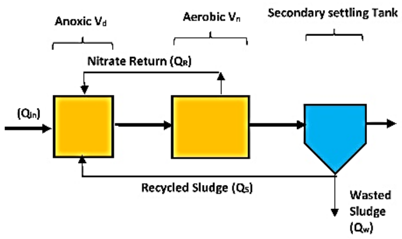	- MPC to optimize the aeration by external carbon source addition under the disturbance of influent flow rate and nitrogen load. - Two step nitrification was modelled by the growth of AOB and NOB.	- The results suggested that optimal external carbon source and aeration can be achieved in biological nitrogen removal by MPC Method.	Jun Wu et. al., (2014)
12.	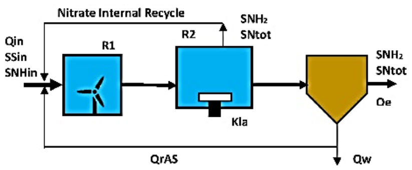	- Real Time Optimization (RTO) - 3 multi-linear structures are compared. - Eliminate nutrients and organic matter.	- Oxygen requirement. - Specific aerator consumption.	P. Vega et al., (2014)
13.	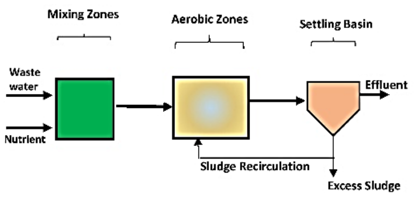	-Homogeneous concentration of solids and substrates in the basin. - System is stable and is less affected by disturbances.	- Successful as long as the dilution rate can be maintained at constant level.	Mircea V et. al., (2014)
14.	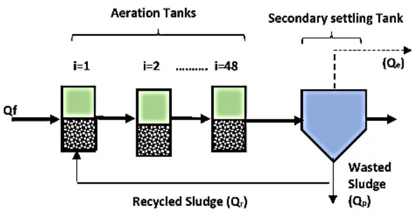	- Fully aerobic without anoxic or anaerobic. - Optimizing the aeration reduces energy by more than 60%. - 48 Diffusers used.	- Focus on reduction of the energy consumption due to the aeration process.	Mustafa Cagdas Ozturk et al., (2016)
15.	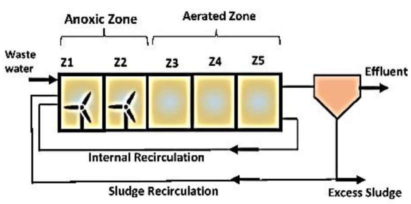	- A PI controller regulates aeration. - controlled by the internal recirculation flow rate. - Nitrification & denitrification.	- Some of the configurations used violated the effluent limits.	Chiara Foscoliano et al., (2016)

2.2 Literature survey on Wastewater Treatment Plant Modelling

In the era of globalization, wastewater management is important to protect our environment from deteriorating. A major investment is required in order to set up a wastewater treatment plant due to high capital cost, operation, and maintenance costs (Shohreh and Thami, 2013). Generally, models are used for analyzing the design (Bayramoglu et al., 2000), treatment ability, and efficiency (Park et al., 2014). Currently, various models have been used in control and optimization (energy consumption) studies (Charpentier and Martin, 1996; Zahir et al., 2012; Mario and Predrag, 2012). Prediction on quality of effluent discharge (COD and Nutrient removal) provides us with the opportunity to measure the effectiveness of treatment processes carried out at the plant (Lukasse et al., 1996; Marta et al., 2016).

A wastewater treatment plant modeling is a mathematical simplification of a real existing system. It is a real challenge due to its complexity, non-linear processes behaviour, and uncertain influent parameters (Sergiu and Maruan, 2007). The wastewater treatment modeling started with the development of a steady state model that includes the hydraulic model. The first dynamic model of an activated sludge system was developed (Goodman and Englande, 1974) to gauge the performance of the system. Wastewater treatment plant modeling is constructed in a simple manner and yet produced the true process behaviour. The most widely applied computer simulation of the activated sludge process is the Activated Sludge Model 1 (ASM1) (Ioana and Ioan, 2016; Ilse et al., 2003; Nejjari and Quevedo, 2004; C. Gomez et al., 2000) created by a group of the International Association of Water Quality. The ASM 1 was further developed in 1995 by introducing nitrogen and phosphorus removal to establish ASM 2 (Damir et al., 2000). Linear time-invariant state-space model, developed can predict the ammonium and nitrate concentration (Lindberg, 1998; Julien et al., 1998). The commonly used networks in the modeling and prediction of the wastewater treatment process are the Feed-Forward Neural Network (Hong and Thomas, 1996), Artificial Neural Network (Hakan et al., 2008), Fuzzy Logic (Turmel et al., 1997). To conclude, the modeling approach could increase the affordability of wastewater management systems.

After referring to various reported mathematical models a model with four nonlinear equations was deduced from the traditional widely accepted activate sludge model (ASM1). The equations included Biomass concentration, substrate concentration, Dissolved oxygen concentration, and Recycle sludge concentration with supporting growth rate equation (refer to Chapter - 3). A few assumptions were made in order to approximate the model to overcome some of the uncertainty.

Since ASP is a MIMO process, extensive mathematical knowledge is a must in order to adopt it for the control study. Hence, to overcome this limitation in this study two model identification approach is considered namely system identification (SysId) and Process Reaction Curve (PRC) method. Both approaches use the input-output data generated from the considered model equations. A review of various modeling approaches and their application is tabulated in Table 2.2. Most of the studies adopted the traditional ASM1 model or a simplified model derived from it. And based on the application and purpose, researchers have modified it accordingly. The review also provides insight into process types and state variables that were considered for respective studies.

Table 2.2: Literature review on WWTP Modeling

Sl. No.	Description – Work done	Remarks	Reference
1.	- Grey box modelling for non-linear time varying DO dynamics - Modelling DO concentration in aerator. - Way to excitate r(act) is by manipulating substrate concentration in aerator unit. - Pilot plant - very minute sampling	- Long range prediction – Model based predictive control (MBPC). - Novelty: Availability of direct measurement of non-DO limited oxygen uptake rate/actual respiration rate – RA 1000.	Lukasse et al., (1996)
2.	- A parallel hybrid model of oxidation ditch to remove organic matter and nitrogen. - Default values by lab experiments. - On-line measurements in wastewater plants is still very limited.	- Hybrid model integrating a simplified first Principle model (FPM) and a neural network is preferable. - Artificial neural networks.	Hong Zhao et al., (1996)
3.	- Alternative method for calculating the electricity cost per kilogram of BOD5 from the quality objective fixed for NH4+.N or TKN in the effluent.	- Satisfactory method for oxygen requirement specific aerator electricity consumed for low-load ASP.	J. Charpentier et al., (1996)
4.	- A linear multivariable time-invariant state-space model used to predict the ammonium and nitrate concentration - A multivariable linear quadratic (LQ) controller designed to control ammonium & nitrate concentration.	- Identification is based on a black-box model (IAWQ model) - Model can predict the ammonium & nitrate concentration.	Carl-Fredrik Lindberg et al., (1998)
5.	- Structural identifiability and practical identification of a reduced order model for an ASP by using on-line measurements of oxygen and nitrate concentrations. - On-line measurements oxygen and nitrate concentrations, Off-line ammonia concentration.	- Good fit between the simulated solution and the actual behavior of a lab scale pilot plant. - Parameter identification problem has been solved - General I.A.W.Q. model no.1.	S. Julien et. al., (1998)
6.	- An integrated model for aerobic and denitrifying biological P removal (Delft bio-P model) was combined with retained equations for COD and N conversion of the ASM No 2. (COD, N, P modeling.) - Simulations were performed in SIMBA3.2	- Batch tests for model evaluation, - Sensitive towards change in kBOD - The combined ASM No. 2 and Delft BPR model for COD, N and P removal proved well capable of describing the performance	Damir Brdjanovic et. al., (1999)
7.	- Proposed reduced nonlinear model of an ASP. - IAWQ activated sludge model. - Identification of model parameters is accomplished by using measurements of ammonia, nitrate and oxygen coming from experimental studies carried out on the pilot plant process.	- A mathematical representation of the main system dynamics during aerobic and anoxic phases for on-line estimation and control purposes. - Final model is a good representation of nitrogen dynamics.	C. Gomez-Quinter et al., (2000)
8.	- Model parameters were found by means of nonlinear regression analysis, - A model for relevant factors was established for the oxygen transfer rate.	- Model for oxygen transfer rate in diffused air systems. - Preliminary design of diffused air aeration tanks - Used plant data. -	M. Bayramoglu et al., (2000)

Sl. No.	Description – Work done	Remarks	Reference
9.	- Reduced nonlinear model of an activated sludge process. - Four state equations and eleven parameters. - Derived from IAWQ N° 1 model - Nitrogen dynamics	- Simple model - Model identified by measuring g measurements of ammonia, nitrate and oxygen coming the pilot plant process. - On-line robust estimation and control	Gomezquintero et al., (2000)
10.	- Activated Sludge Model no. 3 (ASM 3) - Nitrogen removal and biological phosphorus removal - Degradable COD measured by respiration simulation runs	- ASM 3 and the EAWAG BioP Module. - Three real-time WWTP comparison.	Wichern et al., (2001)
11.	- Biotransformation processes in a common activated sludge process with N-removal. - Model reduction procedure: 1: data generation, 2: linear state space model approximation., 3: identification, 4: model interpolation	- A strategy is proposed to reduce the complexity of the activated sludge model no. 1 (ASM1) - Model combines high predictive value with very low computation time	Ilse Y. Smets et al., (2003)
12.	- Mass Balance equations [IAWQ AS Model No.1] - A complex nonlinear model is used in the design of a software sensor and a predictive control techniques.	- Estimate and control of biological nitrogen and carbon removal process. - Modeling, estimation and control of a nutrient removal plant	Fatiha Nejjari et al., (2004)
13.	- Linear model of an alternating-phase activated sludge process. - Two phase : aerobic and anoxic. - Validation thorugh experimental and simulated data. - Derivated from the ASM No. 1.	- Simple to manipulate hence less computational effort. - Online estimation and control purposes. - GPSX simulations.	Claudia et al., (2004)
14.	- Linear multi-model - Three steps followed data generation, local model linearization and model interpolation. - Benchmark configuration, proposed by the COST 682. - Extremal weights avoided while model identification.	- Simple model for the biodegradation processes. - Standard carbon and nitrogen removing. - One anoxic and one aerated tank one point settler. - High predictive power with low complexity	Smets et al., (2004)
15.	- Substrate/biomass reduced-order model - Numerical model calibration structural identifiability and with experimental information. - Hydraulic mass balance and settler mass Balance	- Modelling, estimation and control Techniques. - Implementation of reliable control laws. - PID regulator and linear-quadratic-integral control.	Stefano (2005)
16.	- Dynamic behaviour of simultaneous carbon removal and nitrification process. - Carrousel type aerator. - Wastewater characterization. - Respirometric technique.	- Activated sludge model 1 (ASM1). - GPS-X simulation software. - Erzincan City Wastewater Treatment Plant.	Alper et al., (2005)

Sl. No.	Description – Work done	Remarks	Reference
17.	- Model was applied for 2 cases, one a hypothetical WWTP, second ANN modeling of ASP in the Iskenderun WWTP. - TSS_{eff} was selected model - Prediction of COD_{eff}	- A MATLAB script was developed (ANN) - High correlation coefficient (R) between the observed and predicted output variables.	Hakan Moral et al., (2008)
18.	- Activated Sludge process: biological reactor model without recycle. - Continuation methods to determine the steady-state behaviour	- Activated sludge model number 1. - Model includes eight processes. - 13 differential equations. - Fully understand the dynamics of the system.	Nelson et al., (2009)
19.	- Proposed based on BSM1. - Aerobic/Oxic process. - ASM1 model for reaction mechanism. - Eight biochemical reaction processes. - Considers only carbon oxidation process and removal of carbon.	- Purpose to inspect N and P removal. - Proposed model includes 13 components, 5 stoichiometric parameters and 14 kinetic parameters.	Yao et al., (2010)
20.	- Model to predict the COD. - Only considers the carbon oxidation process, without regard to nitrification process and denitrification process. - Simplified for three reactions .	- Benchmark Simulation Model no.1 (BSM1). - Simplifies Activated Sludge Model No. 1 (ASM1). - Reduces the model components, parameters and computational effort.	Yao et al., (2010)
21.	- Mathematical modelling using three sub models (for oxygen electrode, ideally mixed stirred tank bioreactor and plug flow reactor) - Electrode measuring dissolved oxygen.	- Polarographic oxygen electrodes. - Reduction of electrical power. - Optimisation of aeration process. - Detect the consequences. - Reduction of daily working time	Novak et al., (2012)
22.	- Model for the secondary settler. - Measurements of settling velocities determined using zone settling tests. - The movement of the sludge blanket in the secondary settler using the solid flux theory and the velocity settling.	- To design a model that predicts the outlet water quality from secondary clarifier. - Model will allow better process control.	Zahir Bakiri et al., (2012)
23.	- Seven models : ASM1; ASM2d; ASM3; ASM3 + BioP; ASM2d + TUD; Barker & Dold model; and UCTPHO+. - Mine processes. - Various process conditions.	- New schematic representation. - Gujer matrix notation. - Model are compared so that it can be choosed upon requirements.	Hauduc et al., (2013)
24.	- Two nonlinear ordinary differential equations. - Two hyperbolic partial differential equations. - Two material components; the soluble substrate and the particulate sludge.	- Simplified plant layout. - Controlling effluent dissolved nutrients concentration and the concentration profile in the sedimentation tank.	Stefan et al., (2013)

Sl. No.	Description – Work done	Remarks	Reference
25.	- Varying activated-sludge return rate to observe changes in effluent water quality and treatment efficiency. - Sizes of aeration tank calculated for different activated-sludge return rates. - System Dynamics modeling software, STELLA.	- System dynamics methodology is an effective simulation tool to model the dynamic nature. - Operating rules and policies related to capacity expansion. - Return rate of 90% marked the highest treatment efficiency.	S. Park et al., (2014)
26.	- Use wastewater treatment plant, by means of sensitivity analyse. - Model calibration and parameter estimation prioritization. - Simplified ASP single tank reactor model - Four differential equations through material balance.	- Monte Carlo simulation outputs to priorities the uncertainties on Benchmark Simulation Model (BSM1). - Sensitivity analysis using ANOVA decomposition and RS-HDMR.	Cristescu et al., (2015)
27.	- Propose step by step procedure for modelling ASP for paper mill industry. - Validated on a pilot scale plant. - Better accuracy of the proposed model. - Application specific more efficient than theoretical.	- Proposed BOD based model is compare with CO based ASM1 model. - Three state variables. - Two reactions aerobic growth of bio-mass and the biomass decay.	Cadet et al., (2016)
28.	- Subspace Identification of Dynamical Systems. - Stable and Unstable Systems. - Idification methods: process reaction curve method and optimization methods. - Experimental evaluations.	- Equating coefficients method, pole placement method, synthesis method and stability analysis method; controller design methods. - Subspace identification methods such as N4SID, MOESP, CVA and DSR methods, modified MON4SID.	Chidhambaram et al., (2017)
29.	- Modelling activate sludge aeration reactor - Developed model is fitted with plant data - Operation parameters: Inlet biomass and substrate - Varying substrate concentration yielded optimized process conditions	- Predict and optimize the system behaviour. - Focus on removing organic pollutants. - Inlet and outlet concentration dependency was analysed.	Ashraf et al., (2019)
30.	- Activated Sludge Model No 1. - INtegrated Simulation Environment Language (INSEL). - Explicit Euler method. - Ludzack-Ettinger layout configuration.	- Develop a reliable and accurate model. - Denitrification-nitrification. - Aeration Energy Demand Evaluation.	Calise et al., (2020)
31.	- A novel five-tank integrated activated sludge process (FTIASP) model. - Multi-objective optimization method. - Seven kinetic parameters calibrated using iterative calculation procedure.	- ASM2d. - Experimental validation. - Six different batch tests, sensitivity analysis and genetic algorithm.	Chen et al., (2020)
32.	- Dynamic simulation of Activated sludge unit. - Seven configurations. - CSTR, PFR, SBR. - Taguchi method and Minitab software.	- Activated sludge model No.3 (ASM3) and Wolfram Mathematica. - Biochemical reactions in clarifier is ignored. - Optimized maximum removal efficiency.	Amirfakhri, (2023)

2.3 Literature survey on Wastewater Treatment Plant Control

Wastewater treatment plants (WWTPs) are mainly affected by large disturbances and uncertainties related to the influent wastewater composition. The plants naturally aim to remove suspended substances, organic material, and nutrients from the water before releasing it to the recipient. Manual operation is the traditional method for wastewater process control. These manual adjustments of control elements are made to maintain parameters within desirable ranges, such as dissolved oxygen. The best technology available to control the discharge of pollutants is proven in biological processes. As research advanced online instruments began to be used as a replacement for conventional measurement technology. This enabled better control but there was still a lag between the time of measurement and the adjustment of control elements. The higher level of the controller is the automatic controller, which used online measurements. Based on the changes in wastewater characteristics it causes disturbance to the process, which intern causes feedback response (Nejjari et al., 1999). The typical example of such a controller is blower control for cyclic activated sludge based on online measurements of DO (Burns and Fielden, 1989).

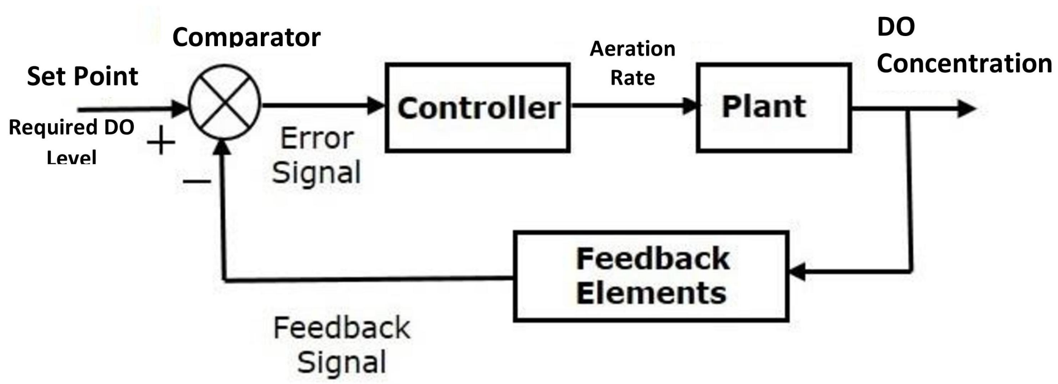

Figure 2.1 Schematic representation of Closed loop feed-back process control system

Major difficulties in controlling the microbial processes lie in the lack of cheap and reliable sensors for online measurement of the key state variables (Nejjari et al., 1999; Nejjari et al., 1997). Nevertheless, online measurement does not give any savings, but it provides ample data with new formations (Marinus and Time, 1995). With the optimal

N removal objective: a Receding Horizon Optimal Control (RHOC) strategy was used to measure NH_4 and NO_3 enabling feedback control of alteration between anoxic and aerobic phases (Lukasse et al., 1998). Meanwhile, feed-forward control strategies have also resulted in optimal performance level (A.Stare et al., 2007). Some of the common types of controllers available are P, P-I, I-P, P-D, P-I-D and advanced controllers like Fuzzy network controllers, Genetic Algorithm based Neural network (Chang et al., 2001) and Artificial Neural Network controllers (Manesis et al., 1998; Santin et al., 2019). Here, the P controller is mostly used in first-order processes with single energy storage to stabilize the unstable process. At the same time, the P controller cannot manage state error and cause oscillations if sufficiently aggressive in the presence of lag/ or dead time. Whereas PI controller is mainly used to eliminate steady-state errors resulting from P controller (Lee et al., 1998). In the case of I-P controller, the proportional part of the controller is fed with the feedback variable and not with the error (Alexandros et al., 2015). PID controller has the optimum control dynamics including zero steady-state error, fast response (short rise time), no oscillations, and higher stability (Turmel et al., 1997). One of the main advantages of the PID controller is that it can be used with higher-order processes including more than single energy storage. Model Predictive Control (MPC) is one such controller where it uses the model of a system to predict its behavior of it (Holenda et al., 2008). It can handle multi-input multi-output systems that may have interactions between their inputs and outputs.

There have been many advanced controllers reported in the literature. However, in order to effortlessly work in a real-world WWTP, a simple and effective controller is a prerequisite. Hence, three control structures, namely, decentralized, decoupled, and centralized are selected to control the MIMO system. To the best of the author's knowledge, there have been limited studies reported in open source where the researchers have used these structures for controlling WWTP. The merits and demerits of the designed control structures are discussed in the upcoming chapters. Taking into consideration of WWTP's initial and operational cost, a simple and effective PI controller is adopted to control the process variables. Various types of controllers with their advantages and disadvantage according to their application are discussed in Table 2.3.

Table 2.3: Literature review on WWTP Control

Sl. No.	Description – Work done	Remarks	Reference
1.	- Quantify the practical and financial benefits from control system. - Automatically Blower to maintain DO. - Supervisory, Control and Data Acquisition (SCADA) system. - Electromagnetic flow meters, liquid level detectors, DO & suspended solids instruments.	- Assessments of several main control functions showed benefits which include cost savings, better operation and early warning of equipment failure. - Monitoring of effluent quality requires further investigations. - Sludge wastage control.	J. M. Burns et al., (1989)
2.	- Four different multivariable control tuning methods - PI Controller. - State space model. - New frequency domain performance and robustness criteria.	- Methods proposed by Davison (1976), extension proposed by Penttinen and Hoivo (1980), modified method presented by Maciejowski (1989) and developed method (Lieslehto, 1990).	J. T. Tanttu et al., (1991)
3.	- Decentralized PI controller. - MIMO stable system. - Robustness analysis. - Comparison of multivariable feedback designs.	- Disturbance rejection. - Linear Quadratic Gaussian control problem. - Synthesis method. - H-Infinity control theory.	Perkins (1991)
4.	- STAR concept for advanced real time control. - Permanent measurement of ammonia, nitrate and phosphate in one of the aeration tanks. - N removal study.	- Control strategies are efficient, robust for practical implementation. Reduction in energy consumption and chemical consumption. - STAR gives full benefit for the cost of measuring systems and maintenance.	Marinus K et al., (1995)
5.	- Fuzzy & artificial neural network controllers. - Manipulated variables: oxygen supply, mixed liquid returns rate from the aerated zone to the anoxic zone, sludge returns rate - Controlled variables: ammonia, Nitrate, DO, temperature, MLSS, BOD.	- The results of this study proved very favourable and the potential of intelligent control of wastewater treatment plants appears unlimited. - Simple, reliable and inexpensive intelligent controller.	S. A. Manesis et al., (1997)
6.	- Decentralized controller. - MIMO stable system. - FORTRAN program used to simulate the dynamics.	- Controlling liquid level. - Manipulating flowrate of liquid pumped. - PI controller is designed with two different process conditions.	Michael L. Luyben et al., (1997)
7.	- Designed a nonlinear adaptive feedback-linearizing control. - Nonlinear controller combined with an estimation algorithm for the on-line estimation of biological states and uncertain parameters of the process.	- Specific growth rate and some of the state variables in interest are not measured on-line, so they are replaced in the control algorithm by on-line estimates provided by a joint observer estimator (JOE).	F. Nejjari et al., (1997)
8.	- The aim for control systems is to reduce the energy needs and/or increase the effluent quality.	- Three control manually tuned PID, auto tuned PID and a fuzzy logic controller. - Best response is the manually tuned PID, more versatile controller is fuzzy logic controller.	Vincent J. Tunnel et al., (1997)

Sl. No.	Description – Work done	Remarks	Reference
9.	- Centralized PI controllers. - Using (1) Davison method, (2) the Maciejowski method, (3) the decoupler design and (4) the Tanttu and Lieslehto method.	- MSF desalination plant. - Robustness analysis. - Perturbation in the system steady-state gains. - Decoupler gave best response.	Reddy et al., (1997)
10.	- ASMI DO. Model. - A Receding Horizon Optimal Control (RHOC) strategy using NH_4 and NO_3 measurements. - Feedback control of the alternation between anoxic and aerobic phases. - Objective optimal N removal. - DO So is treated as control input.	- Developed an aeration strategy yielding optimal N-removal. - Both alternating nitrification/ denitrification DO-levels might be optimal. - RHOC application yields globally optimal control with a prediction horizon.	L. I. S. Lukasse et al., (1998)
11.	- To develop an automatic control system for DO and pH of the ASP in a coke WWTP. - A discrete type auto tuned PI controller using an auto-regressive exogenous (ARX) model. - Controlling the speed of surface aerators. - Nonlinear pH controller using titration curve.	- Automatic control System: on-line data acquisition, auto tuning and data display. - PI controller worked very well and there were small deviations of pH and DO from the set point.	B. K. Lee et al., (1998)
12.	- A non-linear adaptive feedback-linearizing control. - The reduction of the organic matter concentration and control of DO level. -Dilution rate and the air flow rate manipulating variable.	- Lack of cheap and reliable sensors for on-line measurement of the key state variables. - Control action for an acceptable pollutant level; provide the biomass with energy to carry on the oxidation.	F. Nejjari et al., (1999)
13.	- Decentralized PI derivative controller. - Multiplicate model factor (MMF). - Dynamic relative interaction (dRI). - SISO SIMC−PID controller tuning for controller tuning.	- MIMO System. - Very simple and effective.	Mao et al., (2005)
14.	- Evaluated aeration volume control strategy. - Only sensors for measuring the DO concentrations. - Ammonium concentration is controlled by manipulating the DO set-point.	- Suggested aeration volume control strategy could reduce the effluent nitrate and ammonium concentrations significantly without increasing the aeration energy.	Mats Ekman et al., (2006)
15.	- Genetic algorithm-based neural network (GA-NN) designed as a feed forward multi-layered connectionist structure to filter the control strategies from a set of monitoring data measured (SBR). - Petrochemical production process.	- Develops a genetic algorithm-based neural network for the assistance of intelligent controller design. - Cost-effective tool to capture the uncertainties of WWTP.	Ni-bin chang et al., (2007)

Sl. No.	Description – Work done	Remarks	Reference
16.	- Evaluated several control algorithms for N removal using a simulation benchmark. - Various PI and feedforward controllers are evaluated with advanced multivariable and nonlinear model predictive control. - Estimated differences between the controllers in terms of operating costs.	- PI nitrate and feedforward-PI ammonia control closely imitates the optimal operation strategy as the operating costs are only slightly higher compared to the case when model predictive control is applied. - Benchmark simulation model (BSM1).	A. Stare et al., (2007)
17.	- Diagonal main controllers and off-diagonal decoupling controllers - Hankel Interaction Index Array (HIIA) - Relative Gain Array (RGA)	- PI/PID controller for MIMO processes - Method is very simple, straightforward and easy - Higher order processes	Malwaltkar et al., (2008)
18.	- MPC has been applied to control the dissolved oxygen concentration at a certain setpoint based on a linear state-space model. - The control strategy was using systematic evaluation criteria: in a simulation benchmark.	- MPC can be effectively used for dissolved oxygen control. - Performance can be considerably enhanced by decreasing the sampling time.	B. Holenda et al., (2008)
19.	- Robust decentralized PI controller. - New method to controller design for uncertain LTI MIMO systems. - Internal model control (IMC) method for local PI controller.	- Industrial utility boiler system. - Robust stability Analysis. - Nonlinear model is linearized. - Validated with real system. - Crucial conditions robust stability and diagonal dominance.	Marquez et al., (2008)
20.	- To control the free gyroscope seeker scan loop system - Linear model and Nonlinear Model - High Gain PI controller - RGA is used for input-output pairing analysis.	- Centralized and Decentralized control structure - Track patterns like conical and rosette - Proposed methods was effective.	Ramin et al., (2009)
21.	- Decentralized PI/PID controller design. - Method based on gain and phase margin specifications for tuning. - FOPTD using frequency response fitting. - Decoupler design.	- Three TITO systems to measure the performance. - Level–Temperature reactor process.	Maghade et al., (2012)
22.	- Centralized PI controller for MIMO system. - Based on direct synthesis method. - Effective transfer function (ETF). - Maclaurin series get standard PI form.	- Relative gain array and relative normalized gain array concept. - Controller designed from RNGA-RARTA was better than RGA. - Smaller interaction but sluggish.	Vijay Kumar et al., (2012)
23.	- Extension of simplified decoupling. - PID control is obtained by controller reduction. - Process matrix 2x2 and 3x3. - anti-windup schemes	- Set configuration based on complexity of the corresponding decoupler elements or the response of apparent processes. - Experimental quadruple tank system - Slightly complex methodology	Garrido et al., (2012)

Sl. No.	Description – Work done	Remarks	Reference
24.	- Robust decentralized controller design - Pole placement Method. - PI controllers. - Using damping factor closed loop poles region was calculated.	- Reduces the control problem size to subsystem level. - Validated by lab scale two coupled DC motors. - Compared decentralized controller with robust controller.	Holic et al., (2013)
25.	- Relationship between equivalent transfer function (ETF) and the pseudo-inverse of multivariable transfer matrix is derived. - RNGA based ETF parameterization method extended to nonsquare processes.	- PI/PID. - Ideal decoupling. - Resulting controller is simple and easy - Effective for both square and nonsquare processes.	Shen et al., (2014)
26.	- Comparison between PI controller and I – P modified controller. - I – P controller is different from PI controller in that the proportional part of the controller is fed with the feedback variable and not with the error as it is done with the PI controller.	- I – P controller is better for disturbance rejection and process settling times comparing to the same method using PI controller. - Better performance and lower complexity, so as to be easier for the operators to adjust it. - Pole – placement design	Alexandros D. Kotzapetros et al., (2014)
27.	- Parameter optimization technique. - Reduced burden from Feedback controller parameterized using multivariable internal model controller. - A novel technique for estimating the starting values of the controller Parameters.	- MATLAB optimization toolbox. - Constraints like singular values, internal variable magnitude can be directly handed. - PI controller. - Three benchmark process system. - Adopted performance indices.	Taiwo et al., (2014)
28.	- Centralized PI controllers. - Tuning based on steady state gain matrix (SSGM). - Combining Static decoupler design and SISO PI/PID controllers design for centralized controllers.	- Simple method - Results compared with Davison EJ. was better. - Proven by three simulation example. - No knowledge of system dynamics required.	Dhanyaram et al., (2015)
29.	- Simplified centralized PID tuning. - Based on Falb's row by row decoupling (RRDP) concept. - Controller parameters formulated in the statespace framework.	- Zero order, first order and second order systems. - Simultaneous decoupling and set-point tracking. - Accurate sub system dynamics.	Arati et al., (2016)
30.	- MIMO System - Falb's row by row decoupling (RRDP) concept - Decoupling and set-point tracking	- Simplified centralized controller tuning - Centralized PID tuning - Accurate sub system dynamics - Controller settings for zero order, first order and second order systems	Devi et al., (2016)
31.	- Designing decentralised PID controllers for stable systems - Synthesis method extended to unstable systems. - Maclariun Series for controller design	- Two input - two output (TITO) systems - Simple calculations - Decreased interactions - Robustness Analysis	Chandra et al., (2016)

Sl. No.	Description – Work done	Remarks	Reference
32.	- Two tuning methods - PI Controller - Genetic algorithms for desired controller specification - DSM suites for SISO not MIMO	- Modified Direct Synthesis method extended to a multivariable system - Robustness analysis showed better compared to reported methods	Lan et al., (2017)
33.	- Decentralized controller - Equivalent Subsystems Method (ESM) - Unified frequency-domain methodology	- SISO and MIMO system - Frequency-domain plots - Closed-loop stability was verified using the Generalized Nyquist criterion	Alena et al., (2019)
34.	- Influent from BSM1 (ASM1) - An optimal setpoint based control method. - To remove organic substances and N. - ADM1 (Anaerobic digester Model 1)	- Five control strategies were developed. - Control of DO concentration in aeration Unit and N concentration by internal recirculation.	Laurentiu Luca et al., (2019)
35.	- Benchmark simulation model no. 1. - Filters are used to reduce the noise of the sensors (Artificial neural networks-ANN). - Predict DO, to compensate the delay produced by filters and sensors, and anticipate the time needed by actuator to obtain the desired value. - ANN to predict the appropriate S_O - Default control strategy (DEFCS).	- Difficulty of the DO control is due to noise and delay in the sensors and actuators. - The ANN take into account the microorganisms present in the WW, as well as their food and energy source. - PI Control system tries to minimize the effects of sensor noise and sensor & actuator delays, including noise filters.	I. Santin et al., (2019)
36.	- Robust decentralized PI controller. - Predefined reference model transfer function. - Parametric uncertainty. - Set point tracking and disturbance rejection.	- Level maintenance in coupled tank system. - Implemented on real-time experimentation. - Better performance with minimal interactions.	Mahapatro et al., (2019)
37.	- Multi- Objective Particle Swam Optimization (MOPSO) algorithm - PID controller. - Distillation column process. - Fine tune the PID controller using Multi Objective optimization technique.	- ISE, IAE, ITAE performance indices. - Compared with Davison's and Tanttu and Lieslehto methods. - Lesser settling time.	Sivagurunathan et al., (2021)
38.	- Decentralized PI controller. - Biggest Log modulus Tuning method (BLT). - Ziegler-Nichol's tuning method.	- Multivariable coupled tank system. - Closed loop stability measured using characteristic loci method. - Extension of the SISO Nyquist stability criterion.	Mohanraj et al., (2021)
39.	- Centralized PI controller design. - Process matrix inverse calculation. - Controller designed using model matching technique. - Two approach one squares up the process transfer function matrix the other is based on pseudo-inverse evaluation.	- Suitable for low and high-dimensional square/non-square MIMO processes. - Extended for the non-square MIMO processes. - Better performance to reported methods.	Ghosh et al., (2021)

2.4 Literature survey on Data-driven approach for control studies

Advancement in the production units of industries has led to complex production processes. In such a scenario model-based control theory may not work well since the plant model does not consider the assumed model set (Zhong and Zhuo, 2013). This inaccurate model can lead to bad performances and an unstable closed-loop system. The key parameter for this error is the difference between the controlled plant and the assumed plant model. Due to these practical issues, data-driven controller theory is considered over the model-based controller theory in most industries like chemical (Wang et al., 2008; Jong and Jay, 2005; Bei et al., 2018), metallurgy (Yiming et al., 2016), computer security (Han et al., 1999; Chaudhuri et al., 2001), instrumentation (Sridhar et al., 2008), electronics (Shi et al., 2023) and transportation (Murphey et al., 2003; Jiateng et al., 2020; Kah et al., 2023). Moreover, this could be easily adopted since many industrial processes were already generating a huge amount of data at every time instant of every run. And this data contained all valuable information (like state variables, process operation, etc.) of the exact plant upon which the controller was supposed to be designed. This supremacy attracted many researchers in the control theory community to explore more with this technique.

To be specifically defined, the data-driven controller theory is that study in which the controller is designed by directly using the online or offline I/O data from the controlled system without using the implicit or explicit mathematical model of the processes. This approach is absolutely independent of the plant model omitting the estimation and assumptions. Since the first principle model is often complex, time-consuming to derive and reduce, and requires human intervention for model validations, this data-driven approach has clearly an edge over the model-based technique. Most complex to complex industrial process problems could be solved through this data-driven technique (Li et al., 2017; Qiu et al., 2017).

In a recent study, Liang adopts this data-driven approach to model a building energy model that solved many practical problems. The data drive proved to be the effortless technique for Gioia et al., (2022) where in they designed a controller for Wave Energy Converter (WEC) that extracted energy from the ocean (Daniele et al., 2022). Advancing, a real-time data-driven controller is designed for complex equipment by Chaofan et al., (2022) that enhanced the product quality. Sun et al., (2018) presented their study to design a controller for the purification process that adopted a data-driven approach when model parameters were unknown (Bei et al., 2018). To avoid the modeling obstacle, this study utilizes the Adaptive Dynamic Programming (ADP) technique. The identical technique was also used to solve the optimal battery energy management and control problem in a smart grid residential system (Frank et al., 2017). On addressing the key issue of the ship maneuvering model, Xu et al. developed a data-driven controller with the combination of Gaussian Process (GP) and Model Predictive controller (MPC) achieving good generalization ability and robustness (Peilong et al., 2023). The data-driven technique was also adopted in a smart irrigation scheduling for monitoring soil moisture content in real-world tomato farming. The study considered rainfall, evaporation, and irrigation as inputs and soil moisture content as output making it a Multi Input Single Output (MISO) system (Erion et al., 2023). For a nonlinear nonaffine system a data drive optimal control scheme was proposed by Lin et al., (2023). that enhanced the controller performance by introducing an outer set-point updating loop (Na et al., 2023).

Some of the prominent data-driven techniques are discussed here. The technique originated with the Ziegler-Nichols technique that assumed zero initial condition and step responses (Ivan and Paolo, 2008). Later, it was advanced and named as an unfalsified control technique that could identify the control laws (Safonov and Tsao, 1997). This technique recursively falsifies the controller that fails to achieve the desired performance even with the measured data and specified control law. Similarly, Wang et al., 2007 reported a method named Minimum Variance Control (MVC) for multirate systems that adopted a data-driven approach. Iterative Feedback Tuning (IFT) is one such kind wherein it uses the closed loop data for tuning the controller parameters (Hjalmarsson and Birkeland, 1998). The next technique named Virtual Reference Feedback Tuning (VRFT) does not even require parameter initiation nor iterations and specific experiments to design a controller (Campi et al., 2002). Continuation to the above technique, Correlation-based Tuning (CbT) is another type wherein it minimizes the correlation function between closed-loop error and reference signal (Karimi et al., 2007). To overcome the high cost of train control model validations Yin et al., (2019) developed three data-driven model approaches namely Linear regression-based Model (LAM), Nonlinear regression-based Model (NRM), and Deep Neural Network (DNN) based model that used real-world field data from Beijing Metro (Jiateng et al., 2020).

The data-driven approach provided an opportunity for wastewater treatment industries to explore and improve their operations. Various studies were reported based on specific problem statements like energy optimization, coagulant dosages, pH neutralization, process control, management of wastewater - stormwater network and plant monitoring-decision making, etc. A detailed discussion on this topic is presented in Table 2.4. To the best of the authors' knowledge, there have been limited reported studies regarding data-driven approaches to centralized controller design for ASP systems. This approach can attract many researchers who tend to avoid advancement in the research due to the complexity of mathematical modeling techniques.

Table 2.4: Literature review on Data driven WWTP control

Sl. No.	Description – Work done	Remarks	Reference
1.	- Data-driven modelling to support WWTP operation. - Redundant measurement were created and then replaced with existing sensor. - Four different modelling techniques generalized least squares regression, artificial neural networks, self-organizing maps and random forests.	- Presented a procedure to build software sensor based on sensor data available. - Data from SCADA system of the real plant. - Cost effective.	D. J. Durrenmatt et al., (2012)
2.	- Data-driven adaptive optimal controller (DDAOC). - Adaptive dynamical programming. - BSM1.	- Solve optimization problem. - Saving energy. - Target variables $S_{O,5}$ and $S_{NO,2}$.	Qiao et al., (2013)
3.	- k-nearest neighbour (k-NN) method. - Optimized based on the root mean square error. - Influent water qualities Mean absolute percentage error (MAPE).	- Predict the influent flow rate and COD, SS, T-N, T-P. - Both wet and dry weather conditions.	Minsoo et al., (2016)
4.	- Data-driven intelligent monitoring system - Fuzzy neural network (FNN) is applied for designing the soft sensor model, - Principal component analysis (PCA) method is used to select the input variables.	- Combination of data-driven soft sensor and data distribution service - Real-time values of key variables - Tested on several real plants - A hybrid data transfer software insert soft sensor tech. to SCADA.	Han et al., (2018)
5.	- Stochastic optimization algorithm and unidimensional search algorithm used for optimization. - 5 Strategies.	- Remove organic substances and nitrogen. - Control of DO concentration. - PI type controllers.	Luca et al., (2019)
6.	- Data-driven energy optimization strategy of WWTP variable-frequency pumps. - Method combines statistical learning and deep reinforcement learning. - RL control method with data-mining algorithms.	- Designed predictive pump control policies. - Decrease in electrical energy consumption through continuous learning and self-adaptation.	Filipe et al., (2019)
7.	- A data driven decision making method to reduce the membrane fouling. - Self-organizing deep belief network prediction method. - Independent component analysis-principal component analysis technique for multi warning. - Kernel function diagnoses method.	- Long term and multi-step perdition strategy. - Predict membrane permeability. - Diagnose the accurate influencing parameter. - Can extract Gaussian and non-Gaussian information.	Han et al., (2020)

Sl. No.	Description – Work done	Remarks	Reference
8.	- Data-driven and feature based framework. - CART classifier decision tree is used to classify the operation model. - Infrastructure data of Austin Texas pumping system in 2017.	- Improved performance of wastewater management and pumping system. - Minimized the outflow rate to prevent the system from pipe leakage.	Rahimian et al., (2020)
9.	- Sampling approaches. - Two conventional monitoring method. - Multivariate change point detection was applied to identify structural changes in the variables.	- Accurate and efficient method. - Reduce N_2O sampling frequency. - Predict the risk of excess emission.	Vasilaki et al., (2020)
10.	- Calculate predictive controller parameters using subspace. - Identification technique. - Receding window Mechanism. - Direct adaptive model predictive control (DAMPC).	- Direct identification of controller parameters. - Indirect adaptive model-based predictive controller (IAMBPC). - SVD-based optimisation technique.	Razali et al., (2020)
11.	- Data-driven multiobjective predictive control (MOPC). - Adaptive fuzzy neural network identifier to obtain the nonlinear behaviours. - Transfer multiobjective optimization algorithm (TMOOA) to obtain the optimal solutions.	- Multiobjective control strategy. - Improve the operation performance. - Fast control actions of MOPC.	Han et al., (2020)
12.	- Hybrid influent forecasting model based on multimodal and ensemble-based deep learning (ME-DeepL). - Hilbert–Huang transform (HHT) method to identify intrinsic and distinct temporal patterns.	- Forecast the fluctuating influent loads on long-term and short-term with multisteps forecast horizons. - Validated with nine years influent data from a full-scale MBR in Korea.	Heo et al., (2021)
13.	- Data-driven methods based on deep-learning algorithms to process modelling, process analysis, and process forecasting. - Global sensitivity analysis to understand emission characteristics and crucial influencing parameters.	- Plant data driven model coupled with DNN. - Temperature was important factor - Forecasting of dynamic N_2O behaviour.	Soonho et al., (2021)
14.	- Data-driven optimization model. - Combination of genetic algorithm-based optimization and particle swarm optimization technique. - Regression model analyses.	- Optimize coagulant dosage decision in industrial WWT. - Cu removal based on real data. - Lowered cost of the chemicals and sludge treatment.	Wang et al., (2021)

Sl. No.	Description – Work done	Remarks	Reference
15.	- Data-driven strategy consisting of t-distributed stochastic 38 neighbour embedding (t-SNE) and deep neural networks to optimize the processes configuration. - DNNs trained by the classified cluster data from t-SNE.	- 14,647 samples from 10 full-scale WWTPs. - Relationships between key parameters. and configuration of WWTPs - High accuracy.	Xu et al., (2021)
16.	- Data-driven robust model predictive control (DRMPC) method. - Interval type-2 fuzzy neural network (IT2FNN) is used to identify dynamic behaviour of WWTP (predictive model).	- Disturbances are considered. - Robust stability controller to reduce influence of disturbance. - Combining the advantage of fuzzy systems and neural networks.	Han et al., (2022)
17.	- A data driven approach combination of hydraulic modelling and Gaussian processes. - Gaussian process-based predictive control tool. - Uncertainty assessment.	- Aims to reduce the cost of infrastructure expansion - Proposes a combined framework for wastewater and storm water - Tested controller performance with laboratory setup.	K. M. Balla et al., (2022)
18.	- Improved model-free adaptive predictive control scheme - Monte Carlo experiment based multi-parameter sensitivity analysis and hybrid intelligent optimization. - BIBO method to stability check.	- Control the nitrate concentration and dissolved oxygen Concentration. - Sunny days, rainy days and rainstorm days.	Zhang et al., (2022)
19.	- Control of neutralization processes. - Four models - RF, ANN, XGBoost, and KNN exhibited high accuracy. - The cross-validation technique prevented overfitting problems. - Grid search technique importance of tuning hyperparameters.	- Machine learning (ML) models (8). - pH prediction and lime dosage control. - Sensitivity analysis importance of temperature, valve position, and upstream pH.	Xu et al., (2022)
20.	- Mechanism model and data-driven model (ASM model and an ANN Model) are combined. - MLP regression model for online intelligent management.	- Optimize operation strategies. - Complete plan library with 2134 plans. - Less labour, energy and chemicals costs, and higher efficiency and stability.	Wang et al., (2023)
21.	- Intelligent control method with tracking goal representation heuristic dynamic programming. - Data driven model network. - Classical actor-critic scheme in RL.	- Applied in two industrial simulations. - Good performance in tracking both constant and dynamic trajectories. - Theory holds good for robot control and power grid system.	Wang et al., (2023)

2.5 Summary of Literature Review

As a result of rapid urbanization, the implementation of wastewater treatment plants (WWTP) in urban areas has become necessary to protect the environment and address water management challenges. Typically, the conventional biological treatment system, such as the Activated Sludge Process, is chosen as the most effective technique for treating domestic wastewater (sometimes in combination with industrial wastewater), despite its initial investment and maintenance costs. However, the discharge of organic pollutants into receiving water bodies can lead to a sudden decrease in dissolved oxygen (DO) concentration, thereby diminishing the self-purification properties of water.

Organic effluent generally contains a significant amount of suspended and settleable solids, which can alter both the water and reservoir bed characteristics. Additionally, these impurities obstruct sunlight from reaching the bottom surface of the reservoir, resulting in water pollution through eutrophication. Existing literature emphasizes the crucial need to constantly monitor and control effluent characteristics such as DO concentration, biomass, and substrate concentration. Aeration rate, which affects the DO level in wastewater, and recycle sludge (concentration and flow rate) directly influence these parameters.

The mathematical identification of WWTP models is a critical step in studying model parameters and control strategies. This process involves using measured data and statistical methods to build a mathematical model of the dynamic system. To ensure the economical, reliable, and efficient operation of WWTPs, it is imperative to control physical, chemical, and biological parameters. However, due to the multitude of variables and the multivariable nature of biological wastewater treatment, designing a controller for such a complex system is challenging. Various studies have explored different controllers and design techniques based on specific objectives.

Developing an accurate control strategy requires a comprehensive understanding of process behavior, which improves effluent quality while reducing energy consumption. Unregulated aeration rates have been a significant contributing factor to the escalating operating costs of WWTPs. Similarly, controlling the biomass concentration in recycle flow represents the optimal method for organic matter removal in wastewater. Moreover, surveys suggest that a data-driven approach can be adopted to overcome the difficulties and time constraints associated with developing a mathematical model for a plant.

To the best of our knowledge, there are no openly available resources reporting a comprehensive study on mathematical model identification and the design of centralized and decentralized controllers, along with the implementation of a data-driven approach for the activated sludge process.

Chapter 3

SYSTEM DESCRIPTION AND PRELIMINARIES

3.1 Activated Sludge Process Model

The wastewater treatment plant that treats wastewater from both municipalities and industries with soluble organic impurities adopts physical, chemical, and biological zones or stages of treatment, except in a few objectively specific plants. Among these three stages, biological treatment is an integral and important part of any treatment plant. The main reason for this would be due to economic advantages, both in terms of operating costs and initial capital costs. Hence, the modeling, control, and optimization of biological wastewater treatment systems have gained a lot of significance due to stringent effluent norms during the last few decades (Ilse et al., 2003a).

A task group from International Association on Water Quality (IAWQ) worked upon two goals, firstly to review the existing models and, secondly, to formulate the simplest biological wastewater treatment plant model that can predict realistic process variables related to single sludge systems for carbon oxidation, nitrification, and denitrification. In 1987 it got completed, and later it was renamed Activated Sludge Model No. 1. (ASM1) (Henze et al., 2006).

A set of ordinary differential equations from ASM1 is given below. The three processes that affect heterotrophic biomass concentration are aerobic growth, anoxic growth, and decay.

$$\frac{dX_{B,H}}{dt} = \hat{\mu}_H \frac{S_S}{K_S + S_S} \frac{S_O}{K_{O,H} + S_O} X_{B.H} + \eta_g \hat{\mu}_H \frac{S_S}{K_S + S_S} \frac{K_{O,H}}{K_{O,H} + S_O} \frac{S_{N,O}}{K_{NO} + S_{NO}} X_{B,H} - b_H X_{B,H} \tag{3.1}$$

Autotrophic biomass concentration will be less complex to formulate since they do not grow in an anoxic environment.

$$\frac{dX_{B,A}}{dt} = \hat{\mu}_A \frac{S_{NH}}{K_{NH}+S_{NH}} \frac{S_O}{K_{O,A}+S_O} X_{B,A} - b_A X_{B,A} \tag{3.2}$$

As heterotrophic bacteria increase, one can observe a decrease in biodegradable substrate concentration. But it eventually increased by hydrolysis of slowly biodegradable substrate.

$$\begin{aligned}\frac{dS_S}{dt} = \Bigg[&-\frac{\hat{\mu}_H}{Y_H}\left(\frac{S_S}{K_S+S_S}\right)\left\{\left(\frac{S_O}{K_{O,H}+S_O}\right)+\eta_g\left(\frac{K_{O,H}}{K_{O,H}+S_O}\right)\left(\frac{S_{NO}}{K_{NO}+S_{NO}}\right)\right\} \\ &+k_h \frac{X_S/X_{B,H}}{K_X+(X_S/X_{B,H})}\left\{\left(\frac{S_O}{K_{O,H}+S_O}\right)+\eta_h\left(\frac{K_{O,H}}{K_{O,H}+S_O}\right)\left(\frac{S_{NO}}{K_{NO}+S_{NO}}\right)\right\}\Bigg] X_{B,H}\end{aligned} \tag{3.3}$$

According to the death-regeneration hypothesis, the concentration of slowly biodegradable substrate is increased by recycling dead bacteria but decreases with hydrolysis, as given below

$$\begin{aligned}\frac{dX_S}{dt} = (1-f_p)(b_H X_{B,H}+b_A X_{B,A}) - k_h \frac{X_S/X_{B,H}}{K_X+(X_S/X_{B,H})}\Bigg[\left(\frac{S_O}{K_{O,H}+S_O}\right)+ \\ \eta_h\left(\frac{K_{O,H}}{K_{O,H}+S_O}\right)\left(\frac{S_{NO}}{K_{NO}+S_{NO}}\right)\Bigg] X_{B,H}\end{aligned} \tag{3.4}$$

The simplest form of all is the concentration of inert particulate products from biomass decay.

$$\frac{dX_P}{dt} = f_p(b_H X_{B,H} + b_A X_{B,A}) \tag{3.5}$$

As biomass decays, the concentration of particulate organic nitrogen increases and decease by hydrolysis.

$$\begin{aligned}\frac{dX_{ND}}{dt} = (i_{XB}-f_P i_{XP})(b_H X_{B,H}+b_A X_{B,A}) - k_h \frac{X_N D/X_{B,H}}{K_X+(X_S/X_{B,H})}\Bigg[\left(\frac{S_O}{K_{O,H}+S_O}\right) \\ +\eta_h\left(\frac{K_{O,H}}{K_{O,H}+S_O}\right)\left(\frac{S_{NO}}{K_{NO}+S_{NO}}\right)\Bigg] X_{B,H}\end{aligned} \tag{3.6}$$

Both the Ammonification and hydrolysis process impacts the concentration of soluble organic nitrogen.

$$\begin{aligned}\frac{dS_{ND}}{dt} = \Bigg[-k_a S_{ND} + k_h \frac{X_{ND}/X_{B,H}}{K_X+(X_S/X_{B,H})}\Bigg\{\left(\frac{S_O}{K_{O,H}+S_O}\right)+ \\ \eta_h\left(\frac{K_{O,H}}{K_{O,H}+S_O}\right)\left(\frac{S_{NO}}{K_{NO}+S_{NO}}\right)\Bigg\}\Bigg] X_{B,H}\end{aligned} \tag{3.7}$$

A complex differential equation is formulated for ammonia concentration as it is affected by all microorganisms and decreased by the nitrification process.

$$\frac{dS_{NH}}{dt} = \Bigg[-i_{XB}\hat{\mu}_H \left(\frac{S_S}{K_S+S_S}\right)\left\{\left(\frac{S_O}{K_{O,H}+S_O}\right)+\eta_g\left(\frac{K_{O,H}}{K_{O,H}+S_O}\right)\left(\frac{S_{NO}}{K_{NO}+S_{NO}}\right)\right\} \\ +k_a S_{ND}\Bigg] X_{B,H} - \hat{\mu}_A\left(i_{XB}+\frac{1}{Y_A}\right)\left(\frac{S_{NH}}{K_{NH}+S_{NH}}\right)\left(\frac{S_O}{K_{O,A}+S_O}\right)X_{B,A} \quad (3.8)$$

The direct influence of nitrification and denitrification is observed in the concentration of nitrate as shown below

$$\frac{dS_{N0}}{dt} = -\hat{\mu}_H\eta_g\left(\frac{1-Y_H}{2.86Y_H}\right)\left(\frac{S_S}{K_S+S_S}\right)\left(\frac{K_{O,H}}{K_{O,H}+S_O}\right)\left(\frac{S_{NO}}{K_{NO}+S_{NO}}\right)X_{B,H} + \\ -\frac{\hat{\mu}_A}{Y_A}\left(\frac{S_{NH}}{K_{NH}+S_{NH}}\right)\left(\frac{S_O}{K_{O,A}+S_O}\right)X_{B,A} \quad (3.9)$$

Finally, the growth of heterotrophic and autotrophic biomass will directly influence the oxygen concentration in the wastewater.

$$\frac{dS_0}{dt} = -\hat{\mu}_H\left(\frac{1-Y_H}{Y_H}\right)\left(\frac{S_S}{K_S+S_S}\right)\left(\frac{S_O}{K_{O,H}+S_O}\right)X_{B,H} \\ -\hat{\mu}_A\left(\frac{4.57-Y_A}{Y_A}\right)\left(\frac{S_{NH}}{K_{NH}+S_{NH}}\right)\left(\frac{S_O}{K_{O,A}+S_O}\right)X_{B,A} \quad (3.10)$$

Two numerical values, 2.86 and 4.57, are stoichiometric expressions for the anoxic growth of heterotrophic biomass and stoichiometric expression for the aerobic growth of autotrophs. The parameter notations and kinetic parameters are given in Table 3.1. Keeping this classical model as a reference, four simplified model equations are formulated and used by a few of the researchers since a complete biological treatment stage model is not essential for control studies. By considering some of the assumptions, a set of complex ten equations from ASM1 is reduced to four nonlinear equations which were used for the current control studies.

The goal here is to develop a single-stage biological wastewater treatment plant mathematical model. A single-stage biological treatment plant consisting of one aeration unit and one settling tank unit is considered for the study (Figure. 3.1). Some of the sludge from the settling tank is recirculated back to the aeration or biological reactor unit, and the excess is discarded or sent for further utilization or treatment.

The mathematical model of the considered treatment stages will be comprised of a set of four non-linear differential equations (Nejjari et al., 1999). There is one biomass

Table 3.1 IAWQ model parameters (Henze et al., 2006)

Sl. No.	Description	Notation
	Stoichiometric parameters	
1.	Heterotrophic Yield	Y_H
2.	Autotrophic Yield	Y_A
3.	Fraction of biomass yielding particulate products	f_P
4.	Mass N/mass COD in biomass	i_{XB}
5.	Mass N/mass COD in products from biomass	i_{XP}
	Kinetic parameters	
6.	Heterotrophic max. specific growth rate	$\hat{\mu}_H$
7.	Heterotrophic decay rate	b_H
8.	Half-saturation coefficient for heterotrophs.	K_s
9.	Oxygen hsc for heterotrophs	$K_{O,H}$
10.	Nitrate hsc for denitrifying heterotrophs	K_{NO}
11.	Autrotrophic max. specific growth rate	$\hat{\mu}_A$
12.	Autotrophic decay rate	b_A
13.	Oxygen hsc for autotrophs	$K_{O,A}$
14.	Ammonia hsc for autotrophs	K_{NH}
15.	Correction factor for anoxic growth of heterotrophs	η_g
16.	Ammonification rate	k_a
17.	Max. specific hydrolysis rate	k_h
18.	Hsc. for hydrolysis of slowly biodegradable substrate	K_x
19.	Correction factor for anoxic hydrolysis	η_h

component, one substrate component, one dissolved oxygen component, and lastly one recycled sludge concentration. This WWTP model will be based on the First Engineering principle, so exclusively it can be referred to as the white box model (Krist et al., 2004). Accordingly, a few assumptions were considered while developing a mathematical model for WWTP as follows:

- The aeration tank is continuously stirred
- There are no biological reactions in settler
- Only the activated sludge is the recycled component back to the reactor
- Composition of the recycled sludge is neglected
- The flow rate of the reactor is the sum of the flow rate of recycle sludge and WWTP outlet flow

A simplified schematic representation of the ASP stages has been presented in Figure 3.1. The following set of non-linear equations is derived by adopting the mass balance calculations around the aerator and the settler.

The first equation is related to the material balance of the activated sludge from the aerated bioreactor:

$$\frac{dX(t)}{dt} = \mu(t)X(t) - D(t)(1+r)X(t) + rD(t)X_r(t) \tag{3.11}$$

The second equation describes the mass balance of the substrate:

$$\frac{dS(t)}{dt} = -\frac{\mu(t)}{Y}X(t) - D(t)(1+r)S(t) + D(t)S_{in} \tag{3.12}$$

The third equation represents the mass balance of the oxygen in water mass, the oxygen consumed in a biochemical degradation of the organic matter, and the oxygenation process:

$$\frac{dC(t)}{dt} = -\frac{K_o\mu(t)}{Y}X(t) - D(t)(1+r)C(t) + K_{La}(C_S - C(t)) + D(t)C_{in} \tag{3.13}$$

The last and fourth equation deals with the balance of activated sludge from the settling tank:

$$\frac{dX_r(t)}{dt} = D(t)(1+r)X(t) - D(t)(\beta + r)X_r(t) \tag{3.14}$$

where $X(t)$, $S(t)$, $C(t)$, and $X_r(t)$ are state variables representing biomass, substrate, dissolved oxygen concentration, and recycled biomass, respectively. $D(t)$ is the dilution rate. The ratio of recycled flow to influent flow and the ratio of waste flow to influent flow is denoted by r and β, respectively. C_{in} and S_{in} are the dissolved oxygen concentration and substrate concentration in the feed stream, respectively. Specific growth rate μ, and yield cell mass Y represents the kinetics of the cell mass production, the term k_o is constant, C_s represents maximum dissolved oxygen concentration, and oxygen mass transfer coefficient is indicated as K_{La}.

The specific growth rate (μ) is defined as the rate of increase of biomass of a cell population per unit of biomass concentration. Equation 3.15 describes the specific growth rate, which was developed by a series of experiments performed by Monod (NielsenJohn and Liden., 2003). The specific growth rate is the complex function of substrate concentration, dissolved oxygen concentration, pH, and other inhibitors that proclaim to have physicochemical and biological factors affecting it. It is one of the key parameters to describe biomass growth. There exists much analytical law for determining the specific growth rate, but the most commonly used is Monod kinetic Law.

A few assumptions like specific growth rate depends on the substrate, dissolved

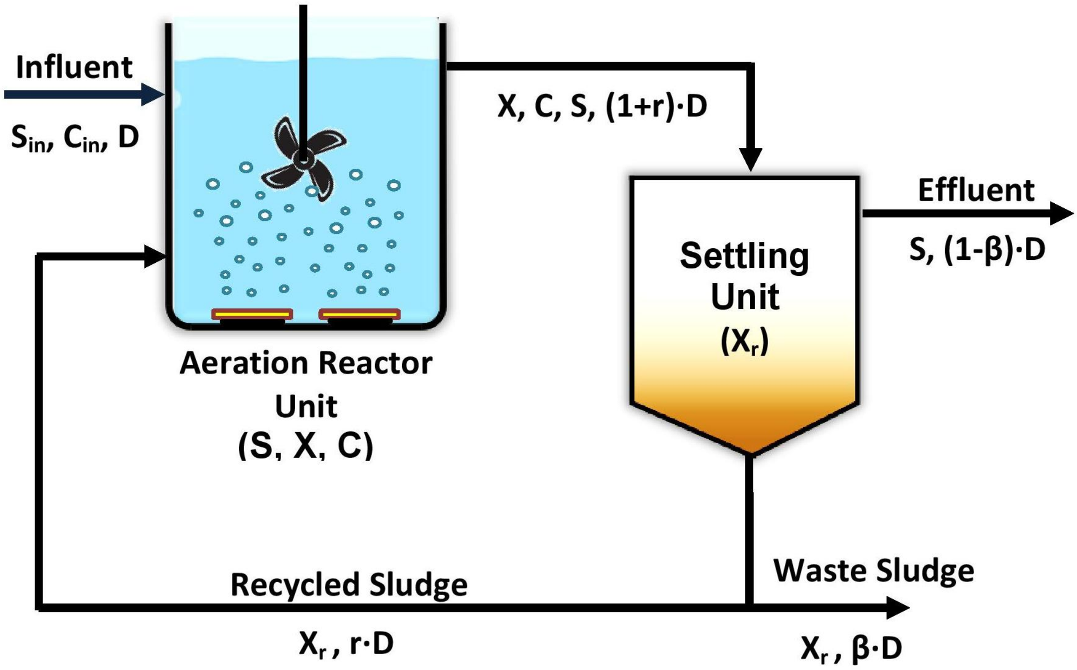

Figure 3.1 Schematic representation of single tank ASP unit

oxygen concentration, and several kinetic parameters, were made while developing the kinetic model, and it is given by

$$\mu(t) = \mu_{max} \frac{S(t)}{K_s + S(t)} \frac{C(t)}{K_c + C(t)} \tag{3.15}$$

Where μ_{max} is the maximum specific growth rate, affinity constant is represented as K_s, S is pollutant concentration and K_c is saturation constant. The major setback in modeling and control of these processes involves, online monitoring of key biological variables to develop an analytical expression for growth rate (Dimitrova and Krastanov, 2012). There exist several parameters in modeling the ASP system. Table 3.2 provides a list of parameters with values used for the modeling and simulations studies.

3.1.1 Model Identification

"Model Identification" refers to the process of developing a mathematical model that represents the behavior and dynamics of a particular system or process. This model is typically derived from data collected from the system or process under study. The purpose of model identification in process control is to understand and predict the behavior of the system, allowing control engineers to design effective control strategies.

Table 3.2 Model parameters of ASP (Muntean I. et al., 2015)

Sl. No.	Parameter	Notation	Value	Unit
1.	Influent dissolved oxygen concentration	C_{in}	0.5	mg/l
2.	Influent substrate concentration	S_{in}	600	mg/l
3.	Maximum dissolved oxygen concentration	C_s	10	mg/l
4.	Maximum specific growth rate	μ_{max}	0.0832	-
5.	The ratio of waste flow to influent flow	β	0.2	-
6.	The ratio of recycled flow to influent flow	r	0.8	-
7.	Biomass yield factor	Y	0.65	-
8.	Affinity constant	k_s	15	-
9.	Saturation constant	k_c	0.5	-
10.	Model constant	k_o	0.4	-
11.	Aeration rate	W	180	m^3/hr
12.	Oxygen transfer rate	σ	0.024	-
13.	Dilution rate	D(t)	0.8	-

The identified model can be used for simulation, analysis, and control algorithm design. Model identification approaches vary depending on the nature of the system and the available data. Some common approaches include: (i) System identification - It involves applying known input signals to the system and measuring the corresponding outputs. The collected input-output data is then used to estimate the system's mathematical model parameters, such as transfer functions or state-space representations. (ii) Regression analysis - This technique involves fitting mathematical models to data using regression algorithms. It can be useful when the system's underlying dynamics are not well-known or when specific models, such as linear regression or polynomial regression, are appropriate. (iii) Machine learning - Machine learning algorithms, such as neural networks, support vector machines, or decision trees, can be employed for model identification. These algorithms learn patterns and relationships from input-output data to construct models that can predict system behavior. (iv) Physical modeling - In some cases, prior knowledge about the system's physics or underlying principles can be used to develop a mathematical model. This approach involves formulating equations based on known physical laws and parameters.

The choice of model identification technique depends on the available data, system complexity, and the desired level of accuracy. It is often an iterative process involving data collection, model estimation, and model validation.

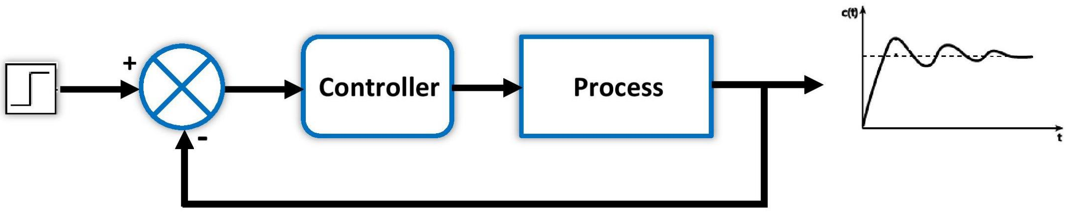

Figure 3.2 closed-loop system identification

A graphical representation of the closed-loop identification is presented in Figure 3.2. Two methods have been adopted to identify the model, namely the system identification method (Ljung and Singh, 2012; Kollar et al., 2006) and the Process Reaction Curve (PRC) method (Huang and Jeng, 2005; Sundaresan and Krishnaswamy, 1978; Chidambaram and C. Sankar, 2017; Prabhu Y. and Sankar, 2019). To solve these identification problems, the data are generated by simulating the above-mentioned nonlinear equations. A detailed procedure followed for both identification techniques is discussed below.

3.1.1.1 System Identification (SysId) to estimate FOPTD Model

System identification is a process of determining the mathematical model of a process in a system based on input-output data rather than its physics. The prime advantage of this approach is that a wide range of system dynamics can be handled without any prior awareness of the physical system (Soumya et al., 2019). In this study, a system identification matrix method is considered to obtain the accurate and simplest form of a dynamic model of the ASP system. Accordingly, the System Identification MATLAB toolbox was used to estimate the desired process parameters. This toolbox utilizes Hammerstein-Wiener and Nonlinear ARX models to estimate the nonlinear system dynamics.

Conventionally, it is widely and commonly chosen for grey box model identification. A step-by-step procedure followed in this technique is shown in Figure 3.3. The data is generated by choosing two inputs, namely, aeration rate and recycle sludge flow rate (manipulating variables), and two output parameters i.e., effluent dissolved oxygen concentration or biomass concentration and substrate concentration (controlled variables), are selected respectively. In order to obtain the model parameters in case-I,

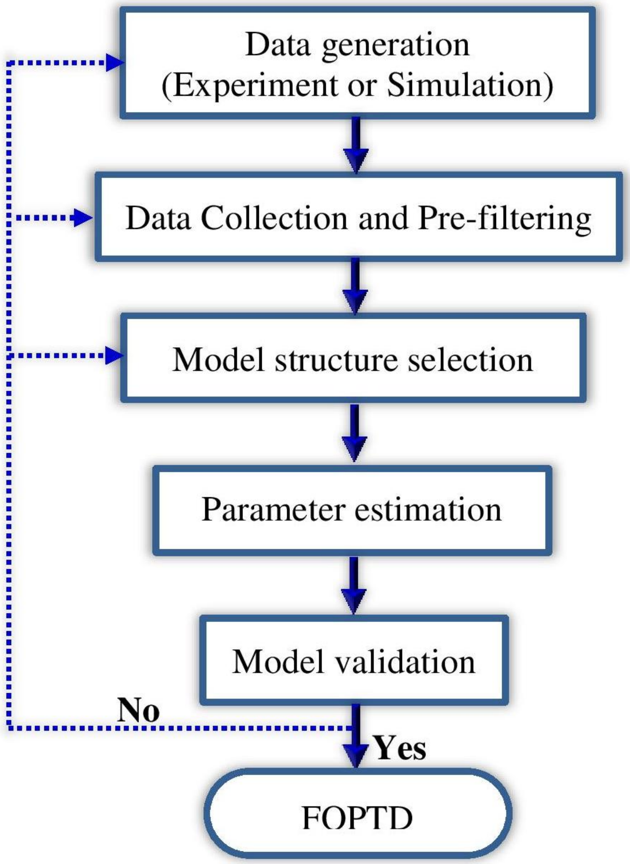

Figure 3.3 Flowchart of procedure for system identification technique

random noise is provided to aeration rate (W), the DO concentration and/or biomass concentration, and substrate concentration are noted down. Similarly, in case II, random noise is fed to recycle sludge flowrate (r), wherein DO concentration and substrate concentration values are recorded. Likewise, 1000 samples of input and output data sets are collected from open loop experiments on simplified WWTP, with a sampling time of 0.1s. Once the data is obtained, the model structure is selected based on the requirements. The Prediction Error Method (PEM) is used to determine the model parameters of the First-Order Plus Time Delay (FOPTD) system. In the final stage, the estimated model is validated by analyzing the curve fitting, aiming for the best fit, preferably close to 100% to conclude the process. If the fit is not satisfactory, the process may return to the data generation step to verify the data or to the data collection stage to re-filter the data. Alternatively, the model structure may be modified to achieve better model estimation.

3.1.1.2 Process Reaction Curve method

PRC is another classical method that is adopted to determine the FOPTD model (Chidambaram and C. Sankar, 2017). The controller gain, integral time, and derivative time are calculated from a process reaction curve which is generated from the step response of the open-loop system. To isolate the impact of controller action and process response, the study is carried out in an open-loop condition. The response of the process variables is recorded by providing a small stipulated disturbance. The process is allowed to reach the steady-state or close to the steady state while generating the process reaction curve.

The transient step responses of the process parameters are utilized to develop an open-loop identification method. The value of t_1 and t_2 are estimated based on the fraction responses $y_1 = 0.353 \triangle y_\infty$ and $y_2 = 0.853 \triangle y_\infty$ respectively from step response curve as shown in Figure 3.4. The generalized form of the FOPTD model and expressions for process gain (K_p), time constant (τ), and time delay (θ) is given by

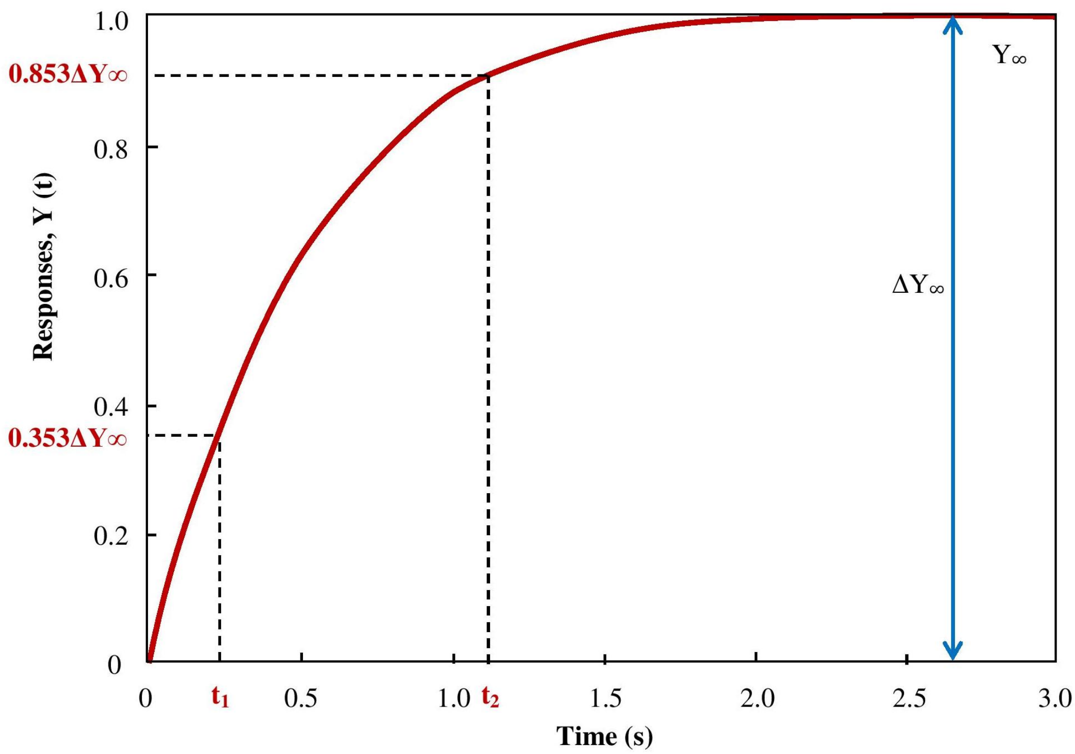

Figure 3.4 Typical process reaction curve

$$G_p(s) = \frac{K_p e^{\theta s}}{\tau s + 1} \tag{3.16}$$

$$K_p = \frac{\triangle Y_\infty}{\triangle U_\infty} \tag{3.17}$$

$$\tau = 0.67(t_2 - t_1) \tag{3.18}$$

$$\theta = 1.3t_1 - 0.29t_2 \tag{3.19}$$

3.2 Wastewater Treatment Plant Control

The objective of multivariable control includes maintaining several controlled variables at independent set points. It mainly depends on the goals of the entire plant and the design of associated equipment. It requires a more complex analysis to control the MIMO systems than that of the SISO system.

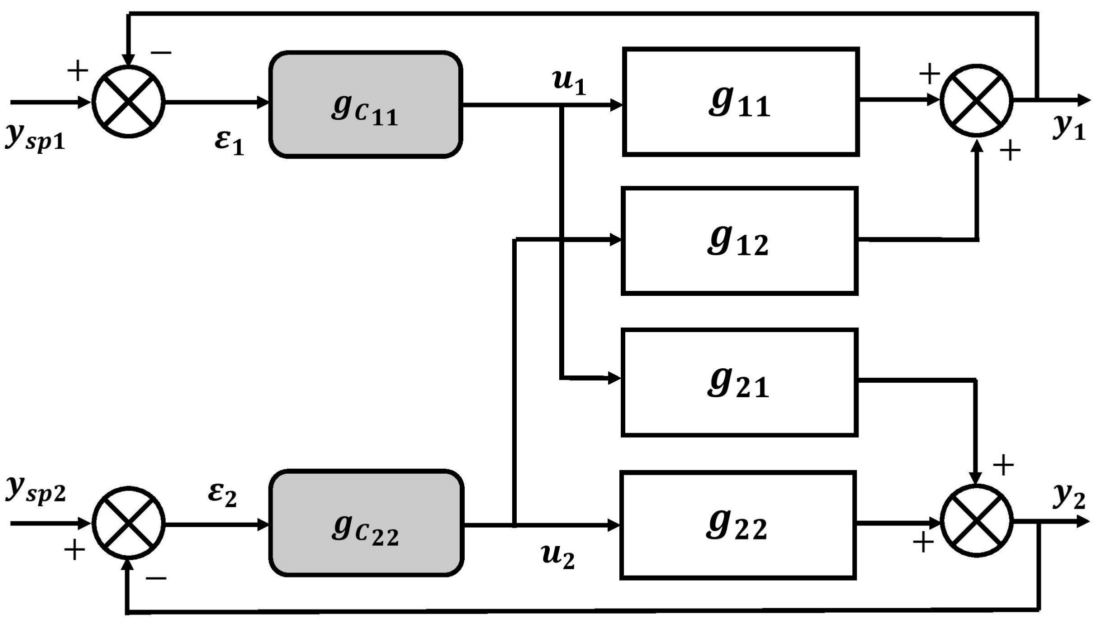

Figure 3.5 Decentralized controller for Two Input and Two Output System (TITO)

The controllers that are widely used are centralized controllers, decentralized controllers, and decouplers. In a decentralized control system, there are only n controllers for n output variables, as shown in Figure 3.5. In the case of a centralized controller for n output variables, there prevails n^2 number of controllers (Figure. 3.6). If there exist two inputs variables, namely u_1 and u_2, and, two outputs variables, namely y_1 and

y_2, then the change in input variable u_1 directly influences output y_1, meanwhile it also indirectly has an impact on output y_2, similarly change in input u_2 directly has an impact on y_2, but also has an indirect influence on output y_1. This condition prevails due to the interaction between the process variables. If the interaction between the loops is moderate or less, the decentralized control system works well; however, they fail if there are more interactions between the loops. Since the decentralized system involves interaction, it can be estimated by the RGA index and Niederlinski method by paring the manipulated and control variables for a stable system. By virtue of its simplicity and the potential to achieve failure tolerance, the decentralized controller has been adopted by most of the process industries (Su et al., 2006).

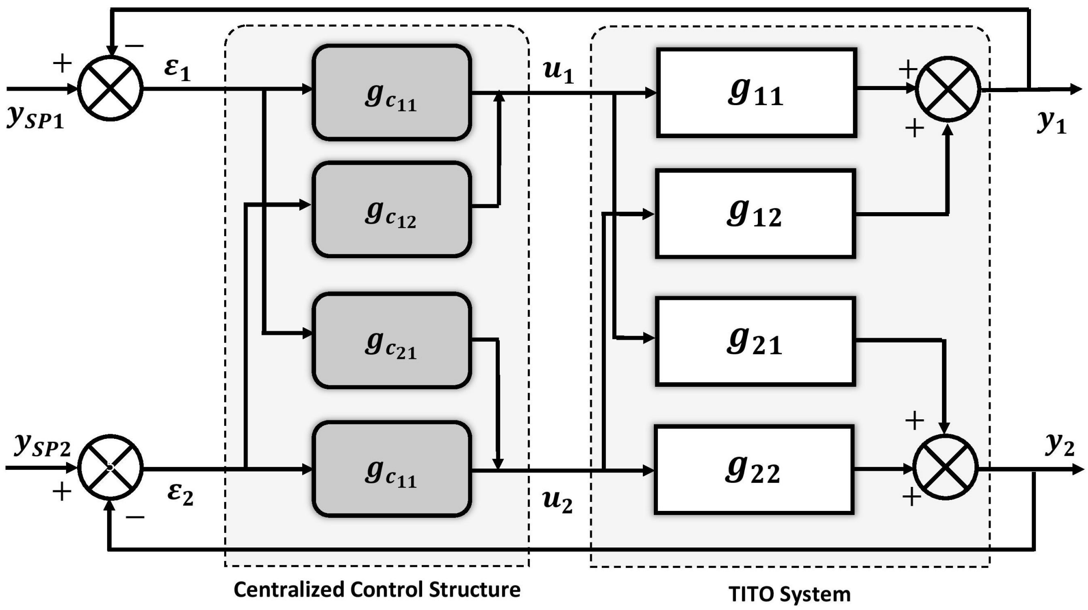

Figure 3.6 Centralized controller for Two Input and Two Output System (TITO)

A decoupler controller structure for a Two-Input Two-Output (TITO) system is depicted in Figure 3.7. It demonstrates the distinct nature of decoupler controllers, which effectively account for the interactions within the MIMO (Multiple-Input Multiple-Output) process compared to decentralized controllers. The design of a decoupler controller involves the utilization of a co-factor matrix, which converts a multivariable process into multiple single loops. By introducing a simplified decoupler matrix into the process model, the multi-loop system is decoupled or transformed into an equivalent set of independent single loops. Subsequently, through an appropriate model reduction technique, the resulting decoupled process model can be approximated as either a First-Order Plus Time Delay (FOPTD) or Second-Order Plus Time Delay (SOPTD) model (Rajapandiyan and Chidambaram, 2012b).

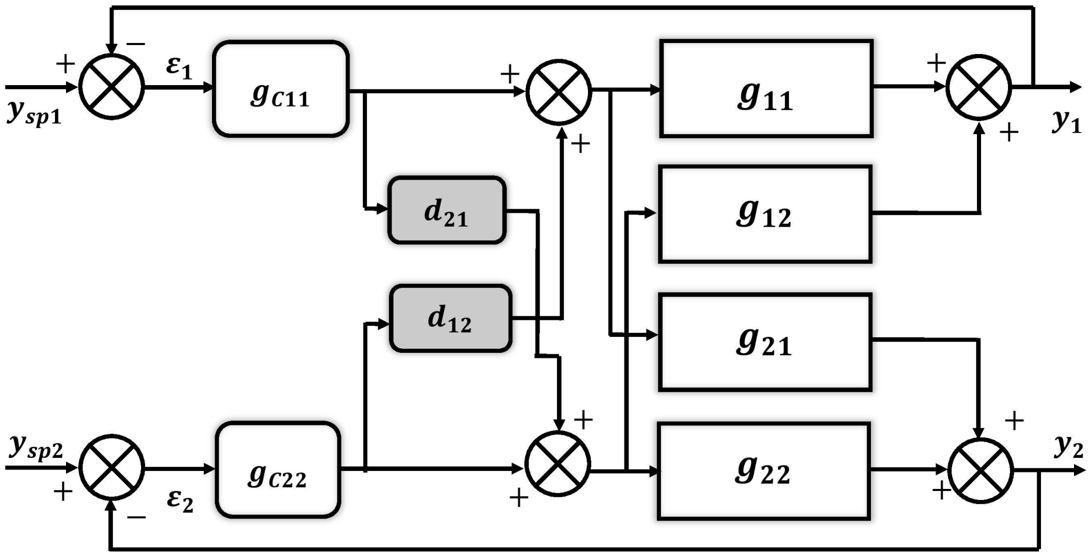

Figure 3.7 Decoupler controller structure for Two Input and Two Output System (TITO)

The PI controller is widely used in industrial applications due to its established position in control theory, taking into account both its advantages and limitations. One of the key benefits of a PI controller is its ability to reduce both the rise time and steady-state errors of a system. Additionally, a PI controller is resilient against measurement channel interference and can achieve zero control error. In the case of nonlinear systems, it is recommended to develop robust PI controllers with uncertainty parameters for improved performance (Aranovskiy et al., 2016). Given that wastewater treatment plants often encounter large disturbances during operations, a PI controller can significantly reduce both disturbances and noise. Moreover, the design process for a PI controller is less burdensome compared to advanced controllers, which tend to be more complex and time-consuming in simulations. In practical implementation, PI controllers are easily applicable since they can operate at lower switching frequencies compared to nonlinear controllers with higher switching frequencies. The use of a PI controller results in better setpoint tracking and reduces unnecessary wear and tear on the instrumentation setup. Hence, for the present study, the PI controller was chosen as the preferred option.

3.3 Performance evaluation

Time Integral Errors (TIE) are used for evaluating the performance of the decentralized and decoupler systems. The three commonly used measures are Integrated Time Absolute Error (ITAE), Integrated Absolute Error (IAE), and Integrated Square Methods (ISE).

$$ITAE = \int_0^\infty t|e(t)|dt \tag{3.20}$$

Integrates the absolute error over time. Compared to the ISE response system, IAE tends to produce a slower response.

$$IAE = \int_0^\infty |e(t)|dt \tag{3.21}$$

ISE integrates the square of the error over time. Using the ISE method in control systems will tend to eliminate large errors quickly, but will tolerate small errors persisting for longer periods.

$$ISE = \int_0^\infty e^2(t)dt \tag{3.22}$$

The best control system can be designed using any of these three mentioned criteria. Total Variance (TV) is defined as

$$TV = \sum_{i=1}^{\infty} |u_i - u_{i-1}|, \tag{3.23}$$

The principle purpose of estimating the TV is to measure the total variance in the controller output signal, which describes the performance criteria through the response of a closed loop. As explained by (Chandra and Chidambaram, 2018), TV is obtained by calculating the total sum of all its moves up and down by manipulating variables. The lesser the value of the TV gives better the result in the form of smoothness of the designed control system

3.4 Robustness Performance

3.4.1 Robust Stability Analysis

The designed control system is said to be robust only if it is insensitive to the difference caused by the actual system and model of the system. This difference is also referred to as model uncertainty. There can be several reasons for the origin of uncertainty. For instance; parameters that are only approximately known, variation of parameters due to non-linearity or change in operating condition, inaccuracy in the measurement device, neglected dynamics, etc. are a few reasons (Maciejowski, 1989). In order to obtain an effective working control system, the sensitivity of the system should not vary much to small changes during the processes. The robustness study becomes important when the parameters containing uncertainties exist in a Multi-loop control system. It is obvious that the MIMO system will experience a larger sensitivity to uncertainty than the SISO system. If there prevails the following condition, then it can be concluded that the system is stable (Chandra and Chidambaram, 2018).

$$||\Delta_I(j\omega)|| < \frac{1}{\sigma_I} \tag{3.24}$$

where σ_I is maximum singular value of following closed loop system $[I + G_c(j\omega)G(j\omega)]^{-1}G_c(j\omega)G(j\omega)]$ Similarly for output multiplicative uncertainty, $G(s)[I + \Delta_o(s)$, if it satisfies the following condition then the closed loop system is stable

$$||\Delta_o(j\omega)|| < \frac{1}{\sigma_o} \tag{3.25}$$

where $\Delta_I(s)$ and $\Delta_o(s)$ are stable, σ_o is maximum singular value of closed loop system

$$[I + G(j\omega)G_c(j\omega)]^{-1}G(j\omega)G_c(j\omega)]. \tag{3.26}$$

A plot is obtained for estimated uncertainties in terms of inverse maximum singular values and frequency. The characteristics of robustness can be evaluated by calculating the area under the curve. The more area under the curve, the more the system will be robust. This method can be utilized for comparing different control settings and their robustness.

3.4.2 Worst-case gain analysis

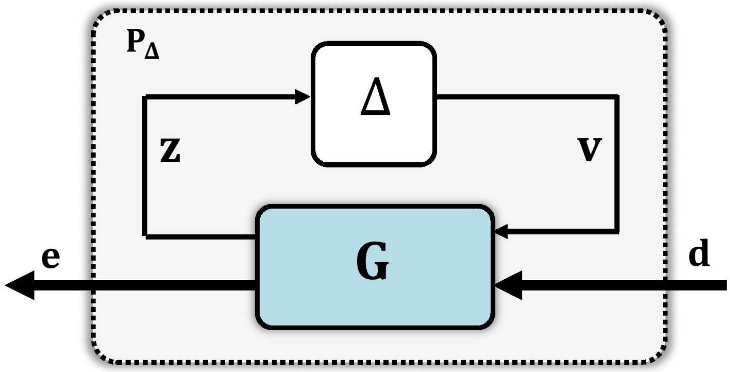

Figure 3.8 Uncertain system interconnection

Figure 3.8 illustrates the block diagram of a stable MIMO linear time-invariant system $G(s)$ and secured dynamic uncertainty $\Delta(s)$. The uncertain system can be given as

$$P_{\Delta}(s) = \digamma_U(G(s), \Delta(s) \tag{3.27}$$

Where dynamic uncertainty is structured and unit-bounded as

$$\Delta := diag(\Delta_1(s), ...\Delta_{N_b}(s)), \Delta_i(s)\, is\, LTI,\; ||\Delta_i(s)||_{\infty} \leq 1, i = 1, ..., N_b \tag{3.28}$$

Since $\Delta_i(s)$ is a MIMO system it has a dimension of $r_i \times c_i$. Worst-case gain is defined as the maximum induced gain upon a set uncertain system. Mathematically,

$$\hat{\gamma} = \max_{\Delta\, \varepsilon\, \mathbf{\Delta}} ||\digamma_U(G(s), \Delta(s))||_{\infty} \tag{3.29}$$

From Figure 3.8 is to be assumed that $P_{\Delta}(s)$ will be robustly stable for all the conditions of $\Delta(s)$ which implies $\hat{\gamma} < \infty$. Here peak gain (γ) at frequency ω of $P_{\Delta}(s)$ is estimated as

$$\gamma = \max_{Q\, \varepsilon\, \vartheta} \bar{\sigma}(\digamma_U(G(j\omega), Q)) \tag{3.30}$$

wherein, the unit norm bounded complex uncertainty for the set of blocked structured is given by

$$\vartheta := diag(_1, ..., Q_{N_b}), Q_i\, \varepsilon\, C^{r_i \times c_i}, \bar{\sigma}(Q_i = 1, rank(Q_i) = 1, i = 1, ..., N_b \tag{3.31}$$

For further details regarding the single-frequency interpolation, kindly refer to the following articles (Patartics et al., 2020, 2023).

In process control, robust control techniques are employed to ensure the stability and performance of a control system in the presence of uncertainties and disturbances. Worst-case gain analysis is one of the methods used to assess the robustness of a control system. The worst-case gain analysis involves evaluating the maximum gain of the uncertain system over a range of possible uncertain parameters (Patartics et al., 2020). The goal is to determine the maximum amplification of disturbances or uncertainties that the control system can tolerate while remaining stable and providing satisfactory performance. The worst-case gain analysis is performed by following the below steps.

- **Define the uncertainty**: Identify the uncertain parameters or disturbances that can affect the system performance. These uncertainties can include variations in process dynamics, model uncertainties, measurement noise, or external disturbances.

- **Formulate the uncertainty set:** Create a set of possible values or ranges for the uncertain parameters. This set represents the uncertainty that the control system needs to handle.

- **Perform worst-case gain analysis:** Evaluate the system's closed-loop transfer function for the entire uncertainty set. Determine the maximum gain (worst-case gain) over this set that can be tolerated while maintaining stability.

- **Assess performance and robustness:** Analyze the closed-loop system's performance with respect to the worst-case gain. Evaluate whether the system meets the desired performance specifications under the worst-case conditions.

- **Iterate and refine:** If the worst-case gain exceeds acceptable limits or the desired performance is not achieved, refine the controller design or modify the uncertainty set. Repeat the analysis until satisfactory robustness and performance are achieved.

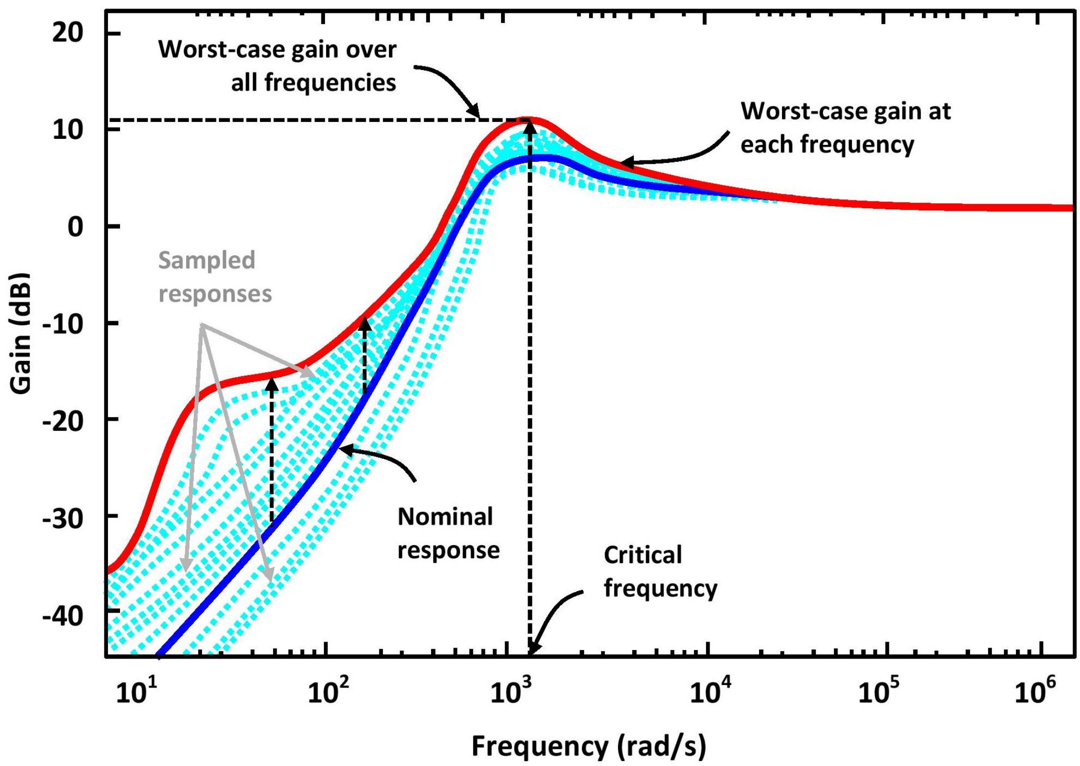

Figure 3.9 Generalized representation of worst-case gain analysis

By performing worst-case gain analysis, one can ensure that the control system remains stable and performs adequately even in the presence of uncertainties and disturbances. It allows for the quantification of robustness and provides insights into the system's sensitivity to various sources of uncertainty, helping to enhance the reliability and performance of the control system.

Figure 3.9 depicts the magnitude of the frequency response for specific systems. The critical frequency corresponds to the frequency at which the worst-case gain occurs among all frequencies. The nominal curves are represented by the blue curve, while the red curve indicates the worst-case gain curve at each frequency. Additionally, the light blue curve represents various sampled responses of the system. This analysis encompasses both dynamic uncertainty, which represents assumed or neglected modeled uncertainty, and parametric uncertainty, which accounts for inaccuracies in physical parameters. The worst-case gain method is highly valuable for assessing the robustness of uncertain systems.

Chapter 4

DECENTRALIZED CONTROLLER DESIGN FOR AN ASP

This chapter begins with an introduction to the multivariable processes, controller configurations with various tuning methods, and the process upon which this study is oriented. The next section presents a detailed approach to the reader about the decentralized controller, the reason and conditions for the best pairing, and the design of the decoupler exclusive with set-by-step flowcharts. The simulation results of the designed controller over the activated sludge process are given in the subsequent section followed by outcomes of robust stability analysis upon parametric uncertainty. And finally, the chapter concludes by summarizing the findings of this study on designing a decentralized and decoupled controller for the ASP system.

4.1 Introduction

Various controllers available in the open literature can be used to control multivariable systems. Some widely adopted controllers are decentralized controllers, centralized controllers, and decouplers. Since there is only n controller for each of n output variables, the decentralized controller becomes the most preferred over the centralized controller. In the case of the centralized controller for n output variables, there prevails n^2 number of controllers. The decentralized controller comprises n controllers for n output variables since single loop controllers or diagonal controllers are used in it. Perhaps, a fully multivariable centralized controller comprises $n \times n$ number of controllers since it is not a diagonal one. In addition, the centralized controllers are individually designed to ensure specified closed-loop performance for a set of operating conditions. If there are two input variables, namely u_1 and u_2, and two output variables, namely y_1 and y_2, then the change in input variable u_1 directly influences output y_1, while it also indirectly has an impact on output y_2, the change in input variable u_2 directly has an impact on y_2, but also has an indirect influence on output y_1. This condition prevails due to the interaction between the process variables. If the interaction between the loops is moderate or less, the decentralized control system works well; however, it fails if there are more interactions between the loops. By virtue of its simplicity and the potential to achieve failure tolerance, the decentralized controller has been adopted by most of the process industries (Su et al., 2006). Meanwhile, the decoupler uses a cofactor matrix of the process in the control loop so that multivariable processes are modified into several multiple single loops (Shen et al., 2010b; Jevtovic and Matausek, 2010). In short, each output variable can be influenced by only one reference signal by isolating loops through a reciprocal system. This allows the designer to tune the controller more tightly because detuning is no longer required to allow delayed effects of interactions. Often switching this can even yield better set point responses.

In most common cases, different process systems interact with one another, which means disturbances are caused among different control loops. This interaction among each loop is commonly faced with challenges in process industries. As discussed in the above sections, nowadays, these challenges are rectified by detuning less important loops so that important loops can achieve goop performance (Nordfeldt and Hagglund, 2006). Theoretically, this approach means one of the loops is made to interact poorly in order to make the other loop have good interaction results, but practically, this is far from optimal. A comprehensive study has been undertaken to know the interactions in control loops, thereby deriving different tuning factors for different classes of interactions. It is to be noted that a constant gain decoupler is always insufficient when it is expected to decouple feedback loops with relatively different dynamic properties (Schei, 1993). Hence, a simple decoupler can be designed for such types of challenges. In the case of full decoupling, it is essential to perform the robustness study for the decoupler to analyze the escalated sensitivity. Perhaps, the existence of significant differences in dynamic characteristics among transfer function elements, the decouple fail to give satisfactory performances (Shen et al., 2010b).

Even under various disturbances and control loop failures, it is been identified that the decentralized controllers will be intrinsically robust (Hanuma et al., 2014). The decentralized control system works well if interaction among the loops is moderate. If not, it is always suggested to opt for centralized controllers (Rajapandiyan and Chidambaram, 2012a). The pairing of controlled and manipulated variables plays a major role in achieving good efficiency for a decentralized control system (Hanuma et al., 2014). The task solved in a decentralized manner will always be easier for the design, implementation, and maintenance of the resulting control system (Teck and Min, 2001).

Since the decentralized system involves interaction, it can be estimated by the RGA index and the Niederlinski method by pairing the manipulated and control variables for a stable system. An optimal input-output pairing for a MIMO system can be achieved through an analytical tool named RGA. In other words, RGA describes the impact of each manipulating variable on the output variables. In its simplest form, it is a normalized form of a gain matrix. This can be obtained by taking the ratio of the open-loop gain to the closed-loop gain (V. Vijay et al., 2012). To overcome the limitations of the RGA method, an improvised version of RGA is proposed called RNGA. When compared with the RGA method, the RNGA method considers transient information along with process-steady state information. Similarly, the dynamic changes caused when all the loops are open and all the loops are closed are represented as the Relative Average Residence Time Array (RARTA). Another new approach proposed by Thomas McAvoy is named Dynamic Relative Normalized Gain Array (dRGA) considers the effect of process dynamics that employ a transfer function model instead of a steady state gain matrix to estimate RGA (Witcher, 1977). In dRGA, the denominator played a vital role in controlling parameters at all frequencies, whereas the numerator was simply an open-loop transfer function. However, dRGA is more difficult to calculate and understand by a control engineer due to its controller-dependent operations. The concepts of RGA, RNGA, and RARTA are adopted in order to obtain the ETF for higher-dimensional models. This ETF takes into account the loop interaction while designing a multi-loop controller. The study by Rajapandiyan has also proven that the Effective Open-loop Transfer Function (EOTF) derived from dRGA is equivalent to the ETF derived from RNGA and the RARTA technique Rajapandiyan and Chidambaram (2012b).

In order to achieve the desired performance level, the controllers are designed based on different methodologies and with different structures. For this study, the Proportional Integral (PI) controller is considered since it will eliminate forced oscillation due to P-action and steady-state errors due to I-action. Any process that eventually returns to the same output, when provided with the same set of inputs and disturbances can adopt a PI controller. Meanwhile Proportional-Integrative-Derivation (PID) controller result in excessive oscillation at set point response, when compared with PI controllers (Seshagiri et al., 2007). In most control systems, the commonly used controller structure is the PID controller because of its several advantages. However, the derivative effect is not always used due to noise in the control process (Concepcion et al., 2010). Further, PI controllers have two parameters to calculate and give good results in most control systems. Apart from this, the forced oscillations and steady-state error can be completely eliminated by adopting a PI controller. In most industrial applications, PI controllers are used where the speed of the response is not a factor of concern (Chidambaram and C. Sankar, 2017). Perhaps for decoupling control, the combination of neural network and layout information achieves a better optimization (Qiao et al., 2019). The standard PI controller dominates the industrial market when it comes to the application of control theory, with its advantages and drawbacks accounted for. If the system is nonlinear, it is always better to develop a procedure to design a robust PI controller with uncertainty parameters (Aranovskiy et al., 2016).

The activated sludge wastewater treatment plant considered for the present study demands a closed-loop control system due to its internal processes nonlinearities and time variability. When viewed as an alternative to a centralized system, decentralized wastewater management has a greater opportunity for wastewater reuse and reclamation (Kara, 2005). Continuing the discussion in this section, inspired me to study the direct and indirect interaction among the system parameters, which was necessary for developing an effective decentralized controller in order to achieve an optimal WWTP. To the best of our knowledge, this work on a decentralized controller with a decoupler design on WWTP has been reported in open sources.

For the current study, a mathematical model for the simplified biological treatment phases has been considered, which consists of four non-linear differential equations. The transfer function matrix (2×2) of WWTP has been determined using the system identification toolbox by considering aeration rate and recycle sludge flow rate as input variables and substrate and biomass concentration as output variables. The primary objective of the present study is to design a multivariable control system for the biological treatment system that can enhance the performance of the WWTP. An attempt has been made to design a decentralized PI controller and study the closed-loop responses. As discussed earlier, the decentralized controller involves interactions, which can be eliminated by the decoupler. A comparative study is also carried out to show the superiority of the designed controllers. The comparison of time integral errors like ITAE, ISE, and IAE minimization is used for designing the controllers. A robustness against process parameters (process gain and time constant) uncertainty was also studied to understand the stability of the control system.

4.2 Methodology

4.2.1 Decentralized Controller

In order to control any process, there should be a manipulated variable that allows one to control the process and obtain the desired outcome. The multivariable process is one that has more than one input variable and more than one output variable, which is known as the MIMO process. Let us consider process G(s) with input variable U and output variable Y, then its relation can be expressed as

$$Y(s) = G(s) \cdot U(s) \tag{4.1}$$

Where $Y(s)$ and $U(s)$ are the output and input vectors, respectively, as shown below.

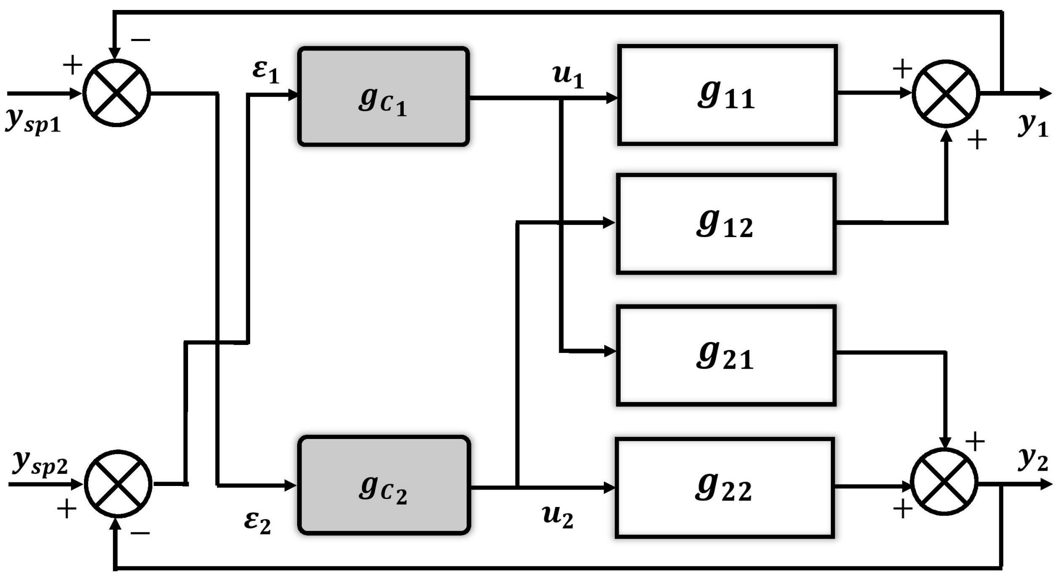

Figure 4.1 Decentralized system for two inputs and two outputs (TITO)

$$Y(s) = \begin{bmatrix} y_1(s) \\ y_2(s) \end{bmatrix} \tag{4.2}$$

$$U(s) = \begin{bmatrix} u_1(s) \\ u_2(s) \end{bmatrix} \tag{4.3}$$

In Equation (4.1), G(s) is the process transfer function matrix and is given as

$$G(s) = \begin{bmatrix} g_{11} & g_{12} \\ g_{21} & g_{22} \end{bmatrix} \tag{4.4}$$

Consider a TITO system (2×2 system) representation with a decentralized controller shown schematically in Figure 4.1. Where g_{11}, g_{12}, g_{21}, and g_{22} are four process transfer function, and g_{c1} and g_{c2} denote the decentralized controllers. The two inputs are expressed as u_1, u_2, and y_1, y_2 which represent two outputs, respectively. Two set points are considered y_{r1} and y_{r1}.
A TITO system with a decentralized controller design is discussed in this section. At the beginning of developing the decentralized controller, all higher-order transfer functions are converted to FOPTD. The decentralized controller matrix can be represented by the following equation:

$$G_c(s) = \begin{bmatrix} G_{c1} & 0 \\ 0 & G_{c2} \end{bmatrix} \tag{4.5}$$

In this study, the decentralized controller is assumed to be the PI controller and given by the following relation

$$G_{C_j} = K_{C_j}\left(1 + \frac{1}{\tau_{ij}}s\right) \tag{4.6}$$

Here controller gain and integral time constant for j^{th} (j = 1,2) are represented as K_{C_j} and τ_{ij} respectively. These controllers are designed by minimizing the time integral errors based on the selected best-paired transfer function models. The selection of the best pairing is discussed in a subsequent section.

4.2.1.1 Selection of best pairing

After estimating the FOPTD model through the system identification technique (as discussed in Chapter-4) the next step is to obtain the best pairing elements. The interactions among the process variables may destabilize the closed-loop system, which tends to make controller tuning more difficult. To overcome these interactions, pairing up the controlled and manipulated variables are must. This operation will increase the controller performance and stability margin. The concept of an RGA was taken up to determine the best pairing between manipulated and controlled variables. The best input-output pairing for a multivariable process control system could be achieved by using the widely accepted RGA method. This method operates by characterizing the degree of interactions between manipulated and control variables. Processes with large RGA indexes are fundamentally difficult to control because of their sensitivity to input uncertainty. This RGA matrix can be calculated as follows:

$$\Lambda = RGA = K \otimes (K^{-1})^T = \begin{bmatrix} \lambda_{11} & \lambda_{12} \\ \lambda_{21} & \lambda_{22} \end{bmatrix} \tag{4.7}$$

where λ_{ij} and K are elements of the relative gain array and gain matrix, respectively. $\otimes$ is the Hadamard product, and the gain matrix is obtained from the process gain matrix (G) by substituting s = 0, and the relative gain array elements can be found as follows.

$$\lambda_{ij} = \frac{\text{gain when all other loops are open}}{\text{gain when all other loops are closed}} \tag{4.8}$$

The two most prominent ways to estimate RGA are experiment and-or theoretical approach. While calculating RGA, the ultimate steady state values are given the most important consideration, not the controller parameters. The RGA value tends to be unity because each row and column sum are normalized. The λ_{ij} values calculated from the steady state gain matrix is unaffected by scaling and invariably dimensionless entity. One of the outputs and manipulated variables are represented by each row and column, respectively. Below are interpretations for various values of λ_{ij}

i. $\lambda_{ij} = 0$: Indicates there is no impact of manipulated variable u_j over controlled variable (y_i)

ii. $\lambda_{ij} = 1$: This means there prevail no interactions among the process variables in the selected control loops. The manipulated variable (u_j) absolutely impacts the controlled variable (y_i). So from the theoretical definition, we can conclude that the gain loop with all loops open is equal to the gain loop for all loops closed, i.e., $g_{11} = g_{11}^*$

iii. $\lambda_{ij} < 0$: This value denotes that the system will be unstable whenever u_j is paired with y_i.

iv. $0 < \lambda_{ij} < 1$: This condition implies that other control loops interact more than the selected control loop $(u_j - y_i)$.

v. $\lambda_{ij} = 0.5$: All the loops selected have equal levels of interactions to the retaliatory effects.

vi. $\lambda_{ij} > 1$: This condition prevails when the control pair is dominant but with the opposite influence of other loops. Theoretically, the open-loop gain is greater than the other closed-loop gain.

The best pairing is selected based on the values closer to unity in a row vector of RGA matrix equation 4.7. Table 4.1 provides the guidelines for selecting the best pairing between manipulated and control variables.

Table 4.1 Guidelines to select and avoid pairing

λ_{ij}	Possible pairing
$\lambda_{ij} = 0$	Avoid pairing u_j with Y_i
$\lambda_{ij} = 1$	Pair u_j with Y_i
$\lambda_{ij} < 0$	Avoid pairing u_j with Y_i
$\lambda_{ij} \leq 0.5$	Avoid pairing u_j with Y_i
$\lambda_{ij} > 1$	Pair u_j with Y_i

4.2.1.1.0.1 Niederlinski Index (NI) By using the result obtain from RGA, the stability of the closed-loop system can be estimated using the Niederlinski index. At steady state, it is given by

$$NI = \frac{|G|}{\Pi_{i=1}^{n} g_{ii}} \tag{4.9}$$

For a TITO system, a negative value of NI indicates that the system is unstable, whereas a positive value of NI represents the system is stable for the pairing. This hypothesis may not be accurate for the larger matrices. since the NI theorem is for system with rational transfer functions where predictions assume apparent feedback, it is suggested in some of the studies to avoid using NI when the system possesses high time delay (dead time).

4.2.2 Design of Decoupler

The principle purpose of designing a decoupler is to reduce the interaction among the loops. A non-iterative control system design is a well-known technique to control interactions between the loops (Prabhu Y. and Sankar, 2019). For the present study, the input parameter aeration rate should affect only the output parameter DO concentration, without altering the substrate concentration. Similarly, in the second instance, the input parameter recycles sludge flow, which should only affect the substrate concentration without interacting with and affecting the output parameter DO concentration. The structure of the closed-loop decoupler is depicted in Figure 4.2. A design method for the decoupler is described in this section.

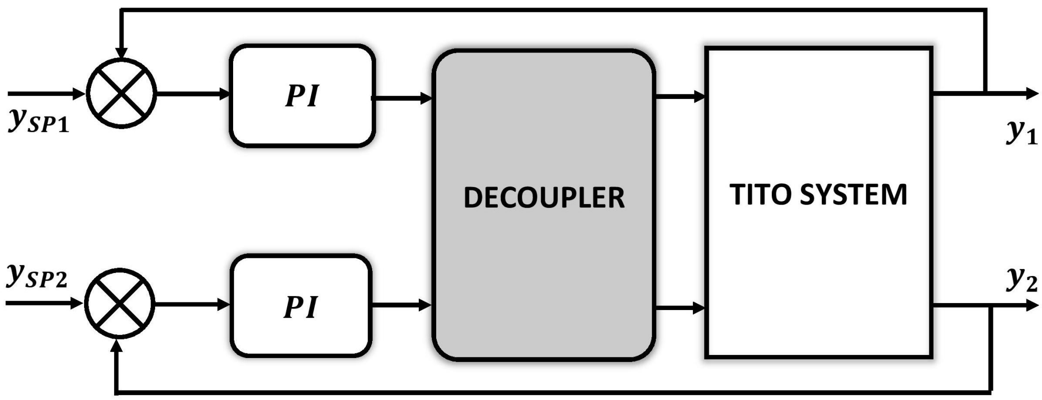

Figure 4.2 Decentralized system for two inputs and two outputs (TITO)

Analytical or empirical methods can be utilized to simplify higher-order transfer function models or nonlinear models to a FOPTD model. This approach is followed for most of the processes in interaction analysis and controller design. Below is the representation of the process transfer function model as the FOPTD model, which relates input i to output j,

$$g_{ij} = \frac{k_{pij}e^{-\theta_{ij}s}}{(\tau_{ij}s+1)} \tag{4.10}$$

From Figure 4.1, following relations can be written

$$y_1(s) = g_{11}(s)u_1(s) + g_{12}u_2(s) \tag{4.11}$$

$$y_2(s) = g_{21}(s)u_1(s) + g_{22}u_2(s) \tag{4.12}$$

There exist two transmission paths when input is introduced from u_i to y_i during the second loop is closed. Usually, two combinations of transmission paths are considered effective open-loop dynamics. Hence comprehensively a closed loop transfer function between u_1 to y_1 is given by

$$\frac{y_1}{u_1} = g_{11} - \frac{g_{12}g_{21}g_{c2}}{1+g_{c2}g_{22}} \tag{4.13}$$

It can be also written as

$$\frac{y_1}{u_1} = g_{11} - \frac{g_{12}g_{21}(g_{c2}g_{22})}{g_{22}(1+g_{c2}g_{22})} \tag{4.14}$$

Similarly for the second loop

$$\frac{y_2}{u_2} = g_{22} - \frac{g_{21}g_{12}(g_{c1}g_{11})}{g_{11}(1+g_{c1}g_{11})} \tag{4.15}$$

The open loop dynamics between controlled variables (y_i) and manipulated variables (u_i) depends on other processes and controllers in other loops apart from corresponding transfer function (g_{ij}). Hence two assumptions were considered to reduce the above two equations;

1. For other loops the perfect controller approximation was used to simplify the above equation

$$\frac{(g_{ci}g_{ij})}{(1+g_{ci}g_{ij})} = 1 \tag{4.16}$$

i = 1, 2, 3..... 2. ETF's when compared with the corresponding open-loop model has the similar structure

$$g_{11}^* = \frac{y_1}{u_1} = g_{11} - \frac{g_{12}g_{21}}{g_{22}} g_{22}^* = \frac{y_2}{u_2} = g_{22} - \frac{g_{21}g_{12}}{g_{11}} \tag{4.17}$$

Because of its complexity it is difficult to use EOTF (g_{11}^* and g_{22}^*) directly for the controller design. Hence using the Maclaurin series the resulting EOTF is reduced to FOPTD models. Adopting this method while formulating EOTFs and in model reduction on higher dimensions systems leads to complications.

4.2.2.1 Equivalent Transfer Function (ETF)

The response from an open-loop stable system is always simplified by analytical or empirical methods to a FOPTD model for designing the controllers. To solve this condition, there are various methods available in the literature. RGA, RNGA, and RARTA concepts are adopted by other researchers to obtain the expression for ETF for higher-dimensional systems. RGA is the fraction of open loop gain to closed loop gain of each element between the same two variables when all other loops are closed (V. Vijay et al., 2012).

$$\Lambda_{ij} = \frac{\text{gain when all other loops are open}}{\text{gain when all other loops are closed}} \tag{4.18}$$

That is

$$= \frac{\left(\frac{\partial y_i}{\partial u_j}\right)_{u_{k\neq j}}}{\left(\frac{\partial y_i}{\partial u_i}\right)_{y_{k\neq j}}} \tag{4.19}$$

Each element of Λ_{ij} for RGA. If the above definition is written in another form of transfer function matrix $G(s) = g_{ij} = (\partial y_i/\partial u_j)_{u_k}$ and its inverse will be $G^{-1}(s) = \hat{g}_{ij} = (\partial y_i/\partial u_j)_{y_k}$ as

$$\Lambda(G) = \left\{\Lambda_{ij}\right\} = \left\{g_{ij}\hat{g}_{ij}\right\} = G(s) \otimes G^{-T}(s) \tag{4.20}$$

where $\otimes$ denotes the Hadamard Product. The transfer function matrix elements are expressed in inverse form as

$$\left\{G^{-T}(s)\right\} = \hat{g}_{iji} = \frac{\Lambda_{ij}}{g_{ij}} \tag{4.21}$$

The normalized gain (K_{Nij}) for a particular transfer function,$(g_{ij}(s))$ which describes the dynamic properties of the transfer function is defined as,

$$K_{Nij} = \frac{k_{ij}}{\sigma_{ij}} = \frac{k_{ij}}{(\tau_{ij} + \theta_{ij})} \tag{4.22}$$

The normalized gain matrix is expressed as

$$K_N = \begin{bmatrix} K_{N,11} & K_{N,12} \\ K_{N,21} & K_{N,22} \end{bmatrix} = \begin{bmatrix} \dfrac{k_{11}}{(\tau_{11}+\theta_{11})} & \dfrac{k_{12}}{(\tau_{12}+\theta_{12})} \\ \dfrac{k_{21}}{(\tau_{21}+\theta_{21})} & \dfrac{k_{22}}{(\tau_{22}+\theta_{22})} \end{bmatrix} \tag{4.23}$$

Here, Average Residence Time (ART) is $\sigma_{ij} = \tau_{ij} + \theta_{ij}$ which represents the response speed of the controlled variable (y_i) to the manipulated variable (u_i). The ART represents the average time it takes for a change in the manipulated variables to be fully reflected in the response of the transfer function. In simpler terms, the smaller the value of ART, the quicker the system responds to changes in the input disturbance. This means that the effects of adjustments made to the manipulated variables are rapidly observed in the behavior of the controlled variable. By reducing the average residence time, the transfer function becomes more sensitive and responsive to any modifications in the manipulated variables. This enhanced sensitivity allows for faster and more efficient control of the process, as deviations from the desired set point can be quickly detected and corrected. Similarly, the larger value of ART indicates slower process dynamics. Compared to RGA, RNGA is an advanced version that scrutinizes the steady-state and transient behavior of the process transfer function through thorough measurement of MIMO systems. Because of this, it provides valuable information without undertaking frequency-dependent analysis (Mao et al., 2009). A normalized gain matrix can be used to express relative normalized gain array (RNGA - ϕ) and hence

$$\phi = K_N \otimes K_N^{-T} \tag{4.24}$$

where,

$$\phi = \begin{bmatrix} \phi_{11} & \phi_{12} \\ \phi_{21} & \phi_{22} \end{bmatrix} \tag{4.25}$$

The ratio of loop y_i - u_j average residence times, during other loops are closed and when other loops are open, yields Relative average residence time (γ_{ij}),

$$\gamma_{ij} = \frac{\hat{\sigma}_{ij}}{\sigma_{ij}} \tag{4.26}$$

When a condition emerges of having all loops open and all other loops closed, the estimation of the RARTA will provide us with the dynamic behavior of the system. The RARTA concept is generally used to approximate a decomposed process model (Shen et al., 2011). RARTA can be secured by estimating the relative average residence time for all the elements of the transfer function matrix,

$$\Gamma = \begin{bmatrix} \gamma_{11} & \gamma_{12} \\ \gamma_{21} & \gamma_{22} \end{bmatrix} \tag{4.27}$$

Which is calculated as

$$\Gamma = \phi \otimes \Lambda = \begin{bmatrix} \phi_{11} & \phi_{12} \\ \phi_{21} & \phi_{22} \end{bmatrix} \otimes \begin{bmatrix} \Lambda_{11} & \Lambda_{12} \\ \Lambda_{21} & \Lambda_{22} \end{bmatrix} \tag{4.28}$$

Here Hadamard division is denoted as $\otimes$. By definition, the relative average residence time can be written as

$$\hat{\sigma}_{ij} = \sigma_{ij}\gamma_{ij} = \tau_{ij}\gamma_{ij} + \theta_{ij}\gamma_{ij} \tag{4.29}$$

$$= \hat{\tau}_{ij} + \hat{\theta}_{ij} \tag{4.30}$$

where $\hat{\tau}_{ij}$ and $\hat{\theta}_{ij}$ denote time constant and time delay when other loops are closed respectively.

The transfer function matrix element of a MIMO process can be possibly obtained by approximating elements of the transfer function matrix that has the same form as the open-loop transfer function, by using the above-discussed methods i.e., RGA, RNGA, and RARTA. Therefore,

$$\hat{g}_{ij}(s) = \frac{\hat{k}_{ij}}{(\hat{\tau}_{ij}} s+1)e^{-\hat{\theta}_{ij}s} \tag{4.31}$$

It can be written as,

$$\hat{g}_{ij}(s) = \frac{\hat{k}_{ij}}{\Lambda_{ij}} \frac{1}{(\gamma_{ij}\hat{\tau}_{ij}} s+1)e^{-\gamma_{ij}\theta_{ij}s} \tag{4.32}$$

When other loops are closed the optimal Effective Transfer Function (ETF) is denoted by $\hat{g}_{ij}(s)$. $\hat{k}_{ij}$, $\hat{\tau}_{ij}$ and $\hat{\theta}_{ij}$ represent closed loop process gain, time constant, and dead time respectively.

4.2.2.2 Relationship between $\hat{g}_{ii}(s)$ and g^*_{ii}

The EOTF can be expressed by the elements of dRGA (Truong and Moonyong, 2010b)

$$g^*_{ii} = \frac{g_{ii}}{\Lambda_{ii}} \tag{4.33}$$

here, dRGA can be expressed as

$$\Lambda_{ij} = G(s) \otimes \hat{G}(s) \tag{4.34}$$

$$\Lambda_{ij} = \begin{bmatrix} g_{11}(s) & g_{12}(s) \\ g_{21}(s) & g_{22}(s) \end{bmatrix} \otimes \begin{bmatrix} \frac{1}{\hat{g}_{11}(s)} & \frac{1}{\hat{g}_{12}(s)} \\ \frac{1}{\hat{g}_{21}(s)} & \frac{1}{\hat{g}_{22}(s)} \end{bmatrix} \tag{4.35}$$

If the controller is Ideal, it is possible to write

$$U(s) = G^{-1}(s)Y(s) \tag{4.36}$$

That is when all other loops are closed the gain from $U_j(s)$ to $Y_j(s)$ is $\frac{1}{[G^{-1}(s)]_{ij}}$ Then

$$\Lambda(s) = G(s) \otimes G^{-T}(s) \tag{4.37}$$

$$\Lambda(s) = \begin{bmatrix} g_{11}(s) & g_{12}(s) \\ g_{21}(s) & g_{22}(s) \end{bmatrix} \otimes \begin{bmatrix} g_{11}(s) & g_{12}(s) \\ g_{21}(s) & g_{22}(s) \end{bmatrix}^{-T} \tag{4.38}$$

Comparing (4.35) and (4.38), it can be noted that

$$\begin{bmatrix} \frac{1}{\hat{g}_{11}(s)} & \frac{1}{\hat{g}_{12}(s)} \\ \frac{1}{\hat{g}_{21}(s)} & \frac{1}{\hat{g}_{22}(s)} \end{bmatrix} = \begin{bmatrix} g_{11}(s) & g_{12}(s) \\ g_{21}(s) & g_{22}(s) \end{bmatrix}^{-T} \tag{4.39}$$

Taking the transpose on both sides,

$$G^{-1}(s) = \hat{G}^{-T}(s) \tag{4.40}$$

From equation 4.40, it can be interpreted that conventional EOTF (from dRGA) is identical to the ETF (from RNGA).

4.2.2.3 Controller Design

It is a well-known fact that the output of the system mainly depends on the input; hence, it is necessary to pair the input and the output in the best possible way. The controllers are designed using ITAE minimization, IAE minimization, and ISE minimization methods. One of the aims of the present study is to obtain the optimal controller parameters (k_c, τ_I, τ_D). Hence, the objective function f is formulated so as to minimize time integral errors such as IAE, ITAE, and ISE. Mathematically, it can be defined as

$$\underset{(k_c,\, \tau_I,\, \tau_D)}{\text{Minimize}} \quad f \tag{4.41}$$

where f is the objective function depending on the time integral error that can be set based on the error function, which will be minimized.

For ITAE minimization, f can be as follows

$$f=\sum_{t=0}^{\infty} t|y(t)-y_r(t)| \tag{4.42}$$

For IAE minimization,

$$f=\sum_{t=0}^{\infty} |y(t)-y_r(t)| \tag{4.43}$$

and for ISE minimization,

$$f=\sum_{t=0}^{\infty} |y(t)-y_r(t)|^2 \tag{4.44}$$

In the ITAE minimization method, the error obtained from comparing the set point and process response for various times is multiplied by the time. The *fminsearch* in Matlab routine is used in this work for solving the optimization problem. The procedure involves developing a single-loop control system in a Simulink environment and then linking it with Matlab. Each time the objective function is evaluated, the Simulink model is executed. The Simpsons One-Third rule is used for obtaining the area under the curve (i.e., IAE, ITAE, and ISE indices). A similar procedure has been followed for the other two methods (i.e., IAE and ISE).

The Nelder-Mead "Simplex" Algorithm implemented in the *fminsearch* function is highly regarded as the most prevalent technique for nonlinear unconstrained optimization. Originally introduced in 1965 by Nelder and Mead (Nelder and Mead, 1965), this algorithm gained widespread adoption in various fields such as chemical engineering, chemistry, and medicine (Lagarias et al., 1998). As a direct method, it operates solely based on the functional values of the scalar-valued nonlinear function with n real variables, making it independent of derivative information. The Nelder-Mead algorithm is a numerical technique for finding the minimum or maximum of a multidimensional function. It uses a shape called a simplex, which consists of a set of vertices. Each vertex represents a point in the function's domain. The algorithm iteratively updates the vertices to converge towards the optimal solution. (Idris et al., 2021; Ghanadzadeh, Gilani, et al., 2019; Moradi and Seyedtabaii, 2022; Erfan et al., 2022).

4.2.2.4 Summary of Decentralized and decoupler controller

This section summarizes the procedure adopted to design a decentralized and decoupled controller. The FOPTD model is estimated using the System Identification technique, which will then be used to obtain the RGA matrix that indicates the best pairing for which the controllers have to be designed. Accordingly, by using this best pair, the controllers are designed to minimize the time integral errors. Figure 4.3 summarizes the steps adopted for designing a decentralized controller

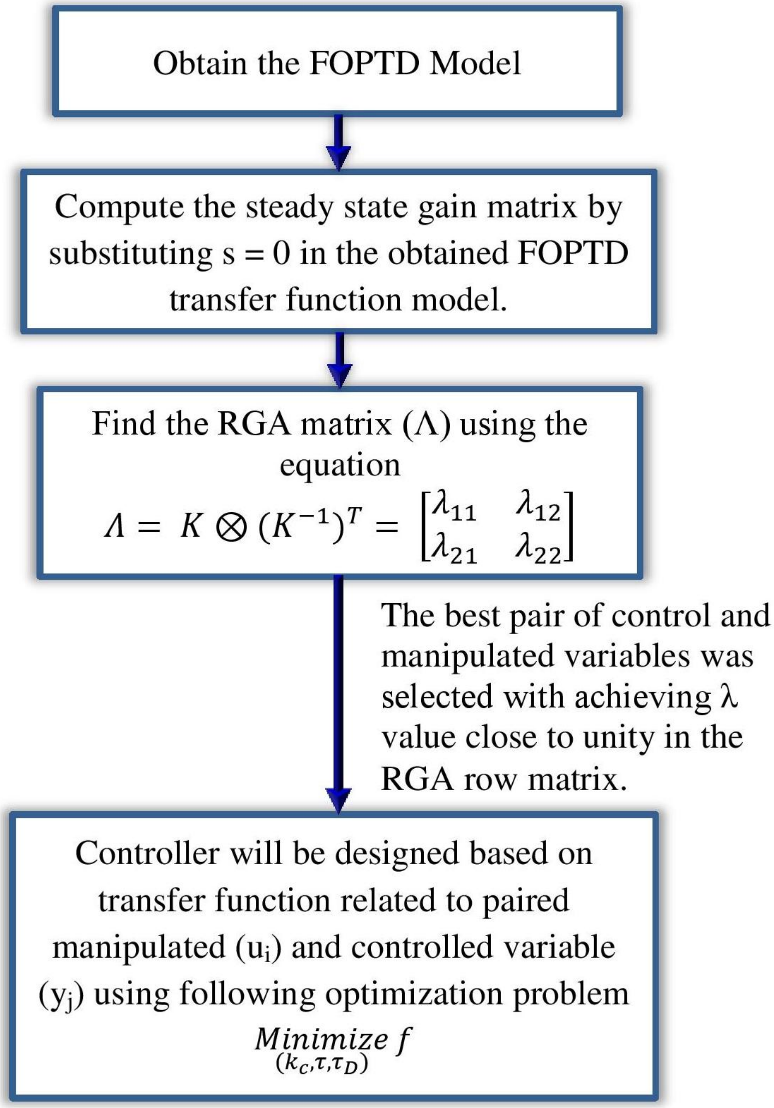

Figure 4.3 Flowchart of steps involved in Decentralized controller design

Similarly, in the case of decoupler controller design, the following steps are carried out (Figure 4.4). This method also endorses the same FOPTD model that was determined using the system identification technique for the decentralized controller. Then followed by a series of steps to estimate RNGA, RART, and RARTA that will lead to estimating the decoupled controller parameters by an optimization technique.

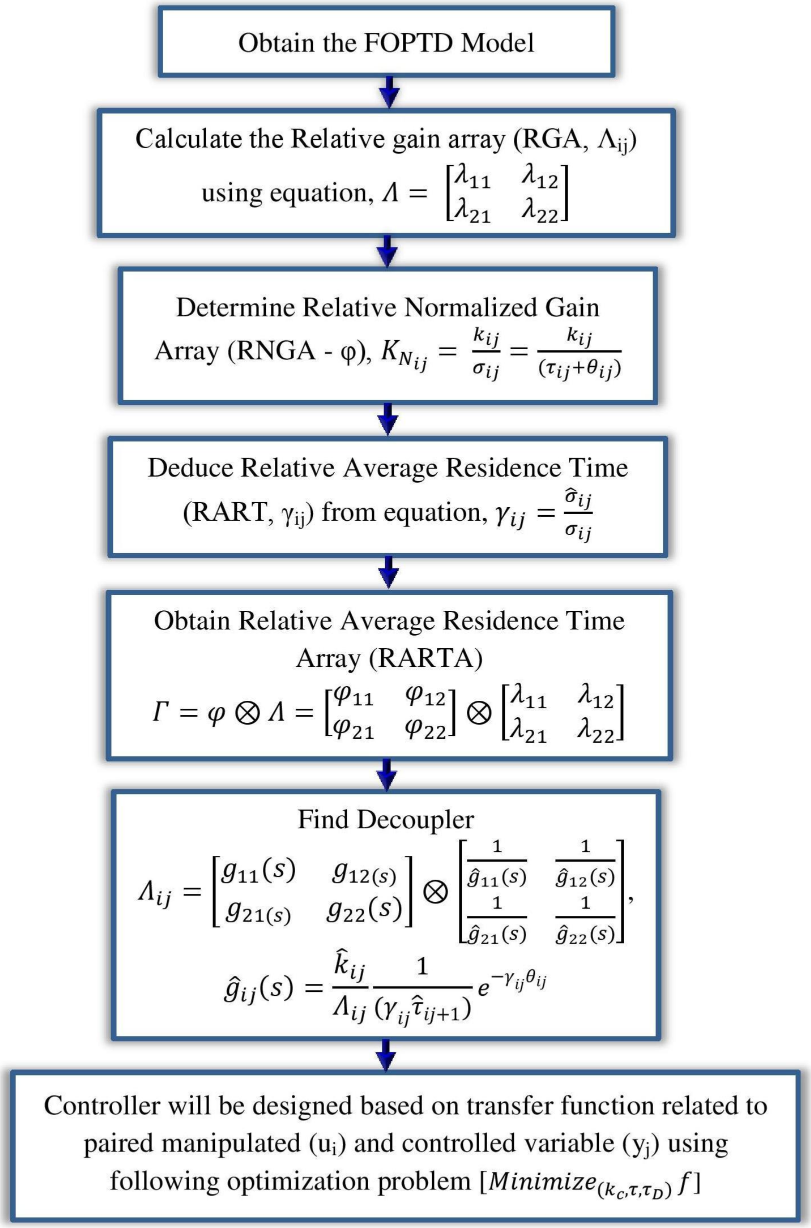

Figure 4.4 Flowchart of steps involved in Decoupler controller design

4.3 Simulation Results and Discussion

To test the performance of the control system, several simulation scenarios were considered using a linear version of a process mathematical model, and the outcome is explained in the following section. The linearized transfer function matrix obtained from the system identification approach is given as

$$G(s) = \begin{bmatrix} \dfrac{0.0007022e^{-0.3s}}{0.60211s+1} & \dfrac{1.3019e^{-0.0306s}}{0.57229s+1} \\ \dfrac{0.94958e^{-0.1781s}}{0.58065s+1} & \dfrac{0.7025e^{-0.0001s}}{0.58347s+1} \end{bmatrix} \tag{4.45}$$

Figure 4.5 represents the dynamic test conducted to validate the model with measured data. On average, good fits of the model were observed, ranging from 82% - 98% from a given percentage. These identified models were controllable and observable. The following expression is adopted for estimating the percentage fit

$$\text{fit} = 100\left(1 - \frac{||y-\hat{y}||}{||y-\text{mean}(y)||}\right) \tag{4.46}$$

Here, the measured output is expressed by y, and $\hat{y}$ indicates output obtained from the identified model.

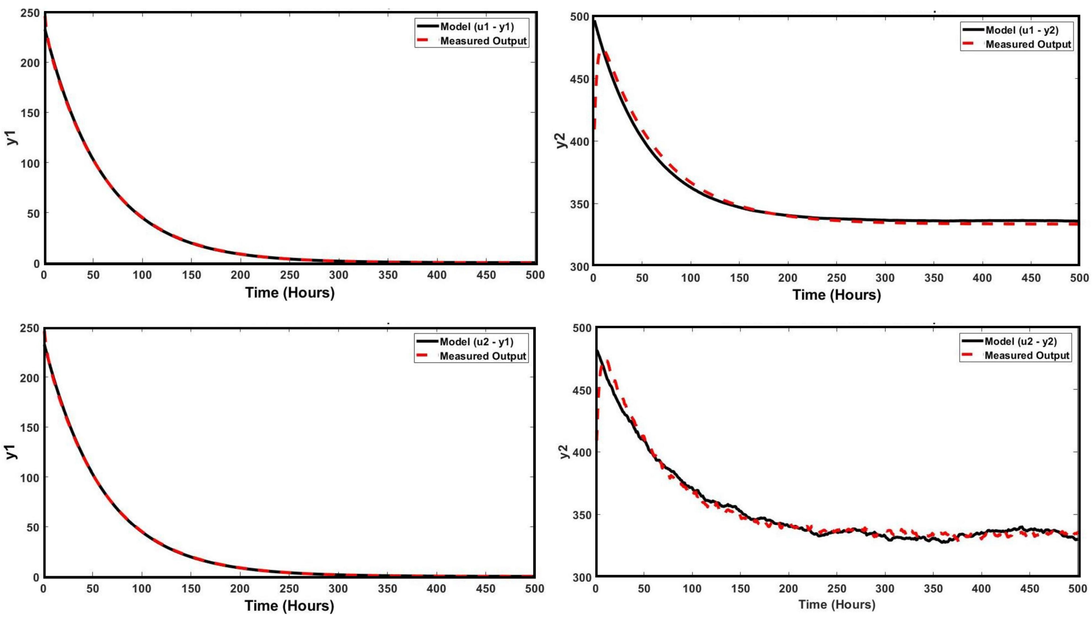

Figure 4.5 Response comparison of the identified model with the measured output

Decentralized controller

The gain array matrix is estimated as follows

$$K = \begin{bmatrix} 0.0007022 & 1.3019 \\ 0.94958 & 0.7025 \end{bmatrix}$$

The RGA can be calculated using Equation 4.7

$$\Lambda = \begin{bmatrix} -3.9918e^{-4} & 1.0004 \\ 1.0004 & -3.9918e^{-4} \end{bmatrix}$$

By utilizing the above calculated RGA values, it becomes possible to determine the most suitable pairing for the values within a row that exhibit proximity to one and are non-negative. It is apparent from the observation of RGA values that input (u_1) and output (y_2) and input (u_2) and output (y_1) can be paired. Hence, a decentralized controller must be designed based on the transfer functions relating recycle sludge flow rate to biomass concentration (G_{12}) and aeration rate to substrate concentration (G_{21}). The controllers are designed using error minimization methods such as ITAE, IAE, and ISE, and identified PI settings are mentioned in Table 4.4. Negative gain initiates direct action on the controller, while positive gain forces the reverse action on the controller. As we increase the two manipulated variables, the ratio of recycled flow to influent flow (u_1) and Aeration rate (u_2), two output variables will favor an inverse action, observing a decrease in biomass concentration (y_1) and substrate concentration (y_2).

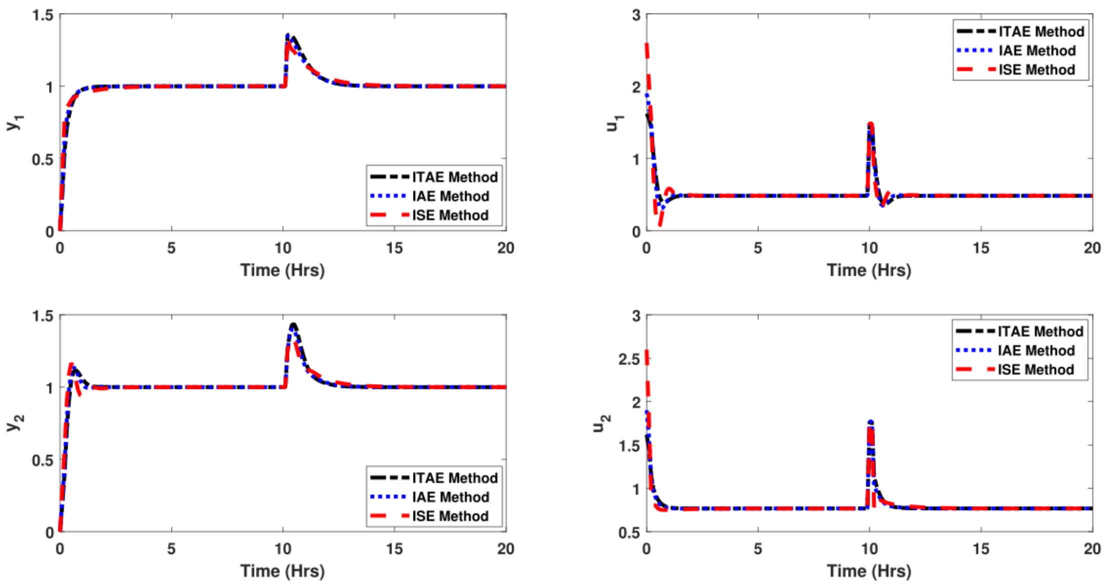

Figure 4.6 Closed loop response and change in manipulated variables for decentralized WWTP

At the time $t = 0$, a unit step input is applied to the set point, followed by the introduction of a disturbance to the process at 10s, enabling the evaluation of the closed-loop performances. Figure 4.6 presents the closed-loop response of output and change in manipulated variables for the decentralized system of WWTP. It is important to highlight that the three methods produced relatively similar types of closed-loop responses. However, when comparing the three methods, such as ITAE minimization, IAE minimization, and ISE minimization, the settings derived from IAE minimization demonstrated a shorter settling time and no oscillation for set point tracking. Additionally, the closed-loop response achieved with IAE minimization PI settings showed lesser errors (as indicated in Table 4.2) compared to the ITAE and ISE methods, respectively.

The quantitative analysis in terms of time integral errors such as IAE and ITAE are given in Table 4.2. It can be found that the IAE minimization method has the lowest value of the IAE and ITAE indexes for both outputs (y_1 and y_2). Meanwhile, the IAE error index when estimated using ITAE, the IAE and ISE minimization methods have 15.44%, 3.67%, and 21.81% of higher percentage Index, respectively. Similarly, for error ITAE, the PP method had 67.55%, 54.05%, and 62.62% lower percentage index when compared with ITAE, IAE, and ISE respectively. The Total variance of the ITAE method, IAE method, and ISE method is shown in Table 4.2. It is clearly noted that the lowest value of the TV is obtained through the ITAE method, while the highest value is obtained by the ISE method in both conditions of the outputs (y_1 and y_2).

Table 4.2 Error Index for Decentralized Controller

	y_1			y_2		
Method	IAE	ITAE	TV	IAE	ITAE	TV
IAE	0.0423	3.5743	1.4158	0.1327	3.6746	1.133
ISE	0.0497	3.7733	2.1144	0.1406	3.847	1.8316
ITAE	0.0471	3.8875	1.1347	0.1453	3.9567	0.8518

An uncertainty of 30% has been introduced in the process gain (k_p) and time constant (τ) to analyze the robust performance of the closed loop system. From Figure 4.7 and 4.8 (right section) it is evident that the system is robustly stable for the significant extent of model uncertainty. These figures exhibit the robustness behavior of the system (for output y_1 and y_2 respectively) towards the stipulated uncertainty. The plot also represents the nominal and worst-case gains of the uncertain system using the dynamic condition with function as frequency. The nominal curve falls well within the 30% perturbation provided for the process gain (Figure 4.7) and time constant (Figure 4.8). The system can tolerate up to 333% of uncertainty in process gain for both the outputs y_1 and y_2, whereas for the time constant it can tolerate upto 321% and 256%, respectively. In the singular value plots (right-hand side) the solid blue line represents the nominal curve, and the red line indicates the worst-case gain for the lower and upper bounds at each frequency. It is distinctly noticeable that the nominal curve falls well with the acceptable range for perturbation provided for process gain and time constant. The light blue curves indicate the various sampled responses of the system. And the peak spike over the worst-case gain curve represents the critical frequency where the worst-case gain over all the frequencies can be estimated. Correspondingly, the closed loop responses over a period of uncertainty at various frequencies in process gain and time constant are presented in Figures 4.7 and 4.8, respectively for both the outputs (y_1 and y_2). In both cases, with acute and swift oscillations, the response curves from outputs (y_1 and y_2 attain a stable state. The nominal value curve falls well within the random sample curves in the closed-loop response plots. The lower and upper bound values of worst-case peak gain tend to be around 1.2 and 1.1 for perturbation is provided to process gain and time constant, respectively (refer Table 4.3). The frequency at which the worst-case peak gain occurs is 5.657 and 6.617 respectively for stipulated perturbation given to process gain and time constant. Then the value for destabilizing elements for uncertain elements and the value of uncertain elements that cause worst-case gain is denoted as *wcu* and *wcug* in Table 4.3.

Table 4.3 Worst-case gain scenario for Decentralized controller

Uncertainty	LB	UB	CF	*wcu*	*wcug*	Tolerance %
K_p	1.2491	1.2518	5.6570	-2.3648E-14	1.2345	y_1 - 333 y_2 - 333
τ	1.1953	1.1979	6.6178	0.1347	0.4065	y_1 - 321 y_2 - 256

LB: Worst case gain lower bound, UB: Worst case gain upper bound,
CF: Critical frequency, wcu: Worst case peak gain at critical frequency,
wcug: Worst case gain at all specified frequency

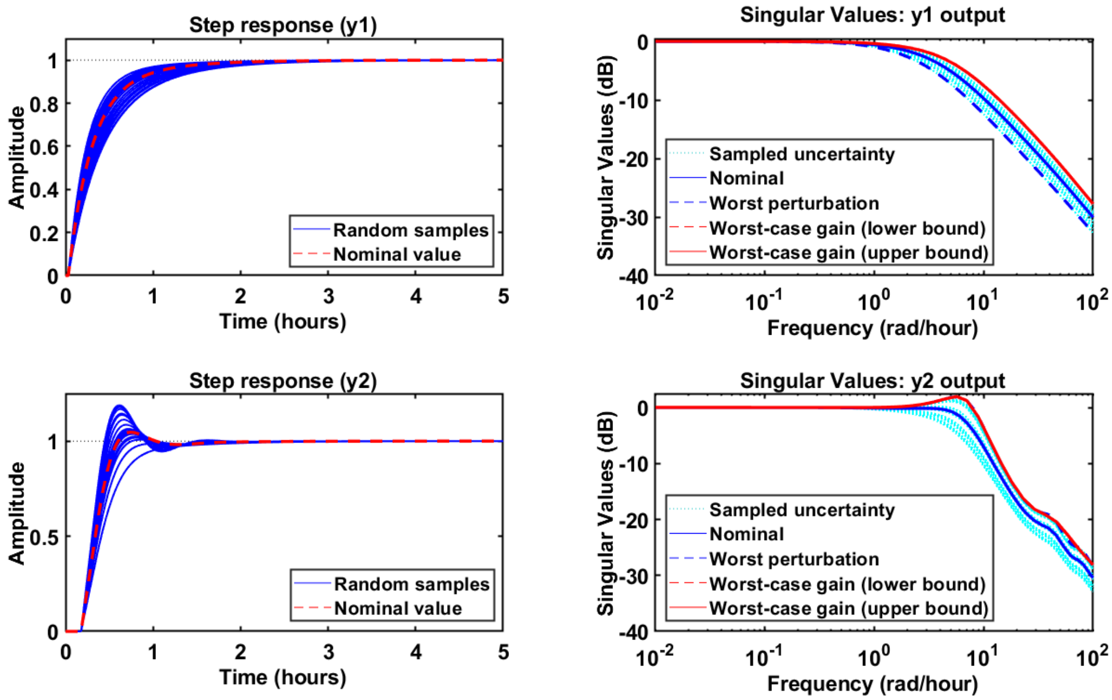

Figure 4.7 Closed loop step responses for 30% uncertainty in process gain (left-hand side), and Singular values for nominal, random samples, and worst-case gain for 30% uncertainty in process gain (right-hand side)(Decentralized)

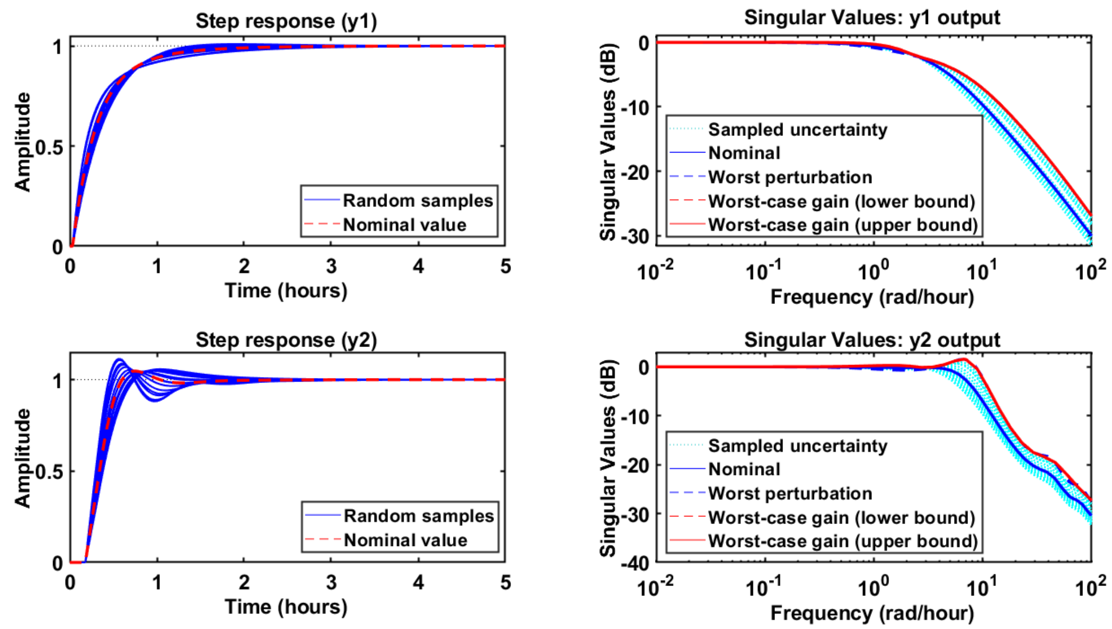

Figure 4.8 Closed loop step responses for 30% uncertainty in time constant (left-hand side), and Singular values for nominal, random samples, and worst-case gain for 30% uncertainty in time constant (right-hand side)(Decentralized)

Decoupler

The normalized gain matrix (K_N), dynamic Relative Gain Array (dRGA - Λ), Relative Normalized Gain Matrix (RNGA - ϕ) , Relative Average Residence Time Array (RARTA - Γ) is calculated as

$$K_N = \begin{bmatrix} 0.0008 & 2.1591 \\ 1.2515 & 0.7952 \end{bmatrix} \qquad \Lambda = \begin{bmatrix} -0.0004 & 1.0004 \\ 1.0004 & -0.0004 \end{bmatrix}$$

$$\phi = \begin{bmatrix} -0.0002 & 1.0002 \\ 1.0002 & -0.0002 \end{bmatrix} \qquad \Gamma = \begin{bmatrix} 0.0008 & 2.1591 \\ 1.2515 & 0.7952 \end{bmatrix}$$

The above estimated RGA and RNGA values are utilized to get the ETF model parameters and are given by

$$\hat{K}_c = \begin{bmatrix} -0.0018 & 0.0013 \\ 0.0009 & -1.7598 \end{bmatrix} \qquad \hat{\tau} = \begin{bmatrix} 0.3456 & 0.5722 \\ 0.5806 & 0.3349 \end{bmatrix}$$

$$\hat{\theta} = \begin{bmatrix} 0.1722 & 0.0307 \\ 0.1781 & 0.1722 \end{bmatrix}$$

Hence the Effective Transfer Function (ETF-$\hat{g}$) can be expressed as

$$\hat{g}(s) = \begin{bmatrix} \frac{-0.0018e^{-0.1722}}{0.3456s+1} & \frac{0.0013e^{-0.0307}}{0.5722s+1} \\ \frac{0.0009e^{-0.1781}}{0.5806s+1} & \frac{-1.7598e^{-0.1722}}{0.3349s+1} \end{bmatrix} \tag{4.47}$$

The decoupler was implemented and tested for the present system, and the performance of the decoupler is shown in Figure 4.9. During its first testing period, the input parameter aeration rate should affect only the output parameter DO concentration without altering the substrate concentration. Similarly, in the second instance, the input parameter recycle sludge flow, should only affect the substrate concentration without interacting with and affecting the output parameter, i.e., DO concentration. Figure 4.9 describes the time response by the system of two inputs and two outputs, where it can be noted that interaction among the loops reduces with interestingly quite intuitive action.

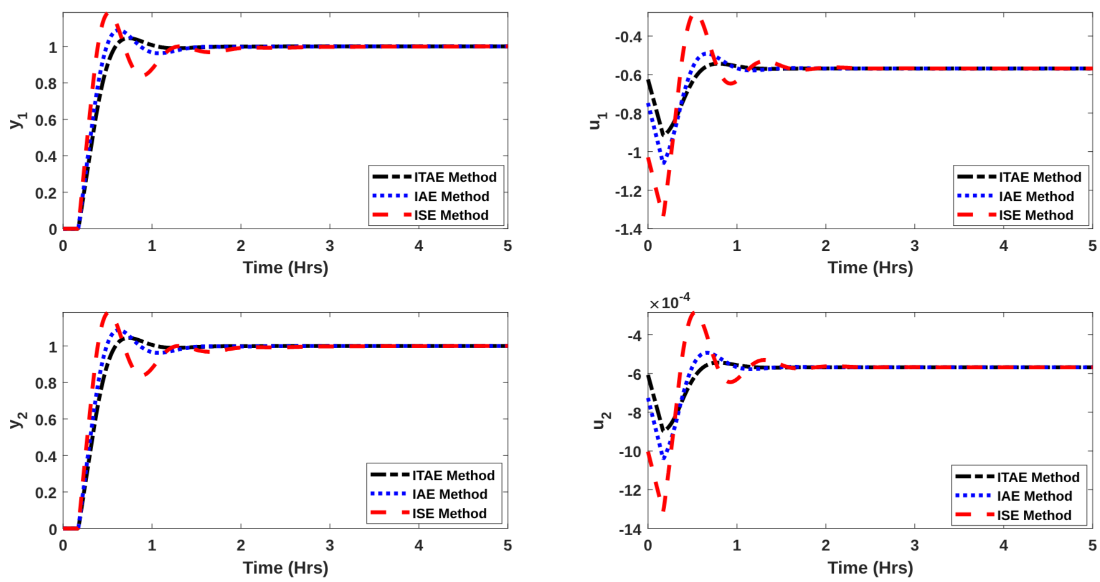

Figure 4.9 Closed loop performance of WWTP with Decoupler

Table 4.4 PI controller Settings

Decentralized controller				
	G_{c1}		G_{c2}	
Method	k_c	τ_I	k_c	τ_I
IAE criterion	1.3788	0.6445	1.9009	0.6359
ISE criterion	1.8767	2.5995	0.9108	0.9126
ITAE criterion	1.1746	0.5922	1.6195	0.5896
Decoupler				
IAE criterion	-0.7473	0.4047	-7.26E-04	0.3937
ISE criterion	-1.0296	0.5653	-0.001	0.55
ITAE criterion	-0.6249	0.3673	-6.07E-04	0.3572

There exist several methods for estimating the robustness of multivariable systems. One method that is easy to apply and compares the different control system stabilities is the inverse of the maximum singular value method (V. Vijay et al., 2012). For the present study, the illustrated robustness stability analysis has been evaluated and is shown in Figure 4.10. This plot describes the frequency plot of the inverse of the maximum singular value, which represents the stability of WWTP. The lower portion of the curve indicates the stability region, whereas the upper portion of the curve describes the instability region. Here, the area under the curve is directly proportional to stability, which indicates that the more area under the curve, the more stable the system's performance. All the methods give almost similar stability, both in the lower and higher frequency regions. It can be seen in the output uncertainty plot that the IAE method curve shows slightly more stabilization than the ISE method curve and almost similar stability conditions with the ITAE method.

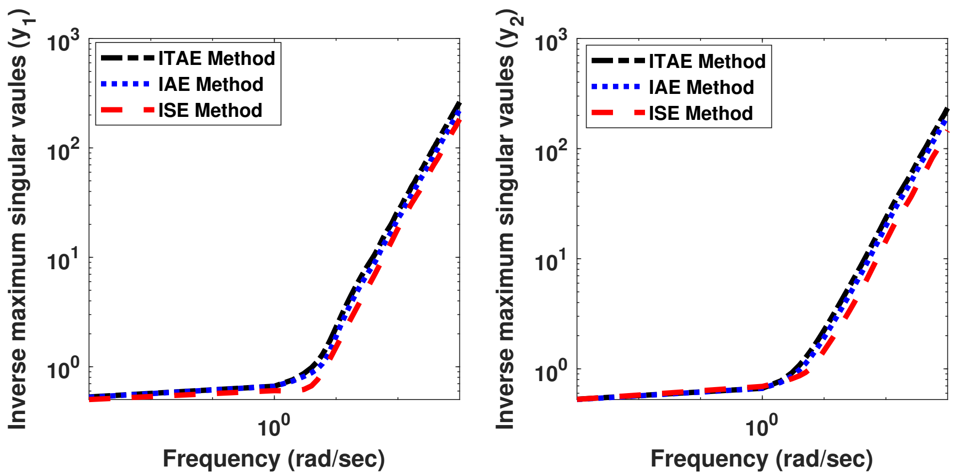

Figure 4.10 Input and Output sensitivity robustness

Table 4.5 Error Index for Decoupler

	y_1			y_2		
Method	IAE	ITAE	TV	IAE	ITAE	TV
IAE criterion	0.3128	0.0599	0.1789	0.3132	0.0600	1.58e-04
ISE criterion	0.3170	0.1116	0.4612	0.3164	0.1099	4.35e-04
ITAE criterion	0.3392	0.0614	0.0564	0.3393	0.0616	3.89e-05

Table 4.5 presents the outcome of quantitative analysis by adopting time integral errors (ITAE, ISE, and IAE) methods. It is clear that the time integral IAE method has better decoupler performance compared with the ITAE method, and the ISE method.

The IAE method has 1.34%, and 8.43% lesser percentage index value, in the IAE index; similarly, in the ITAE index, the IAE method has 86.31% and 2.50% lesser error percentage compared with ISE and ITAE methods, respectively, for output y_1. Identically, for output y_2 also the IAE method has a lesser error response when compared with the other two methods. In the IAE index, the percentage reduction for the IAE method is 1.02% and 8.33%, whereas, in the ITAE index, it is 83.16% and 2.16% reduction when compared with the ITAE method and ISE method, respectively. By comparing the Total Variance (TV) value from Table 4.5, it is clear that the ITAE method gives smoother controller performance when compared with the IAE and ISE methods.

Analysis of the robustness plots (Figure 4.11 and 4.12 right section) reveals a significant observation regarding the system's ability to withstand substantial perturbations while maintaining its stability. Despite subjecting the process parameters (process gain and time constant) to their most extreme magnitudes, with perturbation levels reaching a substantial $\pm$ 30%, the system demonstrates an impressive capacity for stability and prediction. It is apparent that the nominal curve is well within the range of permissible perturbation, whereas serving as robustness indicators, the red line curves act as critical thresholds, defining the upper and lower limits of the process gain and time constant variability. They serve as a tangible benchmark, offering precise guidance on the maximum permissible range of acceptable variability, essential for effective process control. From this uncertainty study, it was evident that the system can tolerate up to 333% variation in process gain, and 267% and 260% of the uncertainty in time constant, respectively. Correspondingly, the closed-loop responses from the process outputs also indicate that the system handles the perturbations exceptionally well caused by model uncertainty with a short oscillation at the beginning (Figure 4.11 and 4.12). It is also noted that the output y_2 response has less oscillation and faster-settling behaviour than the output y_1 response. From Table 4.6, it is observed that the lower and upper bound of worst-case peak gain is around 1.49 and 1.33 when the perturbation is provided to process gain and time constant, respectively. Whereas, 6.995 and 7.939 are two frequencies when the worst-case peak gain occurs for perturbation in process gain and time constant, respectively. *wcug* represents the value of uncertain elements that cause worst-case gain. Next, *wcu* and *wcug* represent the value of the destabilizing elements for uncertain elements and uncertain elements that cause a worst-case gain for stipulated uncertainty, respectively.

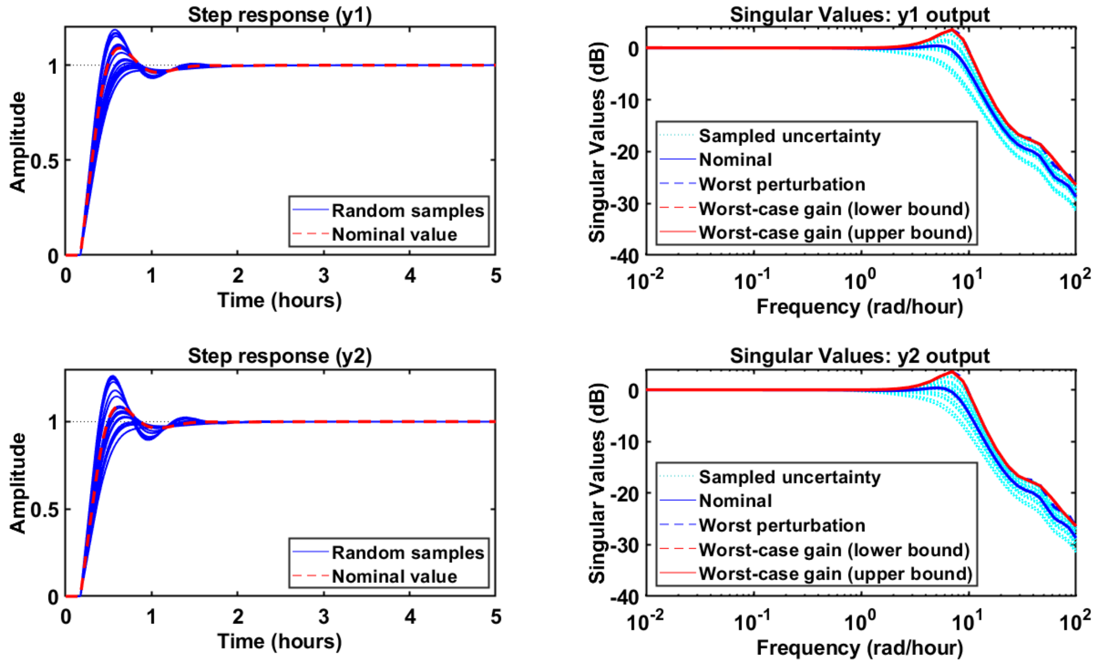

Figure 4.11 Closed loop step responses for 30% uncertainty in process gain (left-hand side), and Singular values for nominal, random samples, and worst-case gain for 30% uncertainty in process gain (right-hand side)(Decoupler)

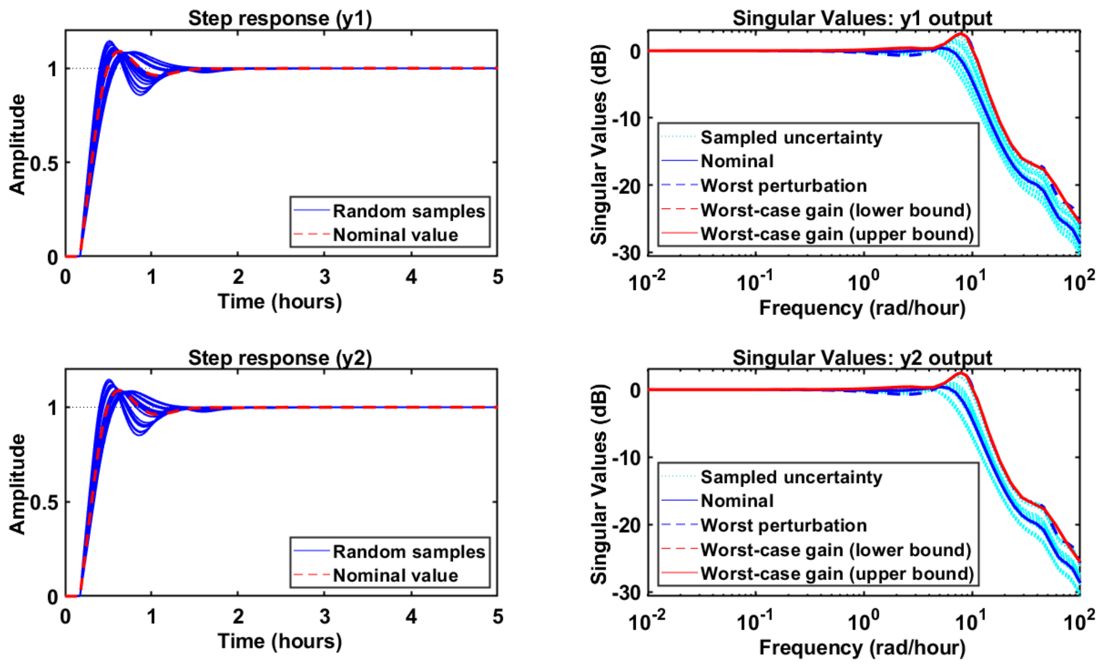

Figure 4.12 Closed loop step responses for 30% uncertainty in time constant (left-hand side), and Singular values for nominal, random samples, and worst-case gain for 30% uncertainty in time constant (right-hand side)(Decoupler)

Table 4.6 Worst-case gain scenario for Decoupler controller

Uncertainty	LB	UB	CF	*wcu*	*wcug*	Tolerance %
K_p	1.495	1.498	6.995	3.024E-11	-2.287E+03	y_1 - 333 y_2 - 333
τ	1.331	1.334	7.939	0.063	0.234	y_1 - 267 y_2 - 260

LB: Worst case gain lower bound, UB: Worst case gain upper bound,
CF: Critical frequency, wcu: Worst case peak gain at critical frequency,
wcug: Worst case gain at all specified frequency

4.4 Conclusion

This article presents a decentralized controller and decoupler controller design for an ASP system. The decentralized controller is mainly preferred for its simplicity, easier maintenance, and fewer tuning parameters when compared to the full multivariable controller. The implemented method utilizes a relative gain array concept, which is obtained by inversing the process transfer function matrix. The closed-loop control system was further improved by adopting a normalized gain array with an equivalent transfer function for each element of the process transfer function matrix. As stated earlier, by choosing a suitable control loop configuration, the interaction strength between two control loops can be nearly reduced. However, it is impossible to completely eliminate the interactions by selecting a favorable pair of manipulating variables.

In the present study, one can appreciate the ability of the controller to track the control parameters using their desired values in response to a step change of the substrate set-point and its robustness by neglecting the disturbances due to changes in kinetic parameters. Simulation studies of the closed-loop system of WWTP indicated that the controller designed based on IAE minimization criteria gives improved performance compared to ISE and ITAE minimization criteria methods. These observations were also supported by error indices, where the IAE method had the lowest error compared to the ITAE and the ISE methods, respectively. The robust stability and performance of the proposed controller are analyzed by undertaking a $\pm 30\%$ parametric uncertainty study for the time constant, and process gain in the normal system. This examination proved that even after providing the stipulated perturbation to process parameters the system retained its robust nature. This method was relatively simple, straightforward to be understood by practical control engineers, and can be easily embedded in the computer control system. To overcome the limitations of the decentralized controller, a decoupler controller is designed for the same ASP system. The closed-loop response was better than the decentralized controller since the decoupler considers a decoupled system that could manage system interactions effectively. In particular, the ITAE method produced almost negligible overshoot, undershoot, and settled faster than the IAE and ISE methods. By providing 30% perturbation to process gain, the system was tested for robustness with a decentralized and decoupler controller. The nominal and worst-case plots clearly showed that the system could tolerate up to 333% of perturbation. Supported by the closed-loop response behavior of two outputs with exceptionally fewer oscillations before achieving stable responses.

Chapter 5

CENTRALIZED CONTROLLER DESIGN FOR AN ASP

This chapter provides an introduction to centralized controllers and their crucial role in effectively managing multivariable processes. The initial section highlights the importance of these controllers and their significance in achieving control objectives. Furthermore, the section presents a comprehensive overview of two interaction methods, namely RNGA and dRGA, which serve as valuable tools for centralized PI controller design. The subsequent section focuses on a detailed design approach for these controllers, offering practical guidelines for implementation. In order to evaluate the effectiveness of the aforementioned methods, a simulation study is performed, comparing their performance and highlighting key insights. Additionally, robust uncertainty analysis is performed to assess the system's resilience against perturbations in process parameters. Finally, the last section summarizes all the obtained results and offers in-depth discussions regarding the centralized PI controller study for an ASP (Activated Sludge Process) system.

5.1 Introduction

The MIMO process with interacting loops stands as the most prevalent process in various process control industries. Its primary objective is to attain exceptional product quality while optimizing energy and material consumption. However, designing a controller that takes into account the interaction among process variables poses significant challenges. Decentralized controllers have gained widespread usage due to their simplicity and ease of operation. To ensure system stability, decentralized controllers are typically loosely tuned, which can impact their efficiency and performance, particularly for systems with mild or less interactive loops. During the course of the study, a decoupled controller was introduced to transform the MIMO system into individual SISO systems, enabling separate controller designs for each component. Subsequently, Ram and Chidambaram combined these decoupled controllers to form a single centralized controller, utilizing a steady-state gain matrix as a basis for integration (V. Dhanya and Chidambaram, 2015). Further advancements led to the direct design of a centralized controller, which exhibited even better performance compared to the combined decoupled controller, even for higher-order multivariable systems (Xiong et al., 2007; X. et al., 2014). Consequently, the centralized controller surpasses both the decentralized and decoupled controllers in terms of performance for interactive MIMO systems (Ghosh and Pan, 2021).

Initially, E. Davison proposed the centralized PI controller design that used just a steady-state gain matrix yet lacked empirically derived controller settings (Davison, 1976). Later by adopting a trial and error approach V. Ram et al., (V. Dhanya and Chidambaram, 2015) further refined the tuning parameters that were suggested by E. Davison. This was further extended to the non-square and unstable MIMO system by K. Sarma et al., (Sarma and Chidambaram, 2013) and V. Ram et al., (V. Dhanya and Chidambaram, 2015). The other simple and popular detuning technique named Biggest Log Modulus tuning (BLT) method was proposed by Luyben (1976) (Luyben, 1986). Eventually, during the last decade, Equivalent Transfer Function (ETF) based controller design has attracted many researchers due to their simple approach (Luan et al., 2015; Shen et al., 2014). V. Kumar et al.,(V. Vijay et al., 2012) suggested ETF-based centralized controller (2×2) design from multi-loop Direct Synthesis (DS) method (Truong and Moonyong, 2010b). However, the complexity of controller tuning increased with the increase in the order of the process. In fact, the ETF-based dRGA method was first presented by Witcher and Mc Avoy (Witcher and McAvoy, 1977) in 1977 where they considered transfer function by replacing the traditional steady-state model, and the RNGA method by He et al. (2009) (Mao et al., 2009). These methods are simple, and easy to implement (Truong and Moonyong, 2010b) but cannot be implemented on the non-square system due to its difficulties in ETF parametrization.

Even though the RNGA method was easy for calculations in practical applications, it was limited to multivariable systems making it only suitable for industrial processes.

The dRGA pairing method considers the process dynamics by overcoming the limitations of the RGA-based loop pairing technique that often uses conjunction with Niederlinski index (NI) to assure system stability. Since the dRGA considers the dynamics so it also takes care of disturbance caused in the MIMO process. In dRGA, the perfect control actions at all frequencies are attained by the denominator, while the numerator is a simple open-loop transfer function. The dRGA method can be useful if at all it involves relatively less interaction among the controller actions (Mc Avoy et al., 2003). Even though these methods include several tuning parameters, these methods are widely adopted in industrial processes due to their simple, straightforward forward, and easy-to-implement operations.

As evident from the above discussions, the current study on WWTP adopts a centralized controller that offers more freedom, plus overcomes the limitation of decoupler for stability challenges as compared to decentralized controller design (Sanjith and Rao, 2020). An ETF-based controller which is easy to implement in real-world engineering processes was considered here. In this chapter, two methods namely RNGA (Shen et al., 2014) and dRGA (Yadav et al., 2020) were adopted for designing a centralized PI controller for an ASP system. The study considers multivariable PI controller since it is a promising alternative for these complex controllers. Full matrix PI controller can constructively achieve the desired performance and independent set-point tracking with interaction suppression goals. The study aims at controlling the effluent DO and Substrate concentration by manipulating the aeration rate and recycle sludge flow rate. The study employs two ETF-based methods to demonstrate the effectiveness of the designed centralized PI controller supported by performance indices and robustness analysis.

5.2 Methodology

The transfer function for the TITO system of size 2 $\times$ 2 with s-domain is represented by $G_p(s)$. This multivariable system is defined as

$$Y(s) = G_p(s) \cdot U(s) \tag{5.1}$$

Here, the output variable is the vector denoted by Y, U is manipulated variable and the transfer function matrix ($n \times n$) is designated as G_p. In this study each transfer function $G_{p,ij}(s)$ is considered as First Order Plus Time Delay (FOPTD) system.

$$G_p = \begin{bmatrix} g_{11} & g_{12} \\ g_{21} & g_{22} \end{bmatrix} \tag{5.2}$$

Accordingly, the 2 × 2 system with a centralized control structure is shown in Figure 1, representing the control structure and corresponding feedback loop. All the manipulated variables are calculated simultaneously by utilizing a single control algorithm in the centralized control system. Converting all higher-order transfer functions to FOPTD is the crucial preliminary stage while designing a centralized controller. The centralized controller matrix can be given by,

$$G_c(s) = \begin{bmatrix} G_{c11} & G_{c12} \\ G_{c21} & G_{c22} \end{bmatrix} \tag{5.3}$$

In this study, the PI Controller type is considered for designing the centralized controller, and it is expressed as

$$G_{C_{ij}} = K_{C_{ij}} \left(1 + \frac{1}{\tau_{ij}} s\right) \tag{5.4}$$

where, $K_{c_{ij}}$ and τ_{ij} are controller gain and integral time constants respectively for i^{th} and j^{th} (i, j = 1, 2) controller. In order to assist the design of the control system, the

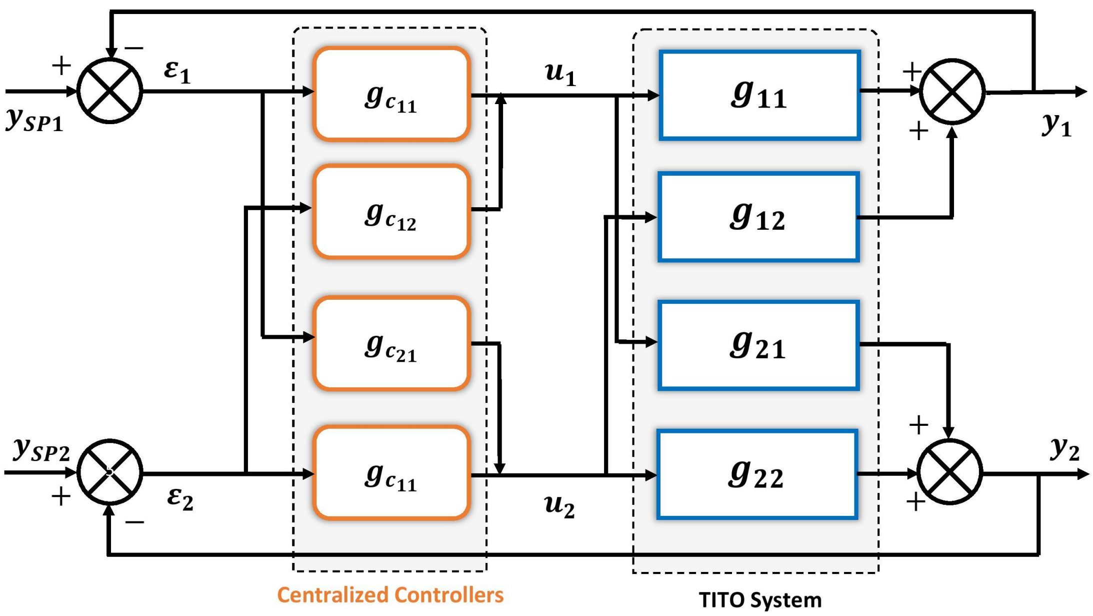

Figure 5.1 Centralized scheme of multivariable system with PI controller

responses from the higher-order processes are simplified to the FOPTD model either by empirical or analytical approach in the below section.

5.3 Effective open-loop Transfer Function (EOTF)

Once the FOPTD model is developed through the PRC method (as discussed in Chapter-4) the next step is to obtain the EOTF elements. Consider a 2 $\times$ 2 system, wherein the input-output relations for the process are given by

$$y_1 = g_{11}(s)u_1 + g_{12}(s)u_2 \tag{5.5}$$

$$y_2 = g_{21}(s)u_1 + g_{22}(s)u_2 \tag{5.6}$$

From the block diagram shown in Figure 5.1, the open loop transfer function for the control variable y_1, and manipulated variable u_1, is defined as,

$$\frac{y_1(s)}{u_1(s)} = G_{11}(s) \tag{5.7}$$

In the case of the closed-loop, it is

$$y_1 = G_{11}u_1 + G_{c2}G_{12}(s)y_2 \tag{5.8}$$

Similarly,

$$y_2 = G_{21}u_1 + G_{c2}G_{22}(s)y_2 \tag{5.9}$$

$$y_2 = \frac{G_{21}u_1}{1 + G_{c2}G_{22}} \tag{5.10}$$

Substituting value of y_2 from equation 5.10 in equation 5.8, we get

$$y_1 = G_{11}u_1 - \frac{G_{c21}G_{12}G_{21}u_1}{1 + G_{c2}G_{22}} \tag{5.11}$$

$$\frac{y_1}{u_1} = G_{11} - \frac{G_{c21}G_{12}G_{21}}{1 + G_{c2}G_{22}} \tag{5.12}$$

Two assumptions are made to reduce the above-complicated relationship. First, the study achieves a perfect controller approximation for the other loop. Second, the respective ETFs have the same structure as the corresponding open-loop model.

$$\frac{G_{cij}G_{ij}}{1 + G_{cij}G_{ij}} = 1,\ i = 1,2 \tag{5.13}$$

Hence, we get

$$\frac{y_1}{u_1} = G_{11} - \frac{G_{12}G_{21}}{G_{22}} = G_{11}^{eff} \tag{5.14}$$

Similarly, when the first loop is closed, the transfer function relating u_2 with y_2 may be expressed as

$$\frac{y_2}{u_2} = G_{22} - \frac{G_{21}G_{12}}{G_{11}} = G_{22}^{eff} \tag{5.15}$$

But the effective open-loop transfer functions (G_{11}^{eff} and G_{22}^{eff}) are complicated and cannot be used directly for the controller design. Hence to adopt EOTF for controller design, it is further reduced to FOPTD models using Maclaurin Series. The present study utilizes RNGA and dRGA concepts to derive the ETF expressions for higher-order systems.

5.4 Equivalent Transfer Function (ETF)

As discussed earlier, the controller is designed by estimating the FOPTD model for a simplified open-loop stable system, using analytical or empirical methods. ETF methods are easy and simple to implement in real-world conditions. Based on the ETF of a closed-loop system, the controller can be designed using existing PI tuning methods. Through RNGA and dRGA methods, the parameters of the ETF model can be easily estimated and are explained in the following sections.

5.5 RNGA Method

The Relative Normalized Gain Array (RNGA) is defined as the ratio of normalized gain to the average residence time for loop i - j. While average residence time represents the response time of a control variable for change in manipulated variables, which can be estimated by (τ + θ). The procedure involved in designing the PI controller using the RNGA method is comprehensively explained in this section. The study utilizes Relative Gain Array (RGA), Relative Normalized Gain Array (RNGA), and Relative Average Residence Time Array (RARTA) concepts to derive the ETF. Mathematically, RGA can be secured by taking a fraction of the open loop gain to the closed loop gain of each element, between the same two variables when all other loops are closed.

$$\Lambda_{ij} = \frac{\text{gain when all other loops are open}}{\text{gain when all other loops are closed}} = \frac{\left(\frac{\partial y_i}{\partial u_j}\right)_{u_{k\neq j}}}{\left(\frac{\partial y_i}{\partial u_i}\right)_{y_{k\neq j}}} \tag{5.16}$$

RGA contains each element of Λ_{ij}. The value closer to unity is selected as the best pairing in a row vector of the RGA Matrix. Meanwhile, the negative values should not be considered for pairing and even the sum of all values within a row should be equal to 1. Transfer function matrix can be used to formulate similar expression $G(s) = g_{ij} = (\frac{\partial y_i}{\partial u_j})_{y_k}$, and its inverse will be $G^{-1}(s) = \hat{g}_{ij} = (\frac{\partial y_i}{\partial u_j})_{y_k}$ as

$$\Lambda(G) = \{\Lambda_{ij}\} = \{g_{ij}\hat{g}_{ij}\} = G(s) \otimes G^{-T}(s) = \begin{bmatrix} \Lambda_{11} & \Lambda_{12} \\ \Lambda_{21} & \Lambda_{22} \end{bmatrix} \tag{5.17}$$

The Hadamard Product is denoted by $\otimes$. Accordingly, the inverse form of transfer function matrix elements will be

$$G^{-T}(s) = \hat{g}_{ij} = \frac{\Lambda_{ij}}{g_{ij}} \tag{5.18}$$

The normalized gain ($K_{N_{ij}}$) in terms of dynamic properties of a particular transfer function ($g_{ij}(s)$) is given by,

$$K_{N_{ij}} = \frac{k_{ij}}{\sigma_{ij}} = \frac{k_{ij}}{(\tau_{ij} + \theta_{ij})} \tag{5.19}$$

And the normalized gain matrix is calculated as,

$$NGA = K_N = \begin{bmatrix} K_{N,11} & K_{N,12} \\ K_{N,21} & K_{N,22} \end{bmatrix} = \begin{bmatrix} \frac{k_{11}}{(\tau_{11} + \theta_{11})} & \frac{k_{12}}{(\tau_{12} + \theta_{12})} \\ \frac{k_{21}}{(\tau_{21} + \theta_{21})} & \frac{k_{22}}{(\tau_{22} + \theta_{22})} \end{bmatrix} \tag{5.20}$$

Where average residence time is given by $\sigma_{ij} = \tau_{ij} + \theta_{ij}$ that represents the response speed of the control variable to manipulated variable.

RNGA can be formulated using the normalized gain matrix as follows,

$$RNGA = \phi = K_N \otimes K_N^{-T} \tag{5.21}$$

here,

$$\phi = \begin{bmatrix} \phi_{11} & \phi_{12} \\ \phi_{21} & \phi_{22} \end{bmatrix} \tag{5.22}$$

Then, the Relative Average Residence Time Array (RARTA) is derived from the ratio of RNGA and RGA and given by

$$\phi = \begin{bmatrix} \phi_{11} & \phi_{12} \\ \phi_{21} & \phi_{22} \end{bmatrix} \tag{5.23}$$

Each element of the matrix can be obtained from

$$\gamma_{ij} = \frac{\hat{\sigma}_{ij}}{\sigma_{ij}} \tag{5.24}$$

This can also be written as

$$\hat{\sigma}_{ij} = \sigma_{ij}\gamma_{ij} = \tau_{ij}\gamma_{ij} + \theta_{ij}\gamma_{ij} \tag{5.25}$$

$$= \hat{\tau}_{ij} + \hat{\theta}_{ij} \tag{5.26}$$

The time constant and time delay are considered when other loops are closed. Ultimately, the above-discussed procedure is adapted to approximate elements of the transfer function matrix that has the same form as the open-loop transfer function. An illustrative step-by-step procedure for the RNGA method is presented as flowcharts in Figure 5.2.

5.6 dRGA Method

This approach utilizes the ETF of a multivariable process. The normalized steady state gain matrix of G(s) is given by

$$K_N = K \odot T_{AR} \tag{5.27}$$

here, the average residence time of $g_{ij}(s)$ is represented as $K = [g_{ij}(0)]_{mxn}$, $T_{AR} = [\tau_{ar.ij}(s)]_{nxm}$. Accordingly, a steady state gain matrix of $\hat{G}(s)$ is expressed as

$$\hat{K}_N = \hat{K} \odot \hat{T}_{AR} \tag{5.28}$$

The generalized relative gain array (GRGA) for MIMO system is calculated as

$$\Lambda = K \otimes K^{\dagger T} \tag{5.29}$$

here the pseudo inverse matrix of K = G (0) is indicated by $K^{\dagger}$. Subsequently, the Generic Relative Normalized Gain Array (GRNAGA) is estimated as

$$\Lambda_N = K_N \otimes \hat{K}_N = K_N \otimes K_N^{\dagger^T} \tag{5.30}$$

By considering the equations (5.28), (5.28) in equation (5.30), we get

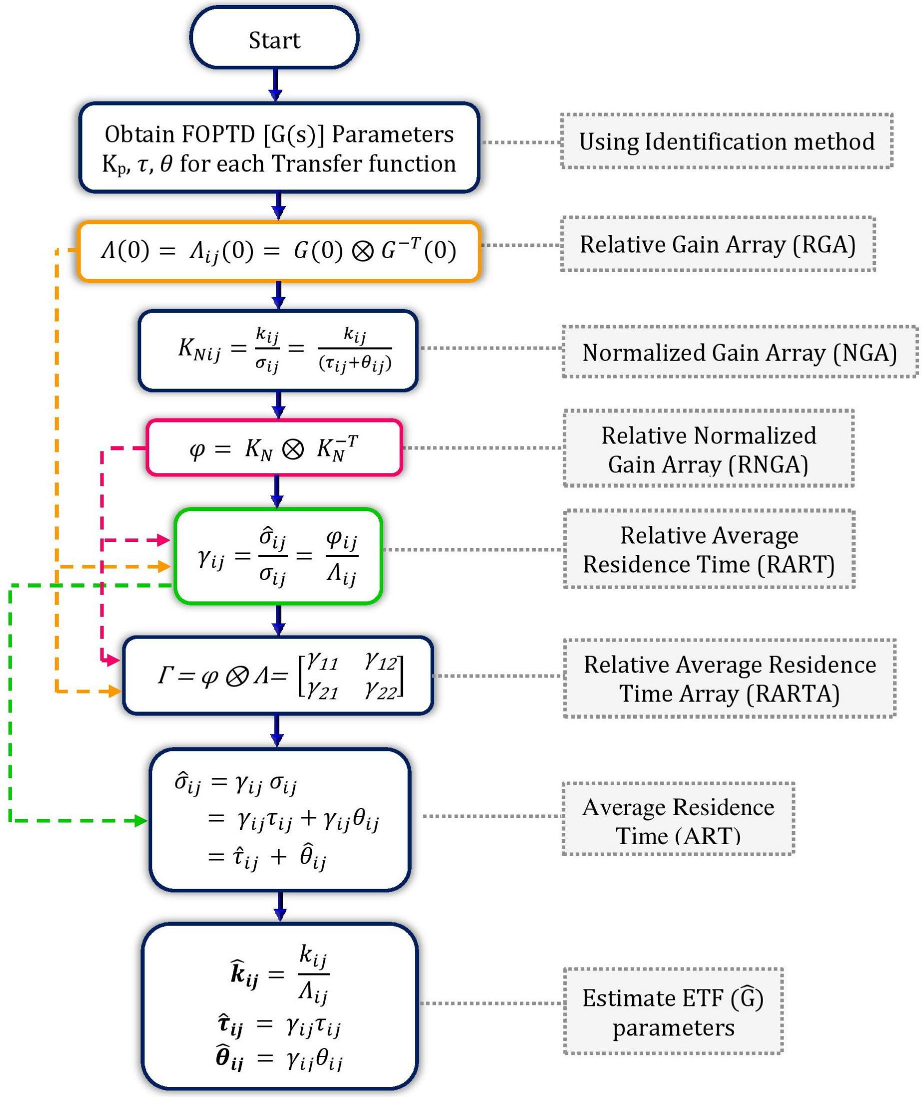

Figure 5.2 Methodology flowchart for RNGA method

$$\Lambda_N = \Lambda \odot \Gamma \tag{5.31}$$

wherein, the RARTA, is defined as

$$\Gamma = [\gamma_{ij}]_{nxm} = \hat{T}_{AR} \odot T_{AR} \tag{5.32}$$

Hence, by utilizing equation (5.30) and (5.32), the equivalent transfer matrix parameters can be expressed as

$$\hat{K} = K \odot \Lambda \tag{5.33}$$

Followed by

$$\hat{T}_{AR} = T_{AR} \otimes \Gamma \tag{5.34}$$

Meanwhile the average residence time matrix of $\hat{g}_{ij}(s)$ can be estimated as

$$\hat{T}_{AR} = \hat{T} + \hat{\Theta} \tag{5.35}$$

Where, time delay $\hat{\Theta} = [\hat{\theta}_{ij}]_{mxn}$ and the time constant of equivalent transfer function matrix $\hat{T} = [\hat{\tau}_{ij}]_{nxm}$ can be also written as

$$\hat{T} = \hat{T}_{AR} - \hat{\Theta} \tag{5.36}$$

$$\hat{\Theta} = \Theta \otimes \Gamma \tag{5.37}$$

Remarks: If there prevails a condition where in zero is divided by zero terms, when $\hat{g}_{ij}(s) = 0$, the ETF of $\hat{g}_{ij}(s)$ is modeled as

$$\hat{g}_{ij}(s) = \hat{k}_{ij} \tag{5.38}$$

Eventually, the generalized form of Relative Dynamic Gain Array (RDGA) for a TITO system is given by

$$\Lambda(s) = G(s) \otimes \hat{G}(s) \tag{5.39}$$

The above-discussed RNGA and dRGA concepts lay the foundation for centralized control design methodology. These obtained ETF parameters are considered while designing the centralized controller by the existing PI tuning rule as discussed in the section below.

5.6.1 Multivariable PI Controller design

The ideal multivariable process control can be related by the following expression

$$G_c(s)G(s) = \frac{1}{s} \Leftrightarrow g_{c,ij}(s)\hat{g}_{ji}(s) = \frac{1}{s} \tag{5.40}$$

The target of the multivariable process control problem

$$G_c(s)G(s) = \begin{bmatrix} \dfrac{k_{\alpha,1}e^{-l,s}}{s} & \\ & \dfrac{k_{\alpha,2}e^{-l,s}}{s} \end{bmatrix} \tag{5.41}$$

This can be calculated by designing a single-loop controller as

$$g_{c,ij}(s)\hat{g}_{ji}(s) = \frac{k_{\alpha,j}e^{-l,s}}{s} \tag{5.42}$$

where, l_j = min $\hat{\theta}_{ji}, I = 1,2,3...,n$; are the regulatory parameters and $0 < k_{\alpha,j} \leq 1$..

$$g_{c,ij}(s) = \frac{I}{s}F(s) \tag{5.43}$$

F value is obtained from the below expression

$$F_{ji}(s) = \frac{k_{\alpha,j}e^{-l,s}}{\hat{g}_{ji}(s)} = \frac{k_{\alpha,j}}{\overline{\hat{g}}_{ji}(s)} \tag{5.44}$$

By using the Maclaurin series above equation can be expanded followed by the controller equation from it

$$g_{c,ij}(s) = \frac{1}{s}[F_{ji}(0) + sF'_{ji}(0) + s^2F''_{ji}(0) + ...] \tag{5.45}$$

From F_{ji} values, equation (5.44) can be written as

$$g_{c,ij}(s) = \frac{k_{\alpha,j}/\overline{\hat{g}}_{ji}(0)}{s}\left[1 - s\frac{\overline{\hat{g}}'_{ji}(0)}{\overline{\hat{g}}_{ji}(0)} + s^2\left(2\frac{\overline{\hat{g}}'^2_{ji}(0)}{\overline{\hat{g}}^2_{ji}(0)} - \frac{\overline{\hat{g}}''_{ji}(0)}{\overline{\hat{g}}_{ji}(0)}\right) + ...\right] \tag{5.46}$$

The standard form of PI controller is expressed as

$$g_{c,ij}(s) = k_{c,ij} + \frac{k_{I,ij}}{s} \tag{5.47}$$

here, $k_{c,ij}$ and $k_{i,ij}$ indicates two control variables. These controller parameters are derived by comparing the following equations

$$k_{c,ij} = k_{\alpha,j}\overline{\hat{g}}_{ji}(0)/\overline{\hat{g}}^2_{ji}(0) \tag{5.48}$$

$$k_{i,ij} = k_{\alpha,j}/\overline{\hat{g}}_{ji}(0) \tag{5.49}$$

Therefore, the designed PI controller can be given by comparing ETF elements with the FOPTD model,

$$k_{c,ij} = k_{\alpha,j}(\hat{\tau}_{ar,ji} - l_j)/\hat{k}_{ji} \tag{5.50}$$

$$k_{i,ij} = k_{\alpha,j}/\hat{k}_{ji} \tag{5.51}$$

A descriptive step-by-step algorithm briefing the methodology for the dRGA method is presented as flowcharts in Figure 5.3.

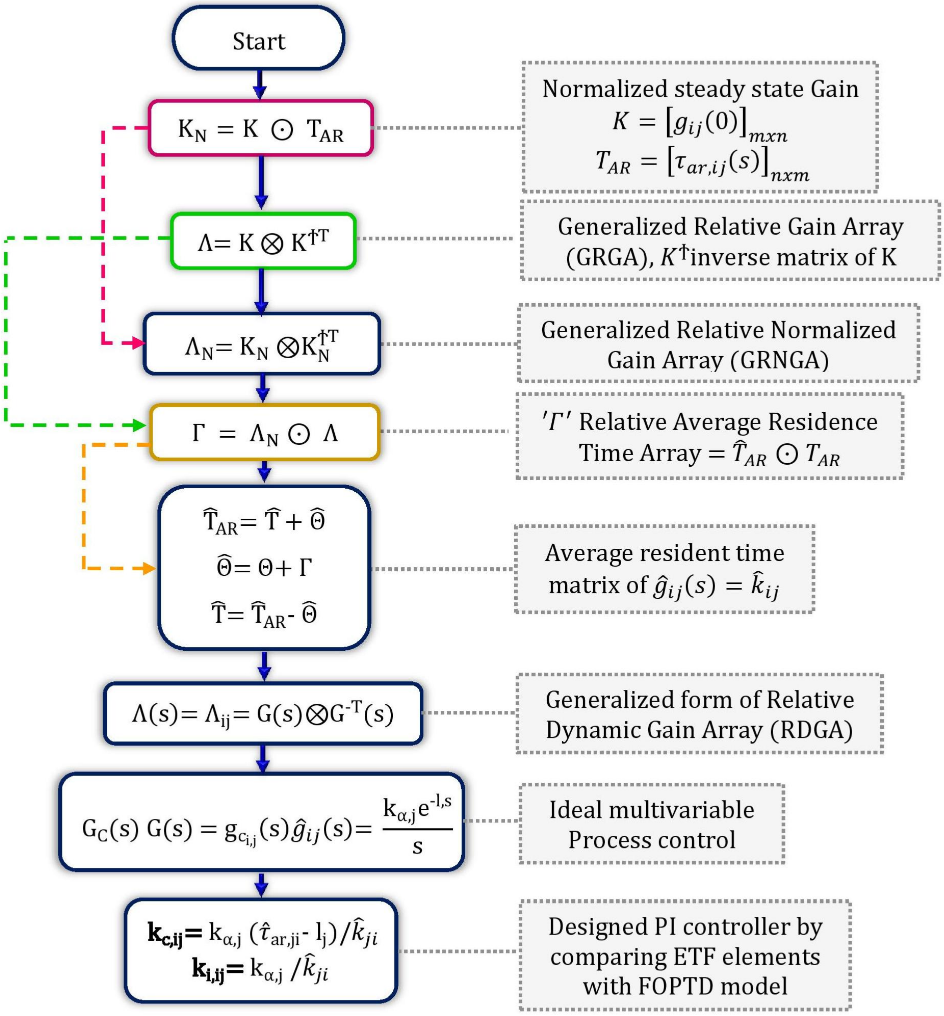

Figure 5.3 Methodology flowchart for dRGA method

5.7 Simulation studies

The purpose of the study is to design a centralized controller to govern the dissolved oxygen (y_1) and substrate (y_2) concentration by manipulating aeration rate (u_1) and recycle sludge flowrate (u_2). Since there exists interaction among each manipulated variable, selecting a suitable pairing will avoid the complication. Controlling the MIMO system like ASP is a tedious task since the interactions within the system have to be addressed (Ujjwal et al., 2017). A skilled operator is required to tune the centralized controller because it requires pairing of input-output variables and trial of error steps (Reddy et al., 1997).

Several simulation studies were executed to understand the performance of the designed centralized controllers with respective tuning strategies. The model input and kinetic parameters considered for the study are recorded in Table 4.1 (refer to Chapter - 4). The study considers the following equation of transfer function obtained through the PRC method:

$$G(s) = \begin{bmatrix} \frac{1.796e^{-0.0491s}}{0.0201s+1} & \frac{0.0017e^{-0.1271s}}{0.0603s+1} \\ \frac{-0.8429e^{-0.0361s}}{0.0134s+1} & \frac{-149.478e^{-0.1473s}}{0.0603s+1} \end{bmatrix} \tag{5.52}$$

5.7.1 RNGA Method

As discussed in the above section the following are estimated Relative Average Residence Time Array (RARTA), Normalized Gain Array (NGA), Relative Normalized Gain Matrix (RNGA)

$$RARTA(\Gamma) = \begin{bmatrix} 1.0000 & 1.5487 \\ 1.5487 & 1.0000 \end{bmatrix}, \quad NGA(K_N) = \begin{bmatrix} 25.9538 & 0.0091 \\ -17.028 & -720.028 \end{bmatrix},$$

$$RNGA(\phi) = \begin{bmatrix} 1.000 & -8.266e^{-6} \\ -8.266e^{-6} & 1.000 \end{bmatrix}$$

By the above-obtained values, the deduced ETF model parameters are given by

$$\hat{K}_c = \begin{bmatrix} 1.7960 & -318.496 \\ 1.579e^{05} & -149.477 \end{bmatrix}, \hat{\tau} = \begin{bmatrix} 0.0201 & 0.0934 \\ 0.0208 & 0.0603 \end{bmatrix}, \hat{\theta} = \begin{bmatrix} 0.0491 & 0.1968 \\ 0.0559 & 0.1473 \end{bmatrix}$$

Hence, the estimated ETF can be expressed as

$$G(s) = \begin{bmatrix} \frac{1.796e^{-0.0491s}}{0.0201s+1} & \frac{-318.496e^{-0.1968s}}{0.00934s+1} \\ \frac{-1.5792e^{-0.0559s}}{0.0208s+1} & \frac{-149.478e^{-0.1473s}}{0.0603s+1} \end{bmatrix} \tag{5.53}$$

5.7.2 dRGA Method

The following are outcomes of dRGA analysis particularly, Relative Average Residence Time Array (RARTA), Normalized Gain Array (NGA), Generalized Relative Normalized Gain Matrix (RNGA)

$$RARTA(\Gamma) = \begin{bmatrix} 1.0000 & 0.6457 \\ 0.6457 & 1.0000 \end{bmatrix}, \qquad NGA(K_N) = \begin{bmatrix} 0.1243 & 3.1857e^{-04} \\ -0.0417 & -31.0316 \end{bmatrix}$$

$$RNGA(\phi) = \begin{bmatrix} 1.000 & -3.1858e^{-04} \\ -3.4465e^{-06} & 1.000 \end{bmatrix}$$

The K_α value estimated after optimization is given below

$$K_\alpha = \begin{bmatrix} 8.9665 & 2.6004 \end{bmatrix} \tag{5.54}$$

By the above-obtained values, the deduced ETF model parameters are given by

$$\hat{K}_c = \begin{bmatrix} 1.7960 & -318.496 \\ 1.5792e^{05} & -149.477 \end{bmatrix}, \qquad \hat{\tau} = \begin{bmatrix} 0.0201 & 0.0389 \\ 0.0087 & 0.0603 \end{bmatrix}$$

$$\hat{\theta} = \begin{bmatrix} 0.0491 & 0.0821 \\ 0.0233 & 0.1473 \end{bmatrix}$$

Hence, the estimated ETF can be expressed as

$$G(s) = \begin{bmatrix} \dfrac{1.796e^{-0.0491s}}{0.0201s+1} & \dfrac{-318.496e^{-0.0821s}}{0.0389s+1} \\ \dfrac{-1.5792e^{-0.0234s}}{0.0087s+1} & \dfrac{-149.478e^{-0.1473s}}{0.0603s+1} \end{bmatrix} \tag{5.55}$$

The controller sets obtained from the RNGA and dRGA methods are shown in Table 5.1.

Table 5.1 PI controller settings from RNGA and dRGA methods

Method	K_c	K_i
RNGA	$\begin{bmatrix} 0.1188 & -0.0005 \\ 1.3517 & -0.0011 \end{bmatrix}$	$\begin{bmatrix} 1.4765 & -0.0079 \\ 1.6592 & -0.0168 \end{bmatrix}$
dRGA	$\begin{bmatrix} 0.1004 & -6.8125e^{-08} \\ 0.0020 & -0.0030 \end{bmatrix}$	$\begin{bmatrix} 4.9925 & 1.6467e^{-05} \\ -0.0282 & -0.0174 \end{bmatrix}$

Figure 5.4 shows the responses of process output and controller performance for set point change at y_{r1}. The designed controller had good set-point tracking and fast disturbance rejection action with minimum settling time. Since controllers are tuned for good disturbance rejection, both methods produced extremely low or negligible overshoot and undershoot. It can be observed that the dRGA method provided better process output and controller output performances when compared with the RNGA method. Even the response action of the dRGA method is quicker than the RNGA method. Similarly, Figure 5.5 presents the process output and controller performance response for set point change at y_{r2}. From the figure, it is clearly noticeable that the dRGA method provides smooth process output and controller output performances when compared with the RNGA method. In addition, here also the dRGA method has faster response behavior when compared with the RNGA method.

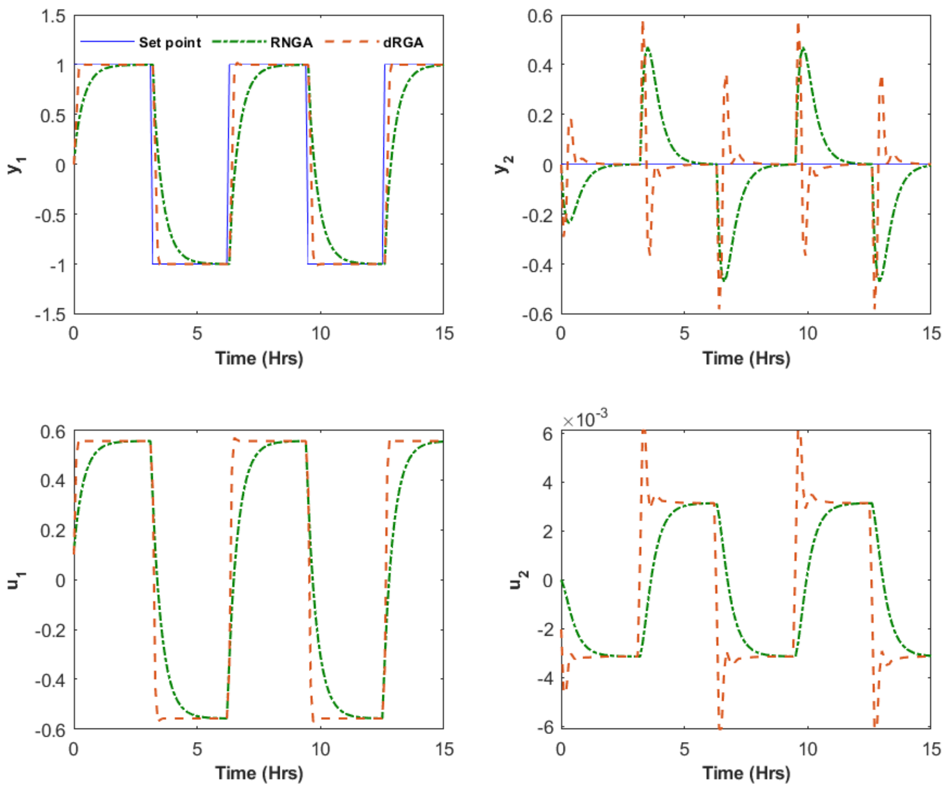

Figure 5.4 Closed loop performance for change in y_1

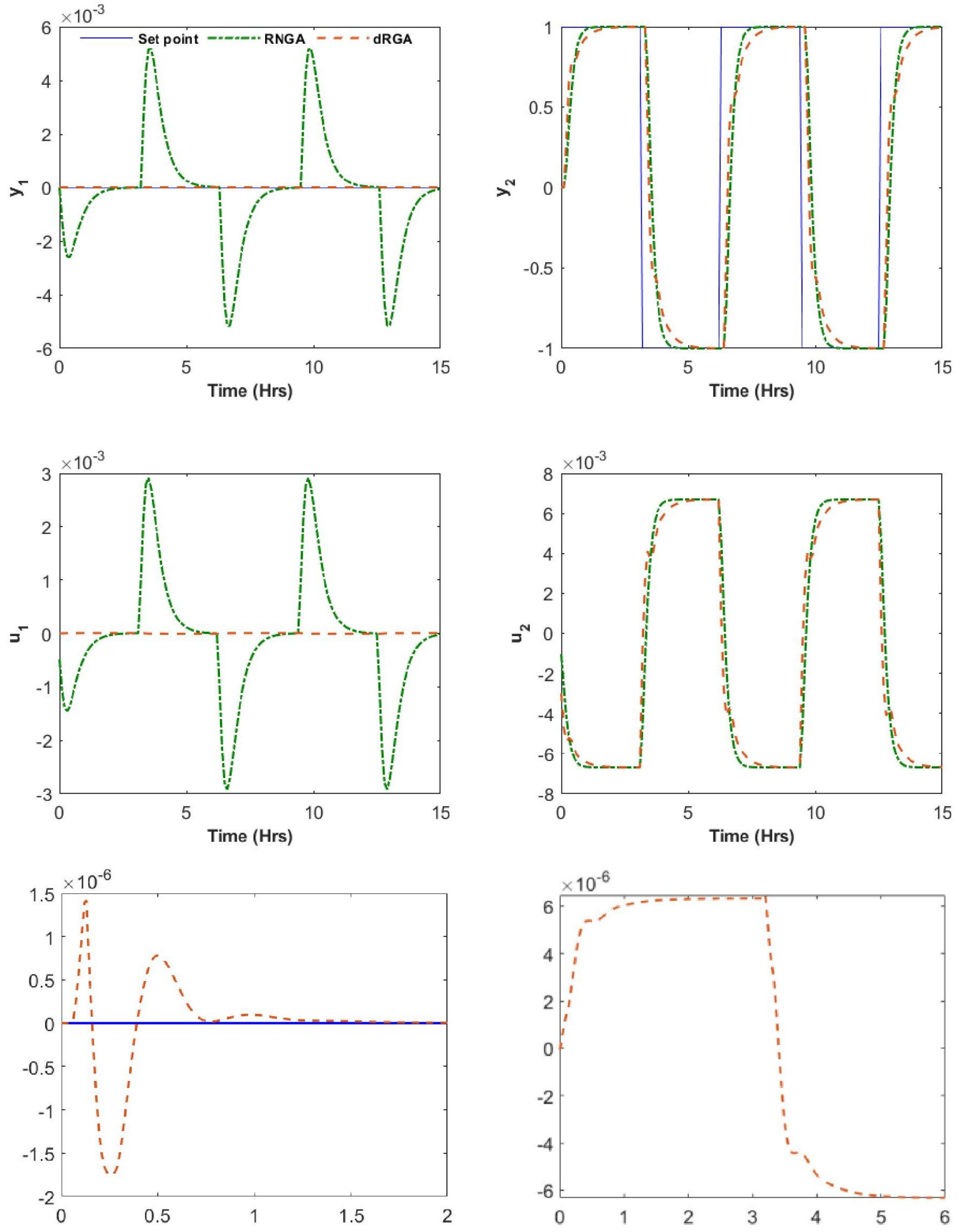

Figure 5.5 Closed loop performance for change in y_2

The closed-loop response of the designed control system is presented in Figure 5.6 for a perturbation provided at d_1. The dRGA method yields more favorable responses with faster dynamics compared to the RNGA method. However, a slightly higher level of oscillation is observed for the dRGA method when compared to the RNGA method. Consequently, Figure 5.7 illustrates the closed-loop response of the process output and controller behavior for a perturbation provided at d_2. The dRGA method demonstrates faster settling time, lower overshoot, and reduced oscillation compared to the RNGA method. Thus, the dRGA method provides acceptable responses for both the process output and controller output when compared with the RNGA method.

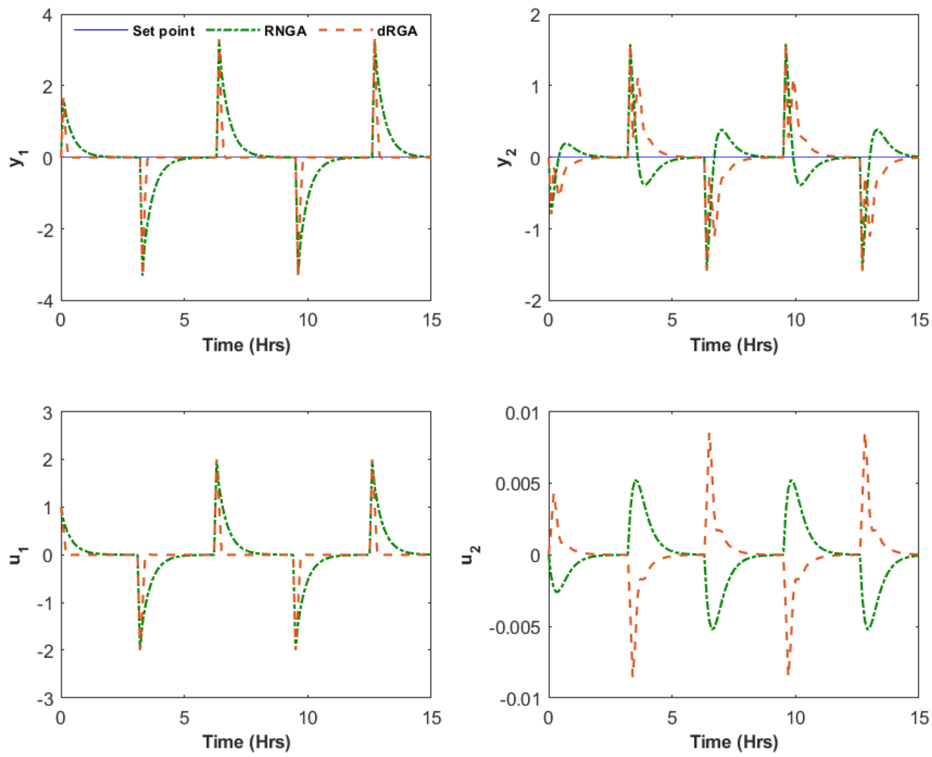

Figure 5.6 Closed loop performance for change in d_1

Table 5.2 illustrates the results of performance index analysis using TIE. The study considers three commonly used error indices, namely IAE, ITAE, and ISE, along with the TV index. The dRGA method exhibits significantly lower error indices and TV values compared to the main responses and interactions for a centralized control scheme. Notably, the dRGA method achieves a remarkable reduction in IAE indices of 79.36% and 4.04% when a step change is applied to y_{r1} and y_{r2}, respectively, compared to the RNGA method. Similarly, the ITAE indices decrease by 79.80% and 2.86% for step changes in y_{r1} and y_{r2}, respectively. The ISE indices also exhibit decreased error values of 44.75% and 0.1% for step changes in y_{r1} and y_{r2}. Moreover, the evaluation of TV indices demonstrates favorable results for the dRGA method in comparison to the RNGA method.

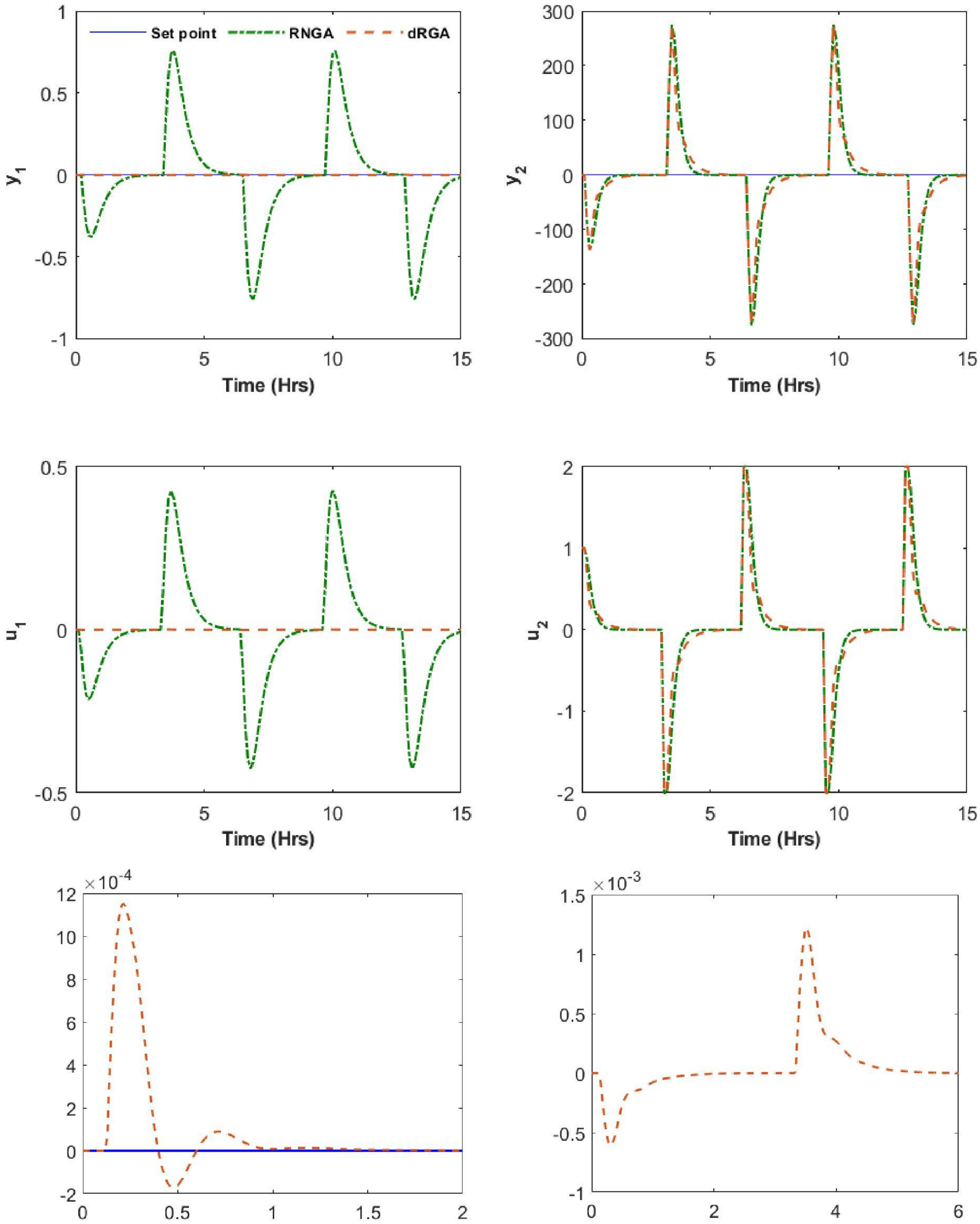

Figure 5.7 Closed loop performance for change in d_2

The stability of the system is examined through robustness analysis (Figure 5.8). The area underneath the curve indicates the stability region, whereas the area above the curve represents instability. Accordingly, the dRGA method is exceptionally robust and stable since the area under the curve is substantially more than the RNGA method. Thus the dRGA method proves to be simple, and effective and offers significantly better control performances than the RNGA method for highly non-linear systems like ASP systems.

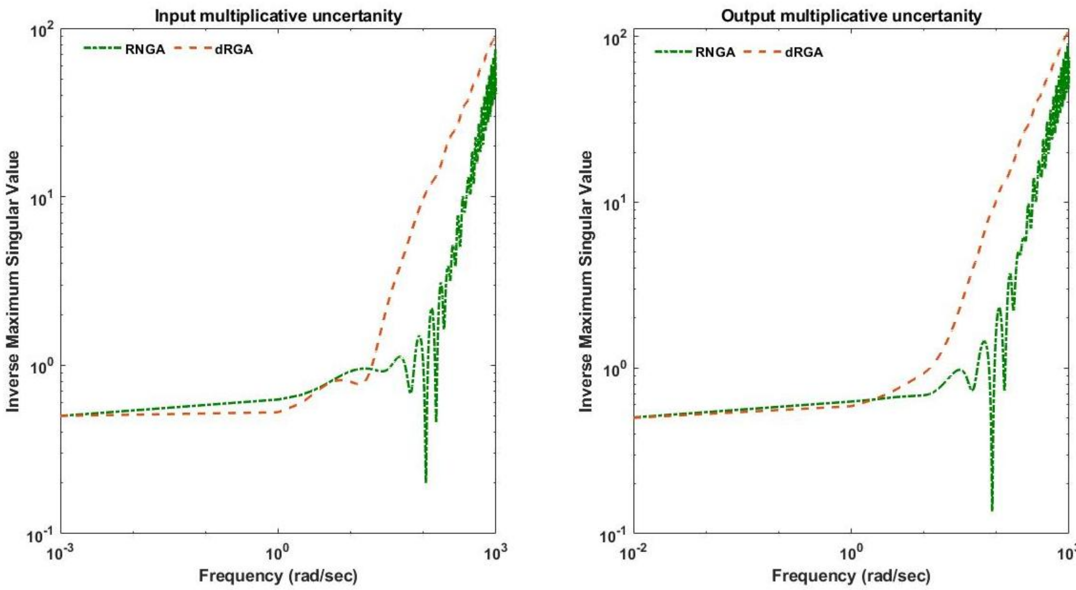

Figure 5.8 Robustness for input and output uncertainty

Table 5.2 TIE and TV values

Step change	Method	IAE			ITAE			ISE			TV		
		y_1	y_2	Sum	y_1	y_2	Sum	y_1	y_2	Sum	u_1	u_2	Sum
y_{r1}	RNGA	3.8137	1.8508	5.6646	48.712	24.038	72.751	35.695	5.0349	37.33	0.4358	0.0031	0.4389
	dRGA	1.1653	0.0036	1.169	14.52	0.1461	14.666	15.8	5.0349	20.844	0.4564	0.0011	0.4575
y_{r2}	RNGA	0.0210	4.0228	4.0439	0.2745	50.879	51.154	0.0006	50.121	50.122	0.0004	0.0056	0.0061
	dRGA	$1.6e^{-8}$	3.8804	3.8804	$4.7e^{-7}$	49.412	49.412	$9.25e^{-11}$	50.121	50.121	$6.38e^{-6}$	0.0036	0.0036
d_1	RNGA	6.7317	0.0335	6.7652	86.447	0.7528	87.2	96.518	18.013	114.53	0.9955	$5.3e^{-5}$	0.99
	dRGA	1.9973	3.2238	5.2211	25.028	41.538	65.566	41.469	18.013	59.482	1	$2.0e^{-5}$	1
d_2	RNGA	3.1218	593.71	596.84	41.261	7634.3	7675.6	13.819	$9.6e^{-5}$	13.819	0.0067	0.9999	1.0067
	dRGA	0.0018	570.91	570.91	0.0240	7387.8	7387.8	$2.8e^{-5}$	$9.6e^{-5}$	$1.2e^{-5}$	$4.4e^{-5}$	0.9961	0.9961

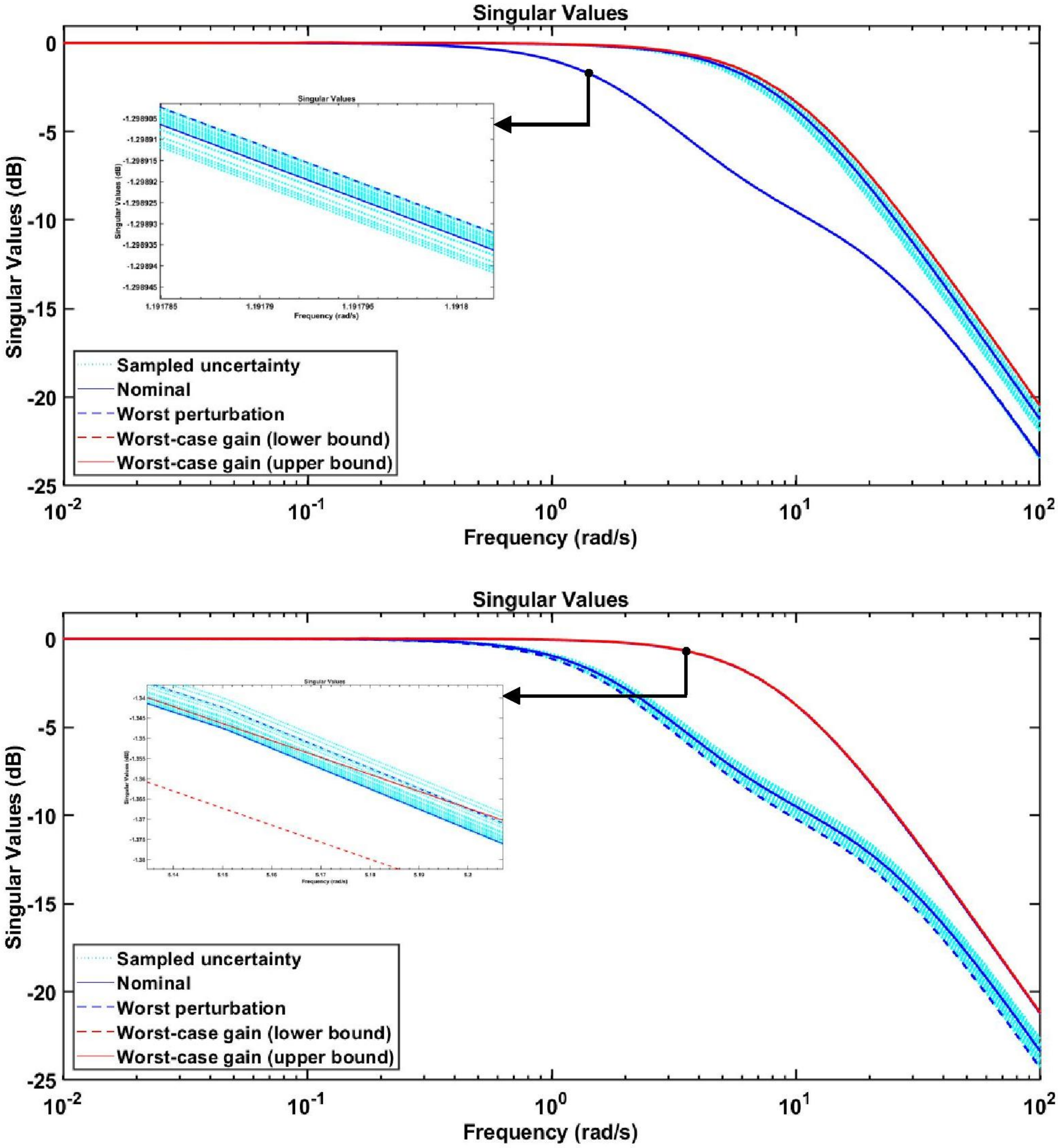

Figure 5.9 Singular values for nominal, random samples, and worst-case gain for 30% uncertainty in process gain.

Figures 5.9 and 5.11 provide a detailed analysis of the worst-case gain uncertainty and its impact on the system. In this analysis, a specified 30% uncertainty is independently applied to the process gain (refer to Figure 5.9) and time constant (refer to Figure 5.11). The purpose of this analysis is to assess the system's stability under varying levels of model parameter uncertainties. Remarkably, both cases demonstrate that the system remains stable even when subjected to significant model parameter uncertainties of up to 1000%. This indicates that the control system is robust and capable of tolerating a wide range of uncertainties without losing stability. To evaluate the impact of the uncertainty on the process outputs, the nominal curve (solid blue) is compared with the worst perturbation curve (blue dotted), and the upper and lower bound curves represent the worst-case gain uncertainty (red). The proximity of these curves suggests that the uncertainty has minimal effect on the process outputs. When the curves are closely aligned, it indicates that the system's performance remains stable and robust despite the presence of uncertainty. Therefore, based on the results of the worst-case gain uncertainty analysis, it can be concluded that the control system exhibits remarkable stability and resilience, even when subjected to significant uncertainties in the model parameters. The close alignment of the curves indicates the system's ability to maintain reliable performance under varying conditions, contributing to its robustness in practical applications.

Figures 5.10 and 5.12 depict the closed-loop responses obtained during the worst-case gain uncertainty analysis. In these analyses, specific uncertainty conditions were imposed to assess the system's dynamic behavior under different scenarios. In the first case, a 30% uncertainty was introduced to the process gain, resulting in a sample curve that exhibited moderation and dispersion. This behavior represents the potential shift in the process output caused by the uncertainty (refer to Figure 5.10). Thus, it is evident that the uncertainty in the process gain can have a noticeable impact on the system's response. Conversely, in the second case, the sample curve closely followed the nominal curve, indicating minimal effects of uncertainty on the close loop system (refer to Figure 5.10). This observation suggests that the system's response remains relatively stable and robust, even when subjected to uncertainty in the process parameter. Importantly, both cases demonstrated stable process outputs without any oscillations induced by the uncertainty. This finding highlights the system's ability to effectively mitigate the effects of uncertainty and maintain reliable performance. To summarize, the results of the worst-case gain uncertainty analysis underscore the significance of considering and understanding the impact of uncertainties in control systems. They reveal that while certain uncertainty conditions may lead to moderate shifts in the process output, the system can still maintain stability and reliable performance overall.

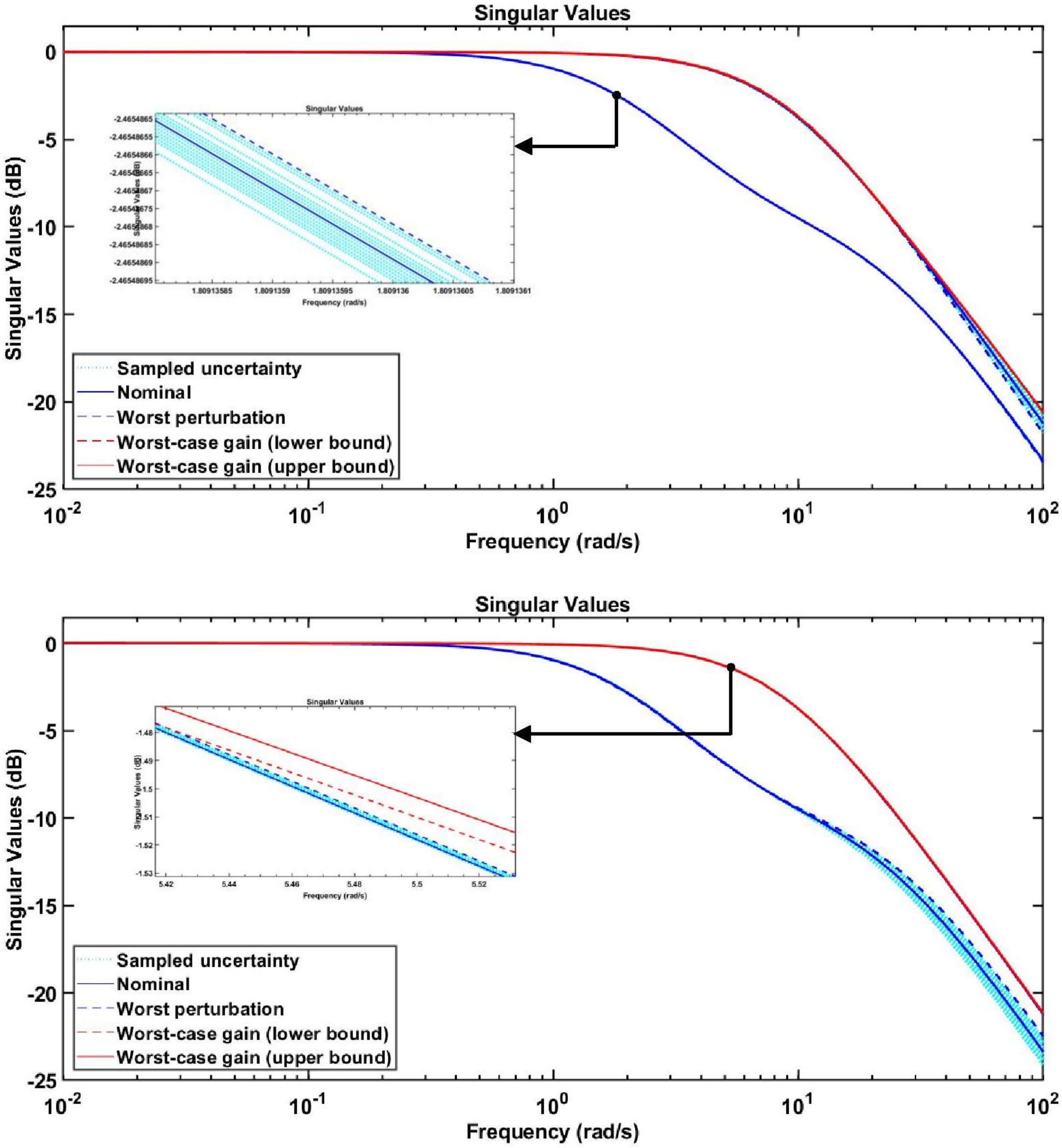

Figure 5.11 Singular values for nominal, random samples, and worst-case gain for 30% uncertainty in time constant.

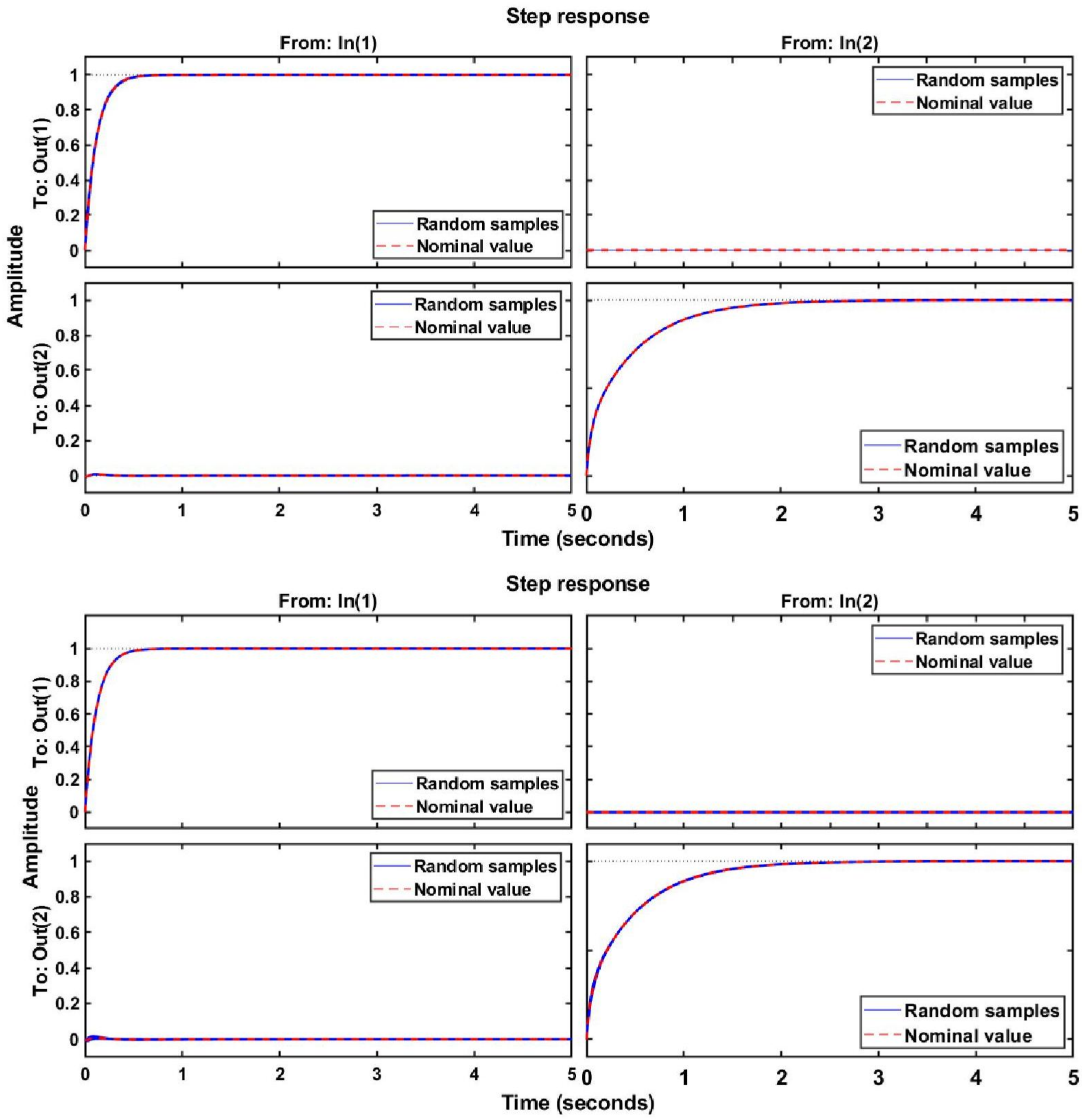

Figure 5.12 Closed loop step responses for 30% uncertainty in time constant.

5.8 Conclusion

Based on the transfer function matrix of a single tank ASP system, a centralized PI controller is designed using RNGA and dRGA methods. A Maclaurin series expansion is used to determine the multivariable PI controller. The aeration rate and recycle sludge flow rate are manipulated to control the dissolved oxygen and substrate concentrations in the effluent stream. The designed controllers were capable of tracking the desired set-point most effectively. The overall outcomes from several simulation studies suggested that the dRGA method provides high stability and less settling time requirement when compared to the RNGA method. Practically, even though the RNGA method is easy to estimate using step response, it might lead to invalid results since it does not consider the system dynamics. The performances of the designed PI controller are tested over operations in terms of IAE, ITAE, ISE error indices, and TV. To obtain the constructive outcome, the minimized error indices of IAE, ITAE, and ISE for the dRGA method were recorded and compared with the RNGA method for cumulative y_1 and y_2 responses. The cumulative error indices of dRGA responses decreased significantly by 79.36%, 79.84%, and 95.21% for IAE, ITAE, and ISE values when compared with the RNGA method. The TV index value of the dRGA method was also observed to be satisfactory as compared to the RNGA method. These outcomes are also authenticated by performing a robustness analysis that justifies the dRGA method to be more robust and stable when compared with the RNGA method. Due to its simplicity, the method can be also used by field engineers for high-dimensional processes with acceptable interactions. Furthermore, the designed controllers were capable of rejecting the uncertain disturbance also.

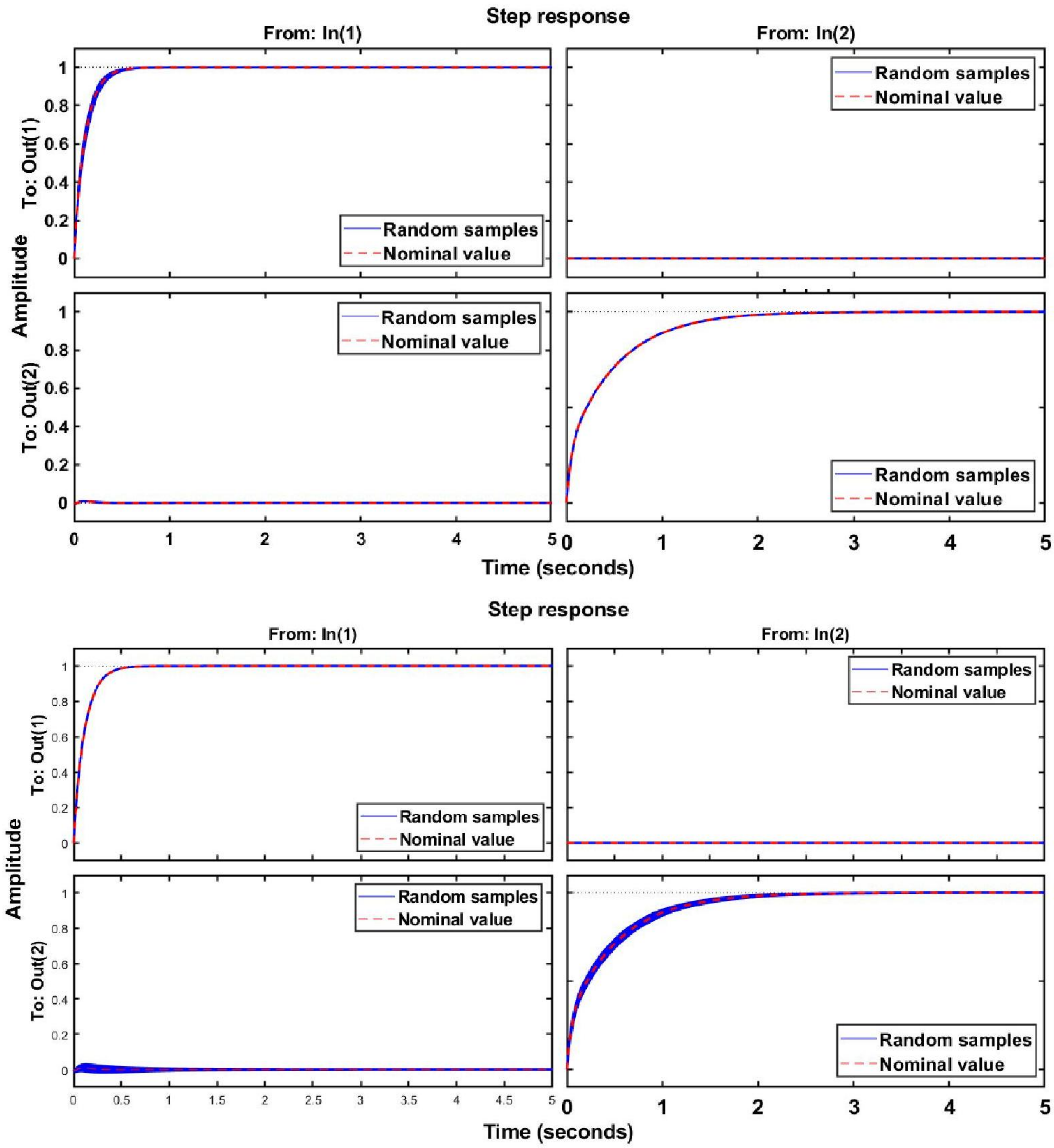

Figure 5.10 Closed loop step responses for 30% uncertainty in process gain.

Chapter 6

CENTRALIZED CONTROLLER DESIGN FOR AN ASP USING DATA-DRIVEN APPROACH

This chapter presents the application of a data-driven approach for modeling and controlling a biological wastewater treatment plant, overcoming the limitations of conventional mathematical modeling. The subsequent section details the approach for designing a centralized controller, including the existing and proposed tuning methods for estimating PI controller parameters. The chapter then proceeds to discuss the results of simulation studies, accompanied by a robust analysis that strengthens the obtained outcomes. Finally, the chapter concludes by summarizing all the outcomes and findings, providing a comprehensive overview of the study.

6.1 Introduction

Water pollution and portable water scarcity have been key challenges for living creatures globally. These circumstances demand treating the used/consumed water through sophisticated wastewater treatment plants. Since economic factor plays a significant role, most consultants follow the biological ASP, which is economical in terms of capital cost and maintenance (Marquez et al., 2022). Due to its dynamic variation of input flow rate and concentrations, the ASP system is highly complex in nature. In a practical scenario, the WWTP faces variation in influent flow rate, influent concentrations, feeding rates, etc., which increases the challenges and complexity for modeling and control operations (Muntean I. et al., 2015; Javier et al., 2011).

Large and complex chemical plants often accumulate vast amounts of data from ongoing processes. However, due to the intricacies involved, researchers have traditionally been cautious about using a data-driven approach to solve problems based on the physical data generated by these plants. Nonetheless, recent advancements in sensors, computers, and data availability have sparked a revolution in various research fields. Control engineering (Mu et al., 2023; Masti et al., 2023; Ding et al., 2023; Mahmood et al., 2023; Sakai et al., 2023), computer security (Shameli-Sendi, 2020; Chaudhuri et al., 2001; Han et al., 1999), power grid and systems (Kim et al., 2023; Grimaldi et al., 2023), energy sectors (Song et al., 2023; Ye et al., 2023), aerospace (Allaire et al., 2012; Hao et al., 2023; Chen et al., 2022), medical research (Hypponen et al., 2019; Bak et al., 2023; Zahid and Sharma, 2023; Chen et al., 2022), environmental sectors (Balla et al., 2022; Zamani et al., 2023; Abraham et al., 2023), and transportation (Huang et al., 2023; Karatug et al., 2023; Kecman and Goverde, 2015; Liu et al., 2023) are just a few examples of domains where the data-driven approach has successfully addressed real-world industrial problems. These advancements have opened up new possibilities for effectively utilizing data-driven approaches in solving real-world industrial challenges.

In the current study, a data-driven approach was adopted for the control study. This approach becomes handy since it does not require a plant mathematical model. The relationship between the system state variables (input and output) can be effortlessly obtained from a data-driven approach without prior knowledge of the system (Layla et al., 2018). All the information regarding the system is obtained by providing sufficiently rich experiments at given operation points from the data. So in specific, the three key points of the data-driven approach are: Firstly, it directly uses the measured I/O data. Secondly, it adopts data-driven modeling in place of first principle modeling; and thirdly, it guarantees the theoretical analysis. Accordingly, the controller in the data-driven approach does not depend on the accuracy of the plant model, and the twin-born problem of unmodeled dynamics does not prevail under a data-driven framework (Zhong and Zhuo, 2013).

In the current study, the control system uses a multivariable PI controller proposed by Penttinen that adopts a manual controller tuning approach based on conventional Ziegler-Nichols tuning (Jaromir and Pavel, 2019) counterparts for SISO systems. Ziegler-Nichols is one of the popular methods for tuning the P, PI, and PID controllers (Ellis, 2012). The proportional gain is raised until the system is unstable when the integral and differential gain is kept at zero. This value of K_p is denoted as K_{max} with frequency oscillation as f_o. In the next step, it backs off the proportional gain and set the integral and differential gain as a function of f_o. But this tuning method involved the tedious task of regulating the tuning values manually until a stable response with minimum performance indices is obtained. In an attempt to overcome the limitations of manual tuning, this study proposes a new tuning method based on optimization principles for designing a centralized controller for the multivariable process. Principally, the Davison (Davison, 1976) and Penttinen (Penttinen and Koivo, 1980) algorithms use a manual tuning approach similar to Ziegler and Nichols for SISO controllers, while the proposed technique poses the controller tuning as an optimization problem. In the optimization problem formulation, Integral Square Error (ISE) was chosen as an objective function, and the fine-tuning parameters of Davison and Pentinen methods as decision variables. The fine-tuning parameters obtained from optimization along with the theoretical results proposed by Pentinen et al., are used to calculate the controller tuning parameters. In addition, the proposed method is compared with the reported method (Shen et al., 2014) to examine their performances and stability properties.

6.2 Methodology

6.2.1 Design of Centralized Controller

The prime objective of the current study is to govern the dissolved oxygen concentration and substrate concentration in the effluent stream. Therefore, the aeration rate and recycle sludge flow rate were chosen as two manipulated variables that have a significant influence on the two control variables. Accordingly, a centralized controller of 2 $\times$ 2 system is considered as shown in Figure 5.1, representing the control structure and corresponding feedback loop. All the manipulated variables were calculated simultaneously by utilizing a single control algorithm in the centralized control system.

Converting all higher-order transfer functions to First Order Plus Time Delay (FOPTD) system is a crucial preliminary stage while designing a centralized controller. The centralized controller matrix can be given below,

$$G_c(s) = \begin{bmatrix} G_{c11} & G_{c12} \\ G_{c21} & G_{c22} \end{bmatrix} \tag{6.1}$$

This study considers PI Controller type while designing the centralized controller, and it is expressed as,

$$G_{C_{ij}} = K_{C_{ij}}\left(1+\frac{1}{\tau_{ij}}s\right) \tag{6.2}$$

where $K_{c_{ij}}$ and τ_{ij} indicates controller gain and integral time constant for j^{th} $(j=1,2)$ controller respectively. By considering the following process transfer function g_{11}, g_{12}, g_{21} and g_{22}, the centralized controllers designed are represented as $g_{c_{11}}$, $g_{c_{12}}$, $g_{c_{21}}$ and $g_{c_{22}}$ respectively.

6.2.2 Davison method

According to the empirical method proposed by Davison (Davison, 1976), the K_c and K_i matrices are obtained from the following equations.

$$K_c = \delta_1[G_P(s=0)]^{-1} \tag{6.3}$$

$$K_i = \delta_2[G_P(s=0)]^{-1} \tag{6.4}$$

where, $[G_P(s=0)]^{-1}$ is referred as rough tuning parameters. This can be obtained by calculating the inverse of the steady-state gain matrix. Generally, the value ranges from 0-1 and recommended values are 0.1-0.5 for δ_1 and 0.05-0.2 for δ_2. In the case of stable and integrating systems, K_P can be substituted for $G_P(s=0)$. The system model was identified using the PRC method, which is discussed in Chapter-4.

6.2.3 Proposed method

Various studies related to the design of control systems for MIMO processes with the known models are reported in numerous literature's (Jin et al., 2016; Nordfeldt and Hagglund, 2006; Fradkov et al., 1999; Yong et al., 2013). A few case studies were found in the reported literature where both model identification and controller design were undertaken simultaneously. This approach will assist researchers while developing a complex first-principles model of the process. Accordingly, Davison (Davison, 1976), and Penttinen (Penttinen and Koivo, 1980) have proposed a method, to simultaneously identify the process model and design only the Integral and the Proportional Integral controller, respectively.

6.2.3.1 Multivariable PI controller system

In the current study, the controller parameters are obtained by adopting the Penttinen and Koivo method of identification till the precursor matrices. The proposed approach differs from the Penttinen and Koivo work in posing the controller tuning problem as an optimization problem. For the tuning rules, the reader is directed to the classical work of Penttinen, and Koivo (Penttinen and Koivo, 1980). This study only refers to the design of the control system and does not include the system identification approach from Penttinen and Koivo. The major advantage of the proposed method is that it eliminates manual tuning approach, as suggested by Penttinen and Koivo, thereby minimizing the effort of tuning the controller.

In general, tuning the PI controller refers to a weighted sum of proportional and integral terms for controller yield that governs the process variables to achieve the desired output. This tuning operation can be accomplished by controller design tools or mathematical methods. The following expressions present the generalized form of the system for multivariable PI tuning,

$$\dot{x} = Ax + Bu \tag{6.5}$$

$$y = Cx \tag{6.6}$$

$$e = y_r - y \tag{6.7}$$

Equations 6.5 and 6.6 represent the state and output equation respectively, x indicates the state vector, u as the control vector, y specifies the output vector, and the set point is represented as y_r. Correspondingly, A, B, and C are the system matrix, input matrix, and output matrix, respectively.

By adopting Laurent series expansion for the plant in state space form,

$$G(s) = C(sI - A)^{-1} + B \tag{6.8}$$

the transfer function matrix can be written as

$$G(s) = \frac{CB}{s} + \frac{CAB}{s^2} + \frac{CA^2B}{s^3} + ... \tag{6.9}$$

As a rule, Penttinen and Koivo observe a multivariable system to be stable and consider it as a significant assumption while designing the PI controller. A system is said to be stable if a bounded input(s) leads to the bounded output(s). Penttinen and Koivo proposed a method to design a feedback PI controller for MIMO systems assuming the system is bounded. Manipulated variable PI controller proposed by Penttinen and Koivo has the structure given in Equation 6.10,

$$U = K_c e + K_i v \tag{6.10}$$

here, the error vector is represented as e, and the integral of the errors summed over time as v. The prime intent of control system design is to obtain K_c and K_i matrices with stable system response for both servo and regulatory cases. This is viable if the designed controller could quickly respond to the change in operating range if needed and eliminate the disturbance effectively. Through Penttinen and Koivo method (Penttinen and Koivo, 1980), the K_c and K_i values are determined from the output data obtained by subjecting the system to the step inputs, which are linearly independent.

$$K_c = \alpha_1 (CB)^{-1} \tag{6.11}$$

$$K_i = \alpha_2 (-CA^{-1}B)^{-1} \tag{6.12}$$

The expressions to obtain K_c and K_i can be Equation 6.13 and Equation 6.14, respectively.

$$K_c = diag(p_1, p_2, p_3, ..., p_n) \times P_0 \tag{6.13}$$

$$K_i = \alpha_2 T^{\dagger} \tag{6.14}$$

where K_c is the proportional gain of a P controller, $diag(p_1, p_2, , p_n)$ is a diagonal matrix with the tuning parameters $p_1, p_2, , p_n$. $'\dagger'$ symbol denotes the pseudo-inverse of a matrix. The precursor matrix P_0 is obtained from the step inputs provided to the system, and outputs are obtained from the system for the proportional part of the controller. The tuning parameter for an integral part of the controller is indicated as α_2, and T is a precursor matrix for an integral part of the controller, which is again obtained from step inputs given to the system and the responses from the systems, respectively. Correspondingly, P_0 and T matrices are determined using Equations 6.15 and 6.16 respectively from the step inputs and responses, and are given by

$$CB = [\dot{y}_1, \dot{y}_2, \dot{y}_3, ..., \dot{y}_m][u_1, u_2, u_3, ..., u_m]^{-1} \tag{6.15}$$

$$T = [y_1, y_2, y_3, ..., y_m][u_1, u_2, u_3, ..., u_m]^{-1} \tag{6.16}$$

where $y_1, y_2, y_3, ..., y_m$ is the response matrices for a set of independent step inputs of unit magnitude vectors $u_1, u_2, u_3, ..., u_m$ respectively, and $\dot{y}_1, \dot{y}_2, \dot{y}_3, ..., \dot{y}_m$ is the matrices containing the slopes of the response matrices for the corresponding input vectors $u_1, u_2, u_3, ..., u_m$. The proportional control segment of the Penttinen and Koivo approach is modified as represented in Equation 6.17 in the proposed method

$$K_c = \alpha_1 P_0 \tag{6.17}$$

Where, α_1 is a tuning parameter, and these fine-tuning parameters (α_1 and α_2) can be obtained from the solution of an optimization problem. Mathematically, the optimization problem can be defined as follows

$$J = \min_{\alpha_1, \alpha_2} \int_0^t (y_r - y)^2 dt \tag{6.18}$$

where, $y = f(K_c, \tau_1, \alpha_1, \alpha_2)$

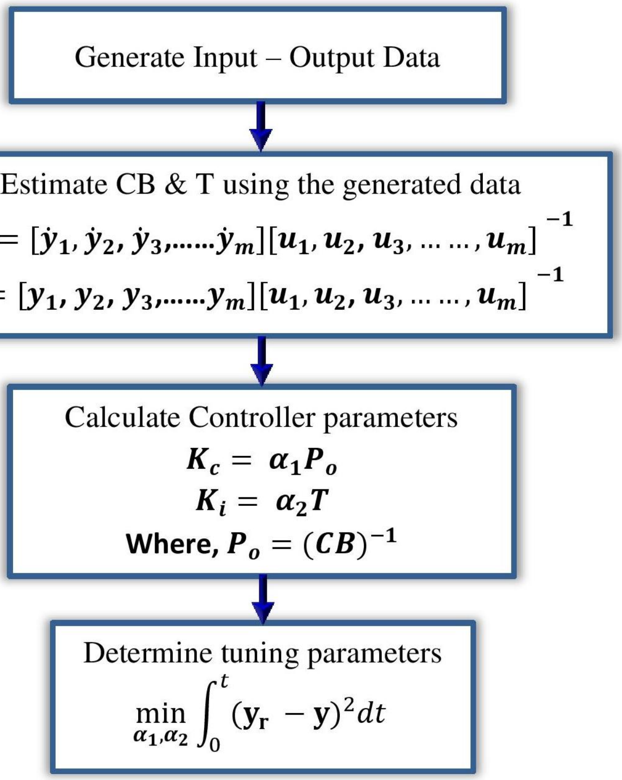

Figure 6.1 Flowchart of methodology to design Data-driven centralized controller

Such modifications to the P-controller part of Penttinen (Penttinen and Koivo, 1980) work was already reported in the article by (Norhaliza et al., 2009). The study by Nor'Azlan et al. has earlier used optimization as a tool to perform the tuning operations (Nor'Azlan et al., 2018). However, the optimization formulations reported in this literature utilize state-space models of process to calculate the precursor matrices and objective function. Meantime the solution to the optimization problems was obtained using Lyapunov's stability criteria to identify the optimal tuning parameters. However, in the proposed work, the input-output data is directly utilized to calculate the precursor matrices. The formulation of an optimization problem comprises ISE as the objective function and the decision variables as the tuning parameters. This modification can directly calculate precursor matrices instead of obtaining them using the state space form of process models to formulate the objective function. This operation will reduce the time taken for tuning the control parameters over the conventional trial and error method.

6.3 Simulation Results

Simulation studies were performed to understand the behavior of the designed centralized PI controller. The principal intent of the study is to control the dissolved oxygen (y_1) and substrate (y_2) concentration by manipulating the aeration rate and recycle sludge flow rate in the ASP unit. Since the system is Two-input, Two-output, a step input change is separately provided among each of the set points. For instance, the step change in y_1 set point outputs y_1 & y_2 will reach 1 and 0 respectively at steady state condition. This is due to the presence of an integral mode in the control system. Corresponding, the steady-state value in the manipulated variables is noted as $u_1 = [u_{1,1} \quad u_{2,1}]^T$. The same procedure is repeated for the step change in y_2 and u_2 values are recorded, respectively. The interaction phenomenon could occur between the control variables by each manipulated variable. In order to reduce the interactions among the process variables, a proper pairing has to be selected, which could be computed through RGA analysis. For the current study, the quantification of these interactions was found to be [1.000 -5.33e-6; -5.33e-6 1.000]. The performance of the designed controller is evaluated through several simulation studies with the two different tuning strategies. These simulation results and subsequent tuning strategies were discussed in this section.

The tuning parameters were estimated by solving the optimization problem (Eq. 6.18) prior to benchmarking the controller. According to the behavior of the system response, the coefficient of the tuning parameters is varied until the desired output responses are obtained. The present study considers a linearized model for the tuning purpose.

The initial step while designing a multivariable PI controller is determining the CB matrix. The constant inputs were chosen and given by,

$$u_1 = [1 \quad 0], u_2 = [0 \quad 1] \tag{6.19}$$

However, the obtained matrix is achieved by providing step inputs for the system with the help of Equations 6.15 and 6.16.

$$CB = \begin{bmatrix} 0.0036 & 3.399e^{-06} \\ \\ -0.0017 & -0.2990 \end{bmatrix} \tag{6.20}$$

that results in,

$$P_o = (CB)^{-1} = \begin{bmatrix} 278.3979 & 0.0032 \\ \\ -1.5699 & -3.3450 \end{bmatrix} \tag{6.21}$$

The P_0 and (in Equation 6.15) and T (in Equation 6.16) are the precursor matrix for the proportional and integral part of the PI controller. They can be computed based on the input-output measurements using Equation 6.15 and 6.16 as calculated above. α_1 and α_2 are the tuning parameter for the proportional gain and integral gain part of the controller. These fine-tuning parameters are determined by solving the optimization problem stated in Equation 6.18. Accordingly, the controller matrix for the proposed method resulted from optimal values α_1 = 0.0013 and α_2 = 5.9568 are given in Table 6.1. The table listed centralized PI controller settings obtained from the optimal fine-tuning parameter from the present method and literature (Shen et al., 2014) method. The study adopted MATLAB numerical optimization solver fminsearch to solve the above problem. Here, the problem description is transformed into a mathematical form by defining the variables, objectives, and constraints. This will be followed by solving the optimization problem with variables that produce optimal values for objective functions within the stipulated constraints. The MATLAB numerical optimization method holds good for solving complex real-world problems for which no closed-form solution is available. The design optimization task, parameter estimation, component selection, and parameter tuning are a few tasks that can be performed in MATLAB. This approach will decrease the time consumed for trial and error manual tuning, especially when the process interactions are strong.

Table 6.1 Parameters for PI controllers

Method	K_c	K_i
M1 (Proposed method)	$\begin{bmatrix} 0.3487 & 3.9659 \\ -0.0012 & -0.0042 \end{bmatrix}$	$\begin{bmatrix} 3.3167 & 3.7720 \\ -0.0187 & -0.0398 \end{bmatrix}$
M2 (Shen et al. (2014))	$\begin{bmatrix} 0.1188 & -0.0005 \\ 1.3517 & -0.0011 \end{bmatrix}$	$\begin{bmatrix} 1.4765 & -0.0079 \\ 1.6792 & -0.0168 \end{bmatrix}$

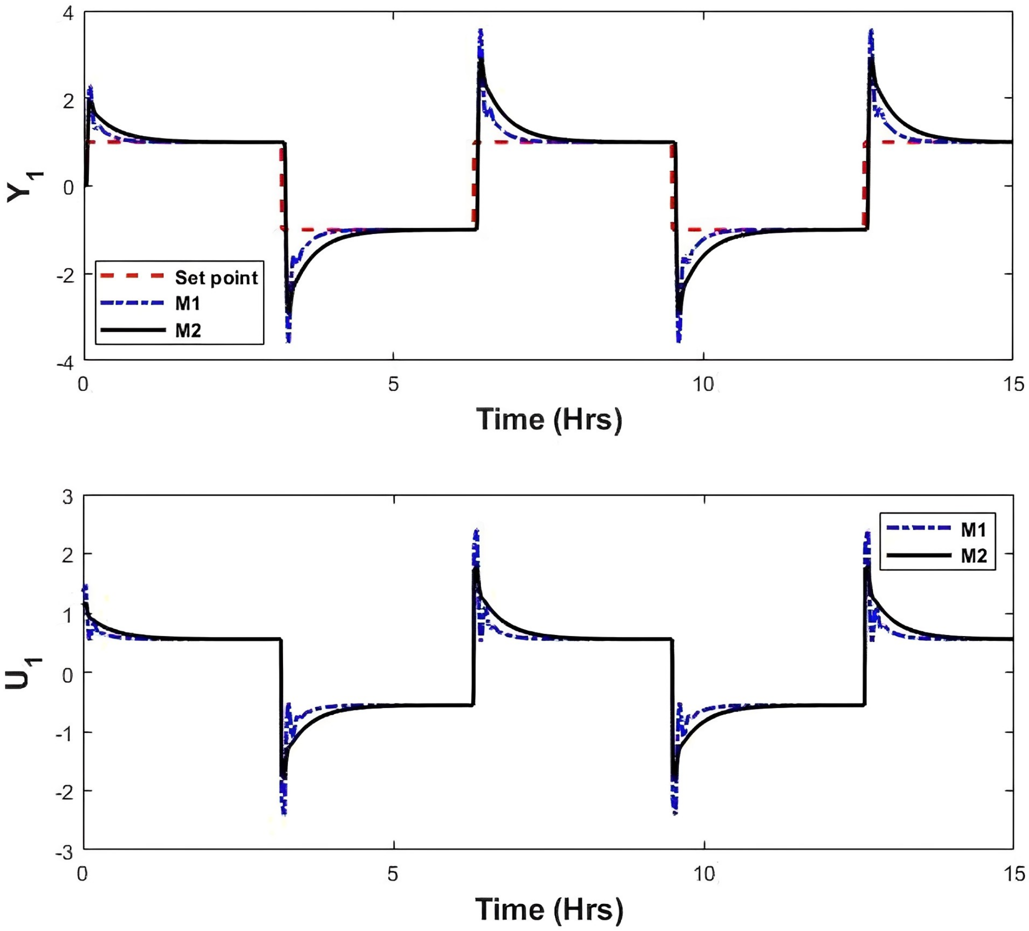

Figure 6.2 Closed loop response (y_1) and Manipulated signal (u_1) behavior to sequential set point (y_{r1}) changes and disturbance rejection

In the context of process automation engineering, Figure 6.2 depicts a comprehensive analysis of two tuning methods applied for controlling the dissolved oxygen concentration (y_1) in response to changes in the set point (y_{r1}). To understand the system responses, various step disturbances were introduced at regular intervals using the waveform generator block in Simulink. The proposed method (M1) demonstrated a notably faster response compared to the method reported by (Shen et al., 2014) (M2). However, a slight overshoot was observed in the proposed method during set point changes, although it exhibited quicker recovery as compared to the approach presented by (Shen et al., 2014). Additionally, Figure 6.2 displays the closed-loop response of the control signals (u_1) for the dissolved oxygen concentration output when step changes are introduced in y_{r1}. The plot showcases the controller action over time for disturbances applied at specific intervals (3.25 hrs, 6.35 hrs, 9.54 hrs, and 12.6 hrs for y_1, and 3.23 hrs, 6.28 hrs, 9.51 hrs, and 12.6 hrs for y_2) for both methods (M1 and M2).

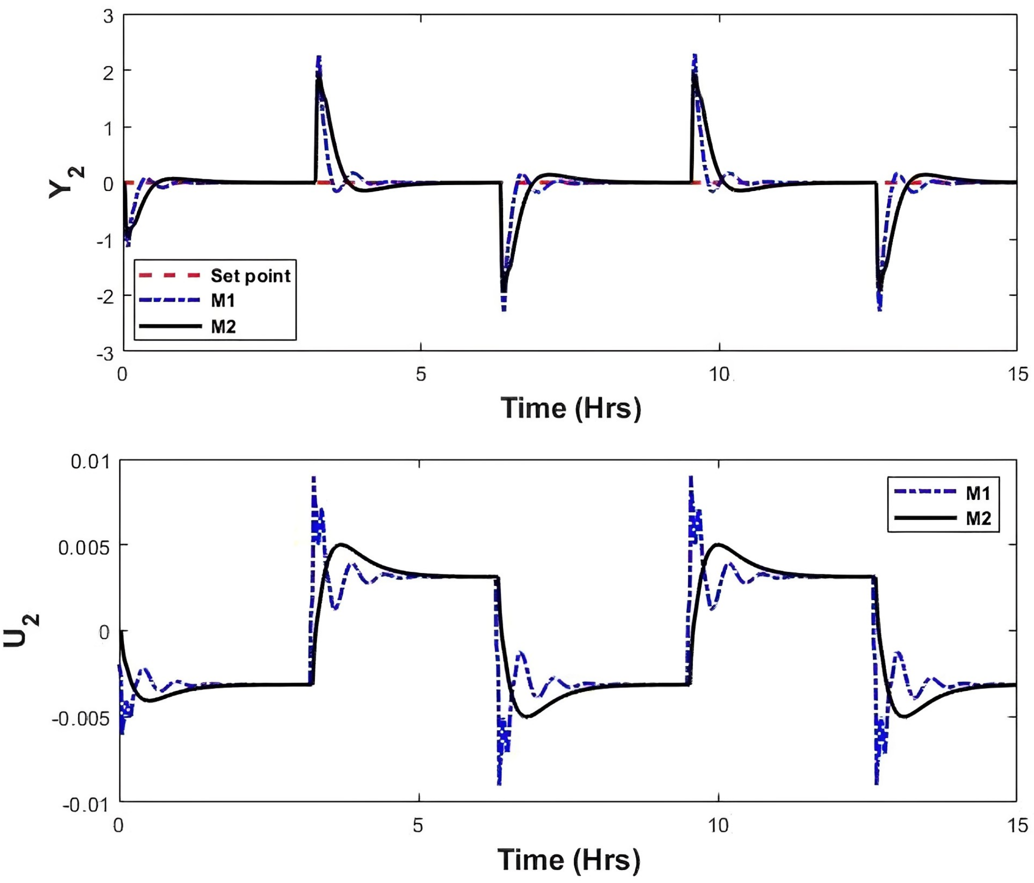

Figure 6.3 Closed loop response (y_2) and Manipulated signal (u_2) behavior to sequential set point (y_{r1}) changes and disturbance rejection

Similarly, Figure 6.3 depicts the closed loop response of two tuning methods on substrate concentration, namely M1 and M2, respectively. It is clearly noticeable how the system reacts to the set point changes and disturbances along the WWTP operation. The classic advantage of adopting a PI controller is its ability to reduce the rise and settling times. Even though the response signal has slight undershoot and overshoot, a faster settling time behavior with less oscillation is observed from the proposed method.

The closed loop response of y_1 (dissolved oxygen concentration) for a step change in y_{r2} is presented in Figure 6.4. On this occasion also, the proposed method (M1) could achieve a quicker response time with less overshoot than the compared reported method (M2) (Shen et al., 2014). Figure 6.4 represents the closed-loop response from control signals (u_1) for the output concentration of dissolved oxygen when step change is introduced in y_{r2}.

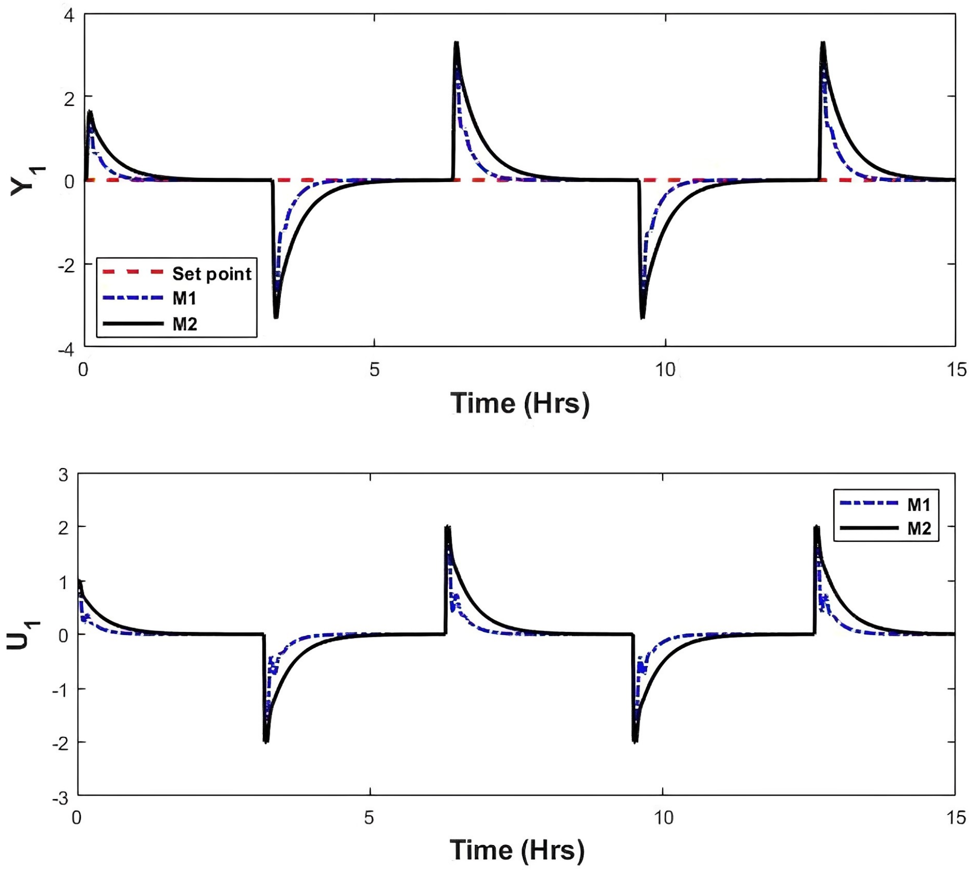

Figure 6.4 Closed loop response (y_1) and Manipulated signal (u_1) behavior to sequential set point (y_{r2}) changes and disturbance rejection

Table 6.2 Comparison of performances indices for the centralized control scheme

Step change in	Method	IAE			ITAE		
		y_1	y_2	Sum	y_1	y_2	Sum
y_{r1}	M1	1.3665	1.503	2.8708	17.435	18.292	36.364
	M2	2.9159	1.8829	4.7988	37.73	23.28	61.01
y_{r2}	M1	3.1987	3.3385	6.5373	40.52	41.896	82.416
	M2	6.7102	4.0572	10.767	86.171	50.13	136.3

Figure 6.5 represents the closed-loop response from y_2 and control signal u_2 for the output (substrate concentration) when step change is introduced in y_{r2}. These plots clearly express the behavior of the output parameter and manipulated variable as time progress in the system. A faster response time towards the imparted disturbances is observed from the proposed method (M1) than the reported method (M2).

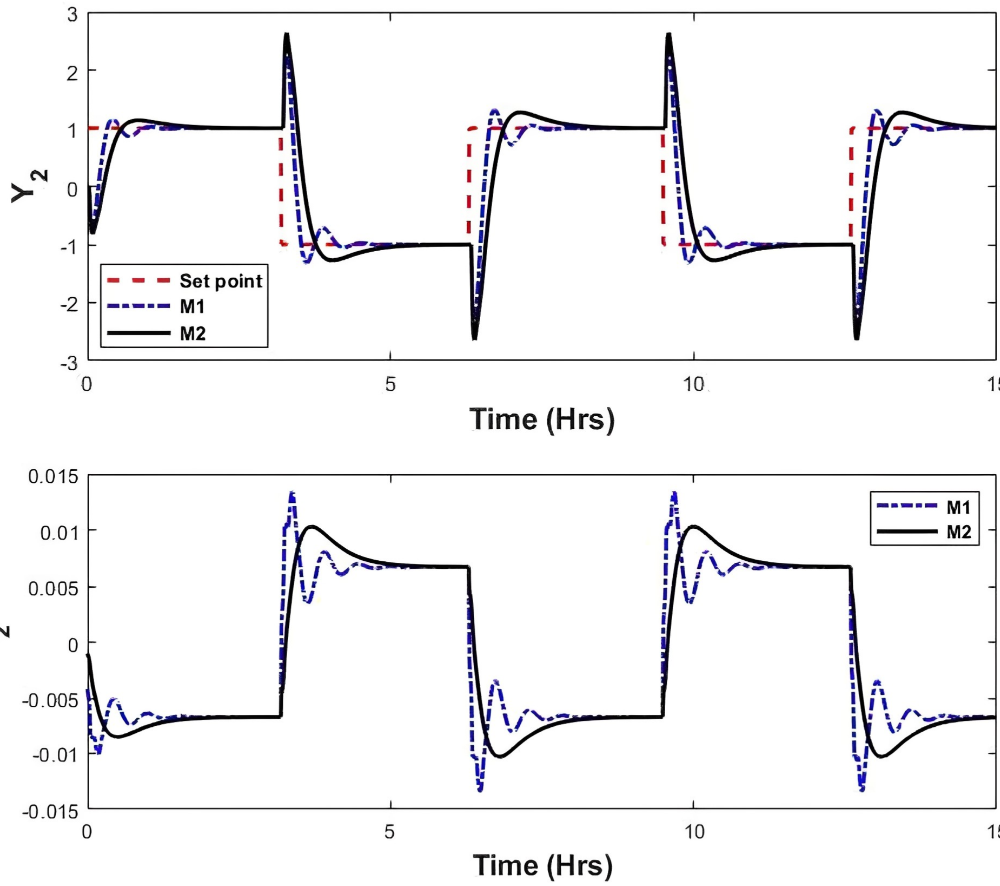

Figure 6.5 Closed loop response (y_2) and Manipulated signal (u_2) behavior to sequential set point (y_{r2}) changes and disturbance rejection

The comparison of performance indices for M1 and M2 methods are presented in Table 6.2. An acceptable level of control performance was achieved by the proposed method when compared with the method proposed by (Shen et al., 2014). For the step change in yr_1, the proposed method secured 53.14% and 53.80% lowered IAE and ITAE error for output y_1 when compared with M2. Identically for y_2, the IAE and ITAE errors decreased to 20.17% and 18.69%, respectively, for the proposed method. Correspondingly, M1 secured 52.33% and 52.97% lowered IAE and ITAE error when compared with M2 for a step change in yr_2 with y_1 as an output. Following it, the output y_2 of M1 produced 17.71% and 16.42% decreased IAE and ITAE errors, respectively, when compared with M2.

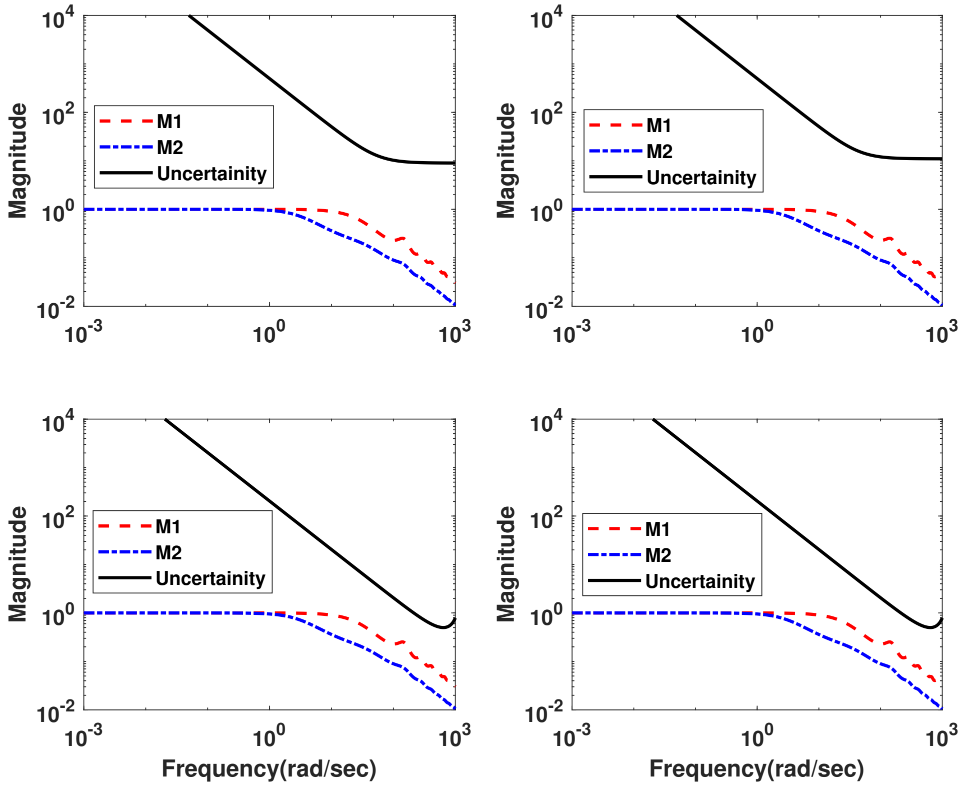

Figure 6.6 Complementary sensitive function with ± 10% uncertainty in time constant (top) and time delay (bottom)

The sensitivity analysis was performed to examine the robustness of the designed controller, and the outcome is presented in Figure 6.6. Since the curve from both the methods (M1 and M2) fall beneath the uncertainty curve, it satisfies the stability condition. Thus, the proposed method proves to be simple and effective and offers satisfactory control performances for a highly non-linear system like the activated sludge process. The proposed method could achieve superior responses for the closed-loop system compared to the reported (Shen et al., 2014) method.

6.4 Conclusion

Observing the need to treat the used water by incorporating a sophisticated control system in WWTP, this study could encourage many sectors to adopt it, especially in small-scale units. This could be a significant step towards the sustainable utilization of water resources. The study put forward a design of a multivariable centralized PI controller to govern the DO and substrate concentration by manipulating the aeration rate and recycle sludge flow rate. A data-driven approach that does not need the plant model becomes functional for the study. The proposed method for tuning the controller by optimization technique provided better responses than the method reported by shen et. al, 2014 (Shen et al., 2014). The responses obtained from the controllers were relatively simple, with less overshoot and undershooting with faster and better response time compared to the reported method. The performance indices (IAE and ITAE) clearly demonstrate the superior response through numerical statistics. Precisely, the error indices for y_1 and y_2 responses lowered substantially between 52-53% and 16-21% respectively than the compared method. This conclusion holds good with the robustness uncertainty analysis too. Finally, the substantial simulation work on the nonlinear model proves that the proposed technique is less time-consuming and achieves better system performance than the compared method. A dynamic optimization tool and Reinforcement learning-based Machine Learning approach to design a controller for the wastewater treatment plant can be taken up for future study.

Chapter 7

Summary and Conclusions

7.1 ASP Model identification

- Two effective and prominent techniques were utilized for identifying the ASP model.
- Even without in-depth knowledge of the physical system, we were able to identify the model that provided the best fit using the system identification technique. This approach significantly reduced the engineering effort required.
- The Process Reaction Curve method demonstrated itself as a classical, straightforward, and simple technique for model identification. It allowed for the estimation of the most basic form of process parameters (FOPTD).
- Both model identification methods offered a simple and optimal approach for designing a controller for the activated sludge process.

7.2 Decentralized controller design for an ASP

- A decentralized controller and decoupler was designed for the wastewater treatment plant by utilizing the relative gain array concept, which is obtained by inversing the process transfer function matrix.
- The closed-loop control system was further improved by adopting a Normalized Gain Array with an equivalent transfer function for each element of the process transfer function matrix.
- Simulation studies of the closed-loop system in the wastewater treatment plant revealed that the controller designed based on the IAE minimization criterion

exhibited improved performance compared to the ISE and ITAE minimization criterion methods.

- These observations were corroborated by the error indices, where the IAE method yielded the lowest error, followed by the ITAE and ISE methods, respectively.

- The simulation studies demonstrated that even after being subjected to a 30% perturbation in process parameters, the closed-loop system maintained its robust nature.

7.3 Centralized controller design for an ASP

- Based on the transfer function matrix of a single tank ASP system, a centralized PI controller was designed using RNGA and dRGA methods.

- A Maclaurin series expansion is used to determine the multivariable PI controller.

- The overall outcomes from several simulation studies suggested that the dRGA method provides high stability and less settling time requirement when compared to the RNGA method. Practically, even though the RNGA method is easy to estimate using step response, it might lead to invalid results since it does not consider the system dynamics.

- The performances of the designed PI controller are tested over operations in terms of IAE, ITAE, ISE, and TV.

- The cumulative error indices for the dRGA responses exhibited a substantial decrease of 79.36%, 79.84%, and 95.21% in IAE, ITAE, and ISE values, respectively, when compared to the RNGA method. Additionally, the TV index value of the dRGA method was found to be satisfactory in comparison to the RNGA method.

- These findings are further supported by a robustness analysis, which confirms that the dRGA method is more robust and stable when compared to the RNGA method.

7.4 Data driven approach Centralized controller design for an ASP system

- A multivariable centralized PI controller was designed to control the DO and substrate concentration by manipulating the aeration rate and recycle sludge flow rate.
- Adopts a data-driven approach where it does not need the plant model to become functional for the study.
- The conventional tuning methods given by Davison (1976) and Penttinen (1980) relied on Ziegler-Nichols or manual tuning. These methods were highly laborious, as the tuning values had to be manually adjusted until a stable response with minimal performance indices was achieved.
- Consequently, an optimization problem was formulated in order to tune the control parameters using the ISE (Integral of Squared Error) technique as the objective function. This article presents a novel approach for obtaining the optimal tuning parameters.
- The proposed method for controller tuning using optimization techniques yielded superior results compared to the method described by Shen (2014).
- It offers relative simplicity and exhibits good transient response. The performance indices (IAE and ITAE) clearly demonstrate their superior performance through numerical statistics.
- This conclusion is further supported by robustness uncertainty analysis.

To summarize, two approaches were used to identify the ASP model, reducing the engineering effort required and providing a simple approach for designing a controller for the activated sludge process. A decentralized controller and decoupler were designed for a wastewater treatment plant using the relative gain array concept, resulting in improved performance compared to other minimization criterion methods. Simulation studies showed that the closed-loop system maintained robustness even after a 30% perturbation in process parameters. For a centralized controller design in an ASP system, the dRGA method exhibited high stability, less settling time requirement, and better performance compared to the RNGA method. A data-driven approach was used for centralized controller design, achieving optimal tuning parameters and superior results compared to other methods, along with good transient response and robustness.

7.5 Future Work

- The implementation of the designed real-time controller on a pilot-scaled WWTP can be conducted to evaluate its performance in an operational setting. This will provide valuable insights into the practicality and effectiveness of the controller in a real-world scenario.

- An optimization study may be undertaken to develop economical operation strategies for WWTPs. By considering factors such as energy consumption, resource utilization, and cost-effectiveness, optimal operational guidelines can be established, leading to more efficient and sustainable wastewater treatment processes.

- Further research should focus on the design and comparison of modern control strategies with the proposed controller. By exploring innovative control approaches and assessing their performances, advancements in the field can be made. This comparative analysis will help identify the strengths and limitations of different control strategies, leading to the development of more effective and efficient controllers for wastewater treatment plants.

LIST OF PUBLICATIONS BASED ON THESIS:

- Sanjith S. Anchan, Chinta Sankar Rao, (2021), Robust decentralized proportional-integral controller design for an activated sludge process. *Asia-Pac J Chem Eng.* 2020; 15(6):e2531.

- Sanjith S. Anchan, and Chinta Sankar Rao, (2022), Centralized Proportional Integral Controller Design for the Activated Sludge Process. *Chem. Eng. Technol.*, 45(3): 467-478.

- Sanjith S. Anchan and Hemanth Kumar Tanneru and Chinta Sankar Rao, (2023), Optimal detuning of multivariable PI controller based on data-driven approach for an activated sludge process, e2919.

- Sanjith S. Anchan and Chinta Sankar Rao, (2023), Activated sludge process for wastewater treatment: A state of art Review, Journal of water process Engineering-Elsevier (**Communicated**)

Conference papers / Presentation

- Sanjith S. Anchan and Chinta Sankar Rao, (2019), Simulation and Control of a Biological Wastewater Treatment Process, Oral presentation at *CTCS 2019, International Conference*, May 23-24, 2019 | N.M.A.M.I.T., Nitte, Karnataka (**Presented**).

- Sanjith S. Anchan and Chinta Sankar Rao, (2019), Design of Decoupler for Wastewater Treatment Plant, Oral presentation at *72nd Annual Session of Indian Institute of Chemical Engineers, CHEMCON 2019 Advances in Chemical Engineering for Industrial Application*, December 16-19, 2019 at Indian Institute of Technology Delhi, Delhi (**Presented**).

- Sanjith S. Anchan and Chinta Sankar Rao, (2021), Centralized PI Controller design for Activated Sludge Process *International Chemical Engineering Conference - 100 Glorious Years of Chemical Engineering & Technology*, September 17 to 19, 2021 at Dr B R Ambedkar National Institute of Technology, Jalandhar, Punjab, India (**Presented**).

Other Publications

- Purushottam Patil, Sanjith S. Anchan, Chinta Sankar Rao (2022), Improved PID controller design for an unstable second order plus time delay non-minimum phase systems, Results in Control and Optimization, 7(1), 100117. (**Published**)

- Sanjith S. Anchan and H.C. Shiva Prasad (2022), Survey on solid waste generated at a South Indian University Campus International Journal of Environment and Waste Management, 30(4), 411-424.(**Published**)

- Sanjith S. Anchan, H.C. Shiva Prasad (2021), Feasibility of roof top rainwater harvesting potential - A case study of South Indian University, Cleaner Engineering and Technology, 4(1), 100206. (**Published**)

- Sanjith S. Anchan, Ateeth Shetty, H Gangadhara Bhat and M. D. Chadaga (2018), Land use and land cover change detection through spatial approach: A case study of Mangaluru Taluk, Karnataka, Journal of Geomatics, 12(2), pp. 167-173. (**Published**)

BIO-DATA

Name : Sanjith S. Anchan

Email Id : sanjithsj@gmail.com

Mobile : +91-9743124106

Address : "SHRIJA" House,
Pulinchandi Kalkar Road, Konaje Post, Konaje
Mangalore, Dakshina Kannada, Karnataka,
India - 574199

Educational Qualifications:

Degree	Graduating year	University
B.E.	2013	Visvesvaraya Technological University, Belgaum
M.Tech.	2017	MIT, Manipal University, Manipal

Work experience:

Position	Year	College/University
Assistant Professor	2013-15	Mangalore Marine College & Technology, Mangalore (VTU)
Intern	2016	Universidad Pontificia Bolivariana Bucaramanga, Colombia
Assistant Professor	2017-18	Sahyadri College of Engineering & Management, Adyar, Mangalore (VTU)

Publications, Conferences, Workshop details:

	Publications		Conference		Workshop	
	International	National	International	National	Offline	Online
	9 (5 under review)	-	4	3	17	7
Total	14		7		24	

Place: NITK, Surathkal

Date: 14.07.2023

Bibliography

Abbassi, B., Dullstein, S., and Rabiger, N. (2000). Minimization of excess sludge production by increase of oxygen concentration in activated sludge flocs; experimental and theoretical approach. *Water Research*, 34(1):139 – 146.

Abdul, Gaffar, S., Tejaswini, E. S. S., and Seshagiri, Rao, A. (2022). Design of intelligent control strategies for full-scale wastewater treatment plants with struvite unit. *Journal of Water Process Engineering*, 49:103104.

Abraham, M. T., Vaddapally, M., Satyam, N., and Pradhan, B. (2023). Spatio-temporal landslide forecasting using process-based and data-driven approaches: A case study from western ghats, india. *CATENA*, 223:106948.

Alena, K., Vojtech, V., and Vladimir, K. (2019). Robust decentralized controller design based on equivalent subsystems. *Automatica*, 107:29–35.

Alexandros, D. K., Panayotis, A. P., and Athanasios, S. S. (2015). Design of a modern automatic control system for the activated sludge process in wastewater treatment. *Chinese Journal of Chemical Engineering*, 23(8):1340 – 1349.

Allaire, D., Biros, G., Chambers, J., Ghattas, O., Kordonowy, D., and Willcox, K. (2012). Dynamic data driven methods for self-aware aerospace vehicles. *Procedia Computer Science*, 9:1206–1210.

Amirfakhri, S. J. (2023). Dynamic simulation and optimization of activated sludge unit using the ASM3 model to maximize removal efficiency of slowly biodegradable substrates. *Journal of Environmental Chemical Engineering*, 11(4):110196.

Aranovskiy, S., Ortega, R., and Cisneros, R. (2016). A robust PI passivity-based control of nonlinear systems and its application to temperature regulation. *International Journal of Robust and Nonlinear Control*, 26(10):2216–2231.

Ashish, G., Varun, A., Shuchi, and Abhishek, G. (2016). Up gradation of activated sludge process for capacity improvement by using high purity oxygen. *Procedia Environmental Sciences*, 35:938 – 942.

Ashraf, A., Hawash, S. I., and Mona A. Abdel, F. (2021). Model of aeration tank for activated sludge process. *ISA Transactions*, 12(4):326 – 337.

A.Stare, Vrecko, D., Hvala, N., and Stmcnik, S. (2007). Control of nutrient removing activated sludge system. *IFAC Proceedings Volumes*, 40(4):61 – 66.

Astrom, K. J. and Hagglund, T. (1988). Automatic tuning of PID controllers. *ISA*, 1(1):1–10.

Bak, M. A., Vroonland, J. C., Blom, M. T., Damjanovic, D., Willems, D. L., Tan, H. L., and Corrette Ploem, M. (2023). Data-driven sudden cardiac arrest research in europe: Experts perspectives on ethical challenges and governance strategies. *Resuscitation Plus*, 15:100414.

Balla, K. M., Bendtsen, J. D., Schou, C., Kallesoe, C. S., and Ocampo-Martinez, C. (2022). A learning-based approach towards the data-driven predictive control of combined wastewater networks an experimental study. *Water Research*, 221:118782.

Banaei, F., Zinatizadeh, A. A. L., Mesgar, M., Salari, Z., and Sumathi, S. (2013). Effect of biomass concentration and aeration rate on performance of a full-scale industrial estate wastewater treatment plant. *Journal of Environmental Chemical Engineering*, 1(4):1144 – 1153.

Bayramoglu, M., Cakici, A., and Tekin, T. (2000). Modelling of oxygen transfer rate in diffused-air aeration tanks. *Process Safety and Environmental Protection*, 78(3):209–212.

Bei, S., He, M., Yalin, W., Weihua, G., Chunhua, Y., and Quanmin, Z. (2018). A data-driven optimal control approach for solution purification process. *Journal of Process Control*, 68:171–185.

Bernardelli, A., S. Marsili, L., Manzini, A., Stancari, S., Tardini, G., Montanari, D., Anceschi, G., Gelli, P., and Venier, S. (2020). Real-time model predictive control of a wastewater treatment plant based on machine learning. *Water Science Technology*, 81(11):2391–2400.

Bhat, Vinayambika, S., Shanmuga, Priya, S., and Thirunavukkarasu, I. (2015). A comparative study on control techniques of non-square matrix distillation column. *International Journal of Control Theory and Applications*, 8(3):1129–1136.

Brdys, M. A., Grochowski, M., Gminski, T., Konarczak, K., and Drewa, M. (2008). Hierarchical predictive control of integrated wastewater treatment systems. *Control Engineering Practice*, 16(6):751 – 767.

Brdys, M. A. and Zhang, Y. (2001). Robust hierarchical optimising control of municipal wastewater treatment plants. *IFAC Proceedings Volumes*, 34(8):531–538.

Burns, J. M. and Fielden, R. S. (1989). The automatic control of wastewater treatment plants. *International Biodeterioration*, 25(1):79 – 86.

C. Gomez, Q., Queinnec, I., and Babary, J. P. (2000). A reduced nonlinear model of an activated sludge process. *IFAC Proceedings Volumes*, 33(10):1001 – 1006.

Cadet, C., F., B. J., and Carlos, S. H. (2004). Multicriteria control strategy for cost/quality compromise in wastewater treatment plants. *Control Engineering Practice*, 12(3):335 – 347.

Cadet, C., Guillet, A., and Aurousseau, M. (2016). Dynamic modeling of an activated sludge process: Case study on paper mill effluents. *Journal of Environmental Engineering: American Society of Civil Engineers*, 142(8):326 – 337.

Campi, M. C., Lecchini, A., and Savaresi, S. M. (2002). Virtual reference feedback tuning: a direct method for the design of feedback controllers. *Automatica*, 38(8):1337–1346.

Chachuat, B., Roche, N., and Latifi, M. A. (2000). Dynamic optimisation of small size wastewater treatment plants including nitrification and denitrification processes. volume 8 of *Computer Aided Chemical Engineering*, pages 853 – 858. Elsevier.

Chandra, Shekar, B. and Chidambaram, M. (2016). Decentralized PID controllers by synthesis method for multivariable unstable systems. *IFAC Papers OnLine*, 49(1):504 – 509.

Chandra, Shekar, B. and Chidambaram, M. (2018). Improved decentralized controllers for stable systems by IMC method. *Indian Chemical Engineer*, 60(4):418–437.

Chang, N.-B., Chen, W. C., and Shieh, W. K. (2001). Optimal control of wastewater treatment plants via integrated neural network and genetic algorithms. *Civil Engineering and Environmental Systems*, 18(1):1–17.

Charpentier, J. and Martin, G. (1996). New approach to oxygen requirement for low-load activated sludge. *Water Research*, 30(10):2347 – 2356.

Chaudhuri, S., Dayal, U., and Ganti, V. (2001). Database technology for decision support systems. *Computer*, 34(12):48–55.

Chen, W., Dai, H., Han, T., Wang, X., Lu, X., and Yao, C. (2020). Mathematical modeling and modification of a cycle operating activated sludge process via the multi-objective optimization method. *Journal of Environmental Chemical Engineering*, 8(6):104470.

Chen, X., Ding, H., Wang, Y., Feng, X., Sun, J., and Shao, W. (2022). Sensitive data-driven tooth surface collaborative grinding model for aerospace spiral bevel gears. *Simulation Modelling Practice and Theory*, 119:102566.

Chidambaram, M. and C. Sankar, R. (2017). Subspace identification of dynamic systems. *Narosa Publishing House Pvt. Ltd.*, First edition.

Chirocca, A., Dumitraccu, G., Ifrim, G., Titica, M., and Caraman, S. (2012). An analysis concerning the robust control of the biological wastewater treatment processes using fuzzy techniques. In *2012 16th International Conference on System Theory, Control and Computing (ICSTCC)*, pages 1–6.

Chotkowski, W., Brdys, M. A., and Konarczak, K. (2005). Dissolved oxygen control for activated sludge processes. *Int. Journal of Systems Sci.*, 36(12):727–736.

Coen, F., Vanderhaegen, B., Boonen, I., Vanrolleghem, P. A., and Van Meenen, P. (1997). Improved design and control of industrial and municipal nutrient removal plants using dynamic models. *Water Science and Technology*, 35(10):53–61.

Coma, M., Verawaty, M., Pijuan, M., Yuan, Z., and Bond, P. (2012). Enhancing aerobic granulation for biological nutrient removal from domestic wastewater. *Bioresource Technology*, 103(1):101 – 108.

Concepcion, A. M., YangQuan, C., Vinagre, B. M., and Dingyu, Xue, a. V. F. (2010). *Fractional-order Systems and Controls*. Springer-Verlag London, 1 edition.

Cristea, M. V. and Agachi, S. P. (2006). Nonlinear model predictive control of the wastewater treatment plant. volume 21 of *Computer Aided Chemical Engineering*, pages 1365 – 1370. Elsevier.

Damir, B., Mark, C. M. van, L., Paul, V., Christine, M. H., Guy, J. A., and Joseph, J. H. (2000). Modeling COD, N and P removal in a full-scale WWTP haarlem waarderpolder. *Water Research*, 34(3):846 – 858.

Daniele, Giovanni, G., Edoardo, P., Paolo, B., and Giuliana, M. (2022). Data-driven control of a pendulum wave energy converter: A gaussian process regression approach. *Ocean Engineering*, 253:111191.

Davison, E. (1976). Multivariable tuning regulators: The feedforward and robust control of a general servomechanism problem. *IEEE Transactions on Automatic Control*, 21(1):35–47.

Day, D. (1996). How australian social policy neglects environments. *Australian Journal of Soil and Water Conservation*, 9:3 – 9.

Degs, Y. A., Khraisheh, M. A. M., Allen, S. J., and Ahmad, M. N. (2000). Effect of carbon surface chemistry on the removal of reactive dyes from textile effluent. *Water Research*, 34(3):927 – 935.

Del Borghi, A., Binaghi, L., Converti, A., and Del Borghi, M. (2003). Combined treatment of leachate from sanitary landfill and municipal wastewater by activated sludge. *Chemical and biochemical engineering quarterly*, 17(4):277–284.

Devi, C. A. and Narayanan, S. (2016). Centralized controller design using state space concept. *IFAC-PapersOnLine*, 49(9):62–67.

Dickin, S. K., Schuster, Wallace, C. J., Qadir, M., and Pizzacalla, K. (2016). A review of health risks and pathways for exposure to wastewater use in agriculture. *Environmental health perspectives*, 124(7):900–909.

Dimitrova, N. and Krastanov, M. (2012). Nonlinear adaptive stabilizing control of an anaerobic digestion model with unknown kinetics. *International Journal of Robust and Nonlinear Control*, 22(15):1743–1752.

Ding, W., Xin, L., Lingzhi, H., and Junfei, Q. (2023). Data-driven tracking control design with reinforcement learning involving a wastewater treatment application. *Engineering Applications of Artificial Intelligence*, 123:106242.

Dongwook, K., James, D. B., and Ertunga, C. O. (2015). Optimization of wastewater treatment plant operation for greenhouse gas mitigation. *Journal of Environmental Management*, 163:39 – 48.

Ellis, G. (2012). Chapter 6 - four types of controllers. In Ellis, G., editor, *Control System Design Guide (Fourth Edition)*, pages 97–119. Butterworth-Heinemann, Boston, fourth edition edition.

Erfan, A., Hossein, M., Emilio, F., Danial, G., Sevda, M., Bracco, G., and Mehdi, N. (2022). Optimization of hydraulic power take-off system settings for point absorber wave energy converter. *Renewable Energy*, 194:938–954.

Erion, B., Felix, K. A., and Geophrey, K. A. (2023). Data-driven modelling of soil moisture dynamics for smart irrigation scheduling. *Smart Agricultural Technology*, 5:100251.

Euan, W. L. and Howard, A. C. (1999). Reducing production of excess biomass during wastewater treatment. *Water Research*, 33(5):1119 – 1132.

Foscoliano, C., Vigo, S., Mulas, M., and Tronci, S. (2016). Predictive control of an activated sludge process for long term operation. *Chemical Engineering Journal*, 304.

Fradkov, A. L., Miroshnik, I. V., and Nikiforov, V. O. (1999). *Nonlinear Control of MIMO Systems*, pages 183–264. Springer Netherlands, Dordrecht.

Francisco, M., Skogestad, S., and Vega, P. (2015). Model predictive control for the self-optimized operation in wastewater treatment plants: Analysis of dynamic issues. *Comput. Chem. Eng.*, 82:259–272.

Francisco, M. and Vega, P. (2007). Integrated design of wastewater treatment processes using model predictive control. In *2007 European Control Conference (ECC)*, pages 5333–5340.

Francisco, M. and Vega, P. (2008). Multi-model approaches for integrated design of wastewater treatment plants with model predictive control. *IFAC Proceedings Volumes*, 41(2):9380–9385.

Francisco, M., Vega, P., and Alvarez, H. (2011). Robust integrated design of processes with terminal penalty model predictive controllers. *Chemical Engineering Research and Design*, 89(7):1011 – 1024.

Frank, L. L., Zhongsheng, H., and Huijun, G. (2017). Data-driven control and learning systems. *IEEE Transactions on Industrial Electronics*, 64(5):4070–4075.

Georgieva, P. G. and Feyo, De, A. S. (1999). Robust control design of an activated sludge process. *International Journal of Robust and Nonlinear Control*, 9(13):949–967.

Ghanadzadeh, Gilani,, A., Ahmadifar, S., and Taki, T. (2019). Experimental and modeling study of liquid phase equilibria for (water+phosphoric acid+sec-alcohols) systems. *The Journal of Chemical Thermodynamics*, 135:305–315.

Ghosh, S. and Pan, S. (2021). Centralized pi controller design method for mimo processes based on frequency response approximation. *ISA Transactions*, 110:117–128.

Gomez-Quintero, C.-S., Queinnec, I., and Sperandio, M. (2004). A reduced linear model of an activated sludge process. *IFAC Proceedings Volumes*, 37(3):219–224.

Goodman, B. L. and Englande, A. J. (1974). A unified model of the activated sludge process. *Journal Water Pollution Control Fed.*, 46:312–332.

Grimaldi, A., Minuto, F. D., Perol, A., Casagrande, S., and Lanzini, A. (2023). Ageing and energy performance analysis of a utility-scale lithium-ion battery for power grid applications through a data-driven empirical modelling approach. *Journal of Energy Storage*, 65:107232.

Grosdidier, P., Morari, M., and Holt, B. R. (1985). Closed loop properties from steady state gain information. *Industrial and Engineering Chemistry Fundamentals*, 24(2):221–235.

Gustaf, O. (1976). State of the art in sewage treatment plant control. *AIChE Symposium Series*, 72(159):52–76.

Gutierrez, G., L. A. Ricardez, S., Budman, H., and Prada, C. (2014). An MPC-based control structure selection approach for simultaneous process and control design. *Computers & Chemical Engineering*, 70:11–21.

Hai, Trung, D., Nam, Van, B., Lanh, Van, N., Hoang, Thuan, T., and Minh, Tuan, N. (2021). A design of higher-level control based genetic algorithms for wastewater treatment plants. *Engineering Science and Technology, an International Journal*, 24(4):872–878.

Hakan, M., Aysegul, A., and Celal, F. G. (2008). Modeling of the activated sludge process by using artificial neural networks with automated architecture screening. *Computers and Chemical Engineering*, 32(10):2471 – 2478.

Han, H., Liu, Z., Hou, Y., and Qiao, J. (2020). Data-driven multiobjective predictive control for wastewater treatment process. *IEEE Transactions on Industrial Informatics*, 16(4):2767–2775.

Han, J., Lakshmanan, L., and Ng, R. (1999). Constraint-based, multidimensional data mining. *Computer*, 32(8):46–50.

Hanuma, Naik, R., Ashok, Kumar, D. V., and Anjaneyulu, K. S. R. (2014). control configuration selection and controller design for multivariable processes using normalized gain. *International Journal of Electrical, computer electronics and communication engineering*, 8:1507–1511.

Hao, W., Tan, L., Yang, X., Shi, D., Wang, M., Miao, G., and Fan, Y. (2023). A physics-informed machine learning approach for notch fatigue evaluation of alloys used in aerospace. *International Journal of Fatigue*, 170:107536.

Hauduc, H., Rieger, L., Oehmen, A., van Loosdrecht, M. C. M., Comeau, Y., Heduit, A., Vanrolleghem, P. A., and Gillot, S. (2013). Critical review of activated sludge modeling: State of process knowledge, modeling concepts, and limitations. *Biotechnology and Bioengineering*, 110(1):24–46.

He, Mao, J., Cai, Wen, J., Wu, Bing, F., and He, M. (2005). Simple decentralized PID controller design method based on dynamic relative interaction analysis. *Industrial & Engineering Chemistry Research*, 44(22):8334–8344.

Henze, M., C. P. Leslie, G., Gujer, W., Marai, G. V. R., and Matsuo, T. (1987). A general model for single-sludge wastewater treatment systems. *Water Research*, 21(5):505 – 515.

Henze, M., Gujer, W., Mino, T., and van Loosedrecht, M. (2006). *Activated Sludge Models ASM1, ASM2, ASM2d and ASM3*. IWA Publishing.

Hjalmarsson, H. and Birkeland, T. (1998). Iterative feedback tuning of linear time-invariant MIMO systems. In *Proceedings of the 37th IEEE Conference on Decision and Control (Cat. No.98CH36171)*, volume 4, pages 3893–3898 vol.4.

Holenda, B., Domokos, E., Redey, A., and Fazakas, J. (2008). Dissolved oxygen control of the activated sludge wastewater treatment process using model predictive control. *Computers and Chemical Engineering*, 32(6):1270 – 1278.

Holger, D., Michael, W. T., and Michael, W. (2006). Wastewater treatment: A model system for microbial ecology. *Trends in Biotechnology*, 24(11):483 – 489.

Holic, I., Rosinova, D., and Vesely, V. (2013). Robust decentralized PI controller design based on subsystem pole placement. *IFAC Proceedings Volumes*, 46(13):260–265.

Hong, Z. and Thomas, J. M. (1996). Modeling of activated sludge wastewater treatment processes using integrated neural networks and a first principle model. *IFAC Proceedings Volumes*, 29(1):6774 – 6779.

Hongbo, L., Fang, Z., Boyang, M., and Xianghua, W. (2012). Enhanced nitrogen removal in a wastewater treatment process characterized by carbon source manipulation with biological adsorption and sludge hydrolysis. *Bioresource Technology*, 114:62 – 68.

Huang, H. P. and Jeng, J. C. (2005). *Process Reaction Curve and Relay Methods Identification and PID Tuning*, pages 297–337. Springer London, London.

Huang, P., Li, Z., Zhu, Y., Wen, C., and Corman, F. (2023). Train traffic control in merging stations: A data-driven approach. *Transportation Research Part C: Emerging Technologies*, 152:104155.

Huoqing, G., Damien, J. B., Morgan, M., Shihu, H., and Jurg, K. (2017). Nutrient removal and energy recovery from high-rate activated sludge processes - impact of sludge age. *Bioresource Technology*, 245:1155 – 1161.

Hypponen, E., Mulugeta, A., Zhou, A., and Santhanakrishnan, V. K. (2019). A data-driven approach for studying the role of body mass in multiple diseases: a phenome-wide registry-based case-control study in the uk biobank. *The Lancet Digital Health*, 1(3):e116–e126.

Idris, A., Goni, Umar, M., Abdullahi, Y., Poom, K., and Ibrahim, Y. (2021). A mathematical model of coronavirus disease (COVID-19) containing asymptomatic and symptomatic classes. *Results in Physics*, 21:103776.

Ilse, Y. S., Jeroen, V. H., Ronald, C., and Jan, F. Van, I. (2003a). Linearization of the activated sludge model asm1 for fast and reliable predictions. *Water Research*, 37(8):1831 – 1851.

Ilse, Y. S., Jeroen, V. H., Ronald, C., and Jan, F. Van, I. (2003b). Linearization of the activated sludge model ASM1 for fast and reliable predictions. *Water Research*, 37(8):1831–51.

Ioana, N. and Ioan, N. (2016). Modelling and optimization of an activated sludge wastewater treatment process. In Zdravko, K. and Milos, B., editors, *26th European Symposium on Computer Aided Process Engineering*, volume 38 of *Computer Aided Chemical Engineering*, pages 1159 – 1164. Elsevier.

Ionut, M., Roxana, B., Ruben, C., and Ioan, N. (1999). RGA analysis and decentralized control for a wastewater treatment plant. *Journal of Biotechnology*, 75(2):229 – 239.

Ivan, M. and Paolo, R. (2008). Data-driven simulation and control. *International Journal of Control*, 81(12):1946–1959.

Jaromir, F. and Pavel, Z. (2019). PID controller tuning via dominant pole placement in comparison with ziegler-nichols tuning. *IFAC-PapersOnLine*, 52(18):43–48.

Jaume, P., Humbert, S., and Joan, G. (2005). Short-term harmful effects of ammonia nitrogen on activated sludge microfauna. *Water Research*, 39(18):4397 – 4404.

Javier, G., Albert, G., Ramon, V., and Juan, A. B. (2011). Improving the performance of a WWTP control system by model-based setpoint optimisation. *Environmental Modelling and Software*, 26(4):492 – 497.

Jeen, L. and Ruey, Jing, L. (2009). Hybrid fuzzy-logic and neural-network controller for MIMO systems. *Mechatronics*, 19(6):972–986.

Jenifer, Benavides, S., Marianna, V., and Davide, D. (2021). Model-based comparison of sequencing batch reactors and continuous-flow activated sludge processes for biological wastewater treatment. *Comput. Chem. Eng.*, 144:107–127.

Jevtovic, B. T. and Matausek, M. R. (2010). Pid controller design of tito system based on ideal decoupler. *Journal of Process Control*, 20(7):869–876.

Jiang, C., Xu, S., Wang, R., Feng, S., Zhou, S., Wu, S., Zeng, X., Wu, S., sZhihui Bai, Zhuang, G., and Zhuang, X. (2019). Achieving efficient nitrogen removal from real sewage via nitrite pathway in a continuous nitrogen removal process by combining free nitrous acid sludge treatment and DO control. *Water Research*, 161(1):590–600.

Jiateng, Y., Shuai, S., Jing, X., Tao, T., and Ronghui, L. (2020). Data-driven approaches for modeling train control models: Comparison and case studies. *ISA Transactions*, 98:349–363.

Jin, Qibing, Z. L., Wang, Q., and Jiang, B. (2016). PI controller design for a TITO system based on delay compensated structure and direct synthesis. *The Canadian Journal of Chemical Engineering*, 94(9):1740–1754.

Joao, Joanaz, d. M. and Antonio, S. C. (1994). Models for the optimization of regional wastewater treatment systems. *European Journal of Operational Research*, 73(1):1 – 16.

Jones, A. B. and Smith, J. M. (2013). Article Title. *Journal Title*, 13(52):123–456.

Jong, Min, L. and Jay, H. L. (2005). Approximate dynamic programming-based approaches for input-output data-driven control of nonlinear processes. *Automatica*, 41(7):1281–1288.

Juan, G., Francisco, V., and Fernando, M. (2012). Centralized multivariable control by simplified decoupling. *Journal of Process Control*, 22(6):1044 – 1062.

Julien, S., Babary, J. P., and Lessard, P. (1998). Theoretical and practical identifiability of a reduced order model in an activated sludge process doing nitrification and denitrification. *Water Science and Technology*, 37(12):309 – 316.

Jun, W., Gang, Y., Guojing, Z., and Ting, X. (2014). Model predictive control of biological nitrogen removal via partial nitrification at low carbon/nitrogen (C/N) ratio. *Journal of Environmental Chemical Engineering*, 2(4):1899 – 1906.

K. Suresh, M., Devakumar, S., Vijayan, V., and Rajinikanth, V. (2016). Design of centralized PI controller for interacting conical tank system. *Indian Journal of Science and Technology*, 9(12).

Kadhar, K. M. A., Baskar, S., and Amali, S. M. J. (2015). Diversity controlled self adaptive differential evolution based design of non-fragile multivariable PI controller. *Engineering Applications of Artificial Intelligence*, 46:209 – 222.

Kah, Y. T., Zhenliang, M., and Carl, W. P. (2023). A review of data-driven approaches to predict train delays. *Transportation Research Part C: Emerging Technologies*, 148:104027.

Kara, L. N. (2005). *Small and Decentralized Systems for Wastewater Treatment and Reuse*. National Research Council.

Karatug, C., Tadros, M., Ventura, M., and Guedes Soares, C. (2023). Strategy for ship energy efficiency based on optimization model and data-driven approach. *Ocean Engineering*, 279:114397.

Karimi, A., van Heusden, K., and Bonvin, D. (2007). Non-iterative data-driven controller tuning using the correlation approach. In *2007 European Control Conference (ECC)*, pages 5189–5195.

Katebi, M. R., Johnson, M. A., Wilkie, and McCluskey, G. (1998). Control and management of wastewater treatment plants. *IFAC Large Scale Systems*, 1(1).

Kaya, I. and Peker, F. (2020). Optimal I-PDcontroller design for setpoint tracking of integrating processes with time delay. *IET Control Theory & Applications*, 14(18):2814–2824.

Kecman, P. and Goverde, R. M. P. (2015). Online data-driven adaptive prediction of train event times. *IEEE Transactions on Intelligent Transportation Systems*, 16(1):465–474.

Khisty, C. J. and Sriraj., P. S. (1999). Transportation project selection through robustness analysis for developing countries. *Transportation Research Record 1695, TRB, National Research Council, Washington, DC*, pages 24–48.

Kim, J., Qi, M., Park, J., and Moon, I. (2023). Revealing the impact of renewable uncertainty on grid-assisted power-to-x: A data-driven reliability-based design optimization approach. *Applied Energy*, 339:121015.

Kiuru, H. J. and Rautiainen, J. A. (1998). Biological nutrient removal at a very low-loaded activated sludge plant with high biomass concentrations. *Water Science and Technology*, 38(1):63 – 70.

Kollar, I., Pintelon, R., and Schoukens, J. (2006). Frequency domain system identification toolbox for matlab: Characterizing nonlinear errors of linear models. *IFAC Proceedings Volumes*, 39(1):726–731.

Krist, V. G., Mark, C. M. v. L., Mogens, H., Morten, L., and Sten, B. J. (2004). Activated sludge wastewater treatment plant modelling and simulation: state of the art. *Environmental Modelling and Software*, 19(9):763 – 783.

Lagarias, J. C., Reeds, J. A., Wright, M. H., and Wright, P. E. (1998). Convergence properties of the nelder–mead simplex method in low dimensions. *SIAM Journal on Optimization*, 9(1):112–147.

Largus, T. A., Khursheed, K., Muthanna, H. A.-D., Brian, A. W., and Rosa, D.-E. (2004). Production of bioenergy and biochemicals from industrial and agricultural wastewater. *Trends in Biotechnology*, 22(9):477 – 485.

Laurentiu, L., Ramon, V., George, A. I., Emil, C., Sergiu, C., and Marian, B. (2019). Control strategies of a wastewater treatment plant. *IFAC-PapersOnLine*, 52(1):257–262.

Layla, Angria, S., Yunita, Dwi, S., Muhammad, Z., and Tulus (2018). Data-driven modelling for decision making under uncertainty. *IOP Conf. Series: Materials Science and Engineering*, 300:012013.

Lee, B. K., Sung, S. W., Chun, H. D., and Koo, J. K. (1998). Automatic control for DO and ph in the activated sludge process in a coke wastewater treatment plant. *Industrial and Engineering Chemistry Research*, 37(12):141–148.

Lee, M., Lee, K., Kim, C., and Lee, J. (2004). Analytical design of multiloop PID controllers for desired closed-loop responses. *AIChE Journal*, 50(7):1631–1635.

Lees-Miller, J., Hammersley, J., and Wilson, R. (2010). Theoretical maximum capacity as benchmark for empty vehicle redistribution in personal rapid transit. *Transportation Research Record: Journal of the Transportation Research Board*, (2146):76–83.

Leon, S. D. and Robert, N. (2008). Total nitrogen removal in a hybrid, membrane-aerated activated sludge process. *Water Research*, 42(14):3697 – 3708.

Li, M., Zhu, Y., Yang, K., Hu, C., and Mu, H. (2017). An integrated model-data-based zero-phase error tracking feedforward control strategy with application to an ultraprecision wafer stage. *IEEE Transactions on Industrial Electronics*, 64(5):4139–4149.

Lindberg, C. F. (1998). Multivariable modeling and control of an activated sludge process. *Water Science and Technology*, 37(12):149 – 156.

Liu, G., Xu, X., Zhu, L., Xing, S., and Chen, J. (2013). Biological nutrient removal in a continuous anaerobic-aerobic-anoxic process treating synthetic domestic wastewater. *Chemical Engineering Journal*, 225:223–229.

Liu, Z., Wang, Q., Sigler, D., Kotz, A., Kelly, K. J., Lunacek, M., Phillips, C., and Garikapati, V. (2023). Data-driven simulation-based planning for electric airport shuttle systems: A real-world case study. *Applied Energy*, 332:120483.

Ljung, L. and Singh, R. (2012). Version 8 of the matlab system identification toolbox. *IFAC Proceedings Volumes*, 45(16):1826–1831.

Luan, X., Chen, Q., and Liu, F. (2015). Equivalent transfer function based multi-loop PI control for high dimensional multivariable systems. *International Journal of Control, Automation and Systems*, 13(2):346–352.

Luca, L., Barbu, M., and Caraman, S. (2014). Modelling and performance analysis of an urban wastewater treatment plant. In *2014 18th International Conference on System Theory, Control and Computing (ICSTCC)*, pages 285–290.

Lukasse, L. J. S., Keesman, K., Klapwijk, A., and van Straten, G. (1998). Optimal control of n-removal in ASPs. *Water Science and Technology*, 38(3):255 – 262.

Lukasse, L. J. S., Keesman, K. J., and Straten, van, G. (1996). Grey-box identification of dissolved oxygen dynamics in activated sludge processes,. In *Proc. 13th IFAC World Congress*.

Luyben, W. L. (1986). Simple method for tuning SISO controllers in multivariable systems. *Industrial and Engineering Chemistry Process Design and Development*, 25(3):654–660.

Maciejowski, J. M. (1989). *Multivariable Feedback Design*. 1st ed., Dagless, E. L. (ed.), Addison Wesley, New York, NY.

Maged, M. H., Mona, G. K., and Ezzat, A. H. (2004). Prediction of wastewater treatment plant performance using artificial neural networks. *Environmental Modelling and Software*, 19(10):919 – 928.

Maghade, D. and Patre, B. (2012). Decentralized PI/PID controllers based on gain and phase margin specifications for TITO processes. *ISA Transactions*, 51(4):550–558.

Mahmood, F., Govindan, R., Bermak, A., Yang, D., and Al-Ansari, T. (2023). Data-driven robust model predictive control for greenhouse temperature control and energy utilisation assessment. *Applied Energy*, 343:121190.

Malwatkar, G. M., Khandekar, A. A., Asutkar, V. G., and Waghmare, L. M. (2008). Design of centralized PI/PID controller: Interaction measure approach. In *2008 IEEE*

Region 10 and the Third international Conference on Industrial and Information Systems, pages 1–6.

Manesis, S. A., Sapidis, D. J., and King, R. E. (1998). Intelligent control of wastewater treatment plants. *Artificial Intelligence in Engineering*, 12(3):275 – 281.

Mao, Jun, H., Wen, Jian, C., Wei, N., and Li, Hua, X. (2009). RNGA based control system configuration for multivariable processes. *Journal of Process Control*, 19(6):1036 – 1042.

Marinus, K. N. and Time, B. O. (1995). Improvement of a recirculating plant by introducing STAR control. *Water Science and Technology*, 31(2):171 – 180.

Mario, N. and Predrag, H. (2012). Mathematical modelling and optimisation of a waste water treatment plant by combined oxygen electrode and biological waste water treatment model. *Applied Mathematical Modelling*, 36(8):3813 – 3825.

Marquez, H. J., Labibi, B., and Chen, T. (2008). Decentralized robust PI controller design for an industrial utility boiler - an IMC method. *IFAC Proceedings Volumes*, 41(2):14235–14240.

Marquez, P., Gutierrez, M. C., Toledo, M., Alhama, J., Michan, C., and Martin, M. A. (2022). Activated sludge process versus rotating biological contactors in WWTPs: Evaluating the influence of operation and sludge bacterial content on their odor impact. *Process Saf. Environ. Prot.*, 160:775–785.

Marta, R., Berta, G., and Javier, R. V. (2016). Analysis and modelling of predation on biofilm activated sludge process: Influence on microbial distribution, sludge production and nutrient dosage. *Bioresource Technology*, 220:572 – 583.

Martin, C., Grandjean, P. A. B., Paul, L., and Jules, T. (1995). Dynamic modeling of the activated sludge process improving prediction using neural networks. *Water Research*, 29:995–1004.

Masti, D., Breschi, V., Formentin, S., and Bemporad, A. (2023). Auto-tuning of reference models in direct data-driven control. *Automatica*, 155:111110.

Mats, E., Berndt, B., and Mikael, A. (2006). Control of the aeration volume in an activated sludge process using supervisory control strategies. *Water Research*, 40(8):1668 – 1676.

Mc Avoy, T., Arkun, Y., Chen, R., Robinson, D., and Schnelle, P. (2003). A new approach to defining a dynamic relative gain. *Control Engineering Practice*, 11(8):907–914.

Mervyn, C. G., Gunnar, D., and Mark, N. (1997). Aerated denitrification in full-scale activated sludge facilities. *Water Science and Technology*, 35(10):103 – 110.

Metcalf and Eddy (2003). *Wastewater Engineering, Treatment and Reuse fourth Edition*, volume 4. McGraw Hill Education.

Michela, M., Stefania, T., Francesco, C., Henri, H., Paula, L., Mari, H., Riku, V., and Roberto, B. (2013). An application of predictive control to the viikinmaki wastewater treatment plant. *IFAC Proceedings Volumes*, 46(31):18 – 23.

Mohanraj, S., Murugesh, T., and Senthilkumar, M. (2021). Design of decentralized controller for coupled tank system using BLT method. *Materials Today: Proceedings*, 46:11198–11201.

Moradi, M. and Seyedtabaii, S. (2022). Intelligent fuzzy controller design: Disturbance rejection cases. *Applied Soft Computing*, 124:109015.

Mu, Y., Xu, Y., Zhang, J., Wu, Z., Jia, H., Jin, X., and Qi, Y. (2023). A data-driven rolling optimization control approach for building energy systems that integrate virtual energy storage systems. *Applied Energy*, 346:121362.

Muntean, I., Both, R., Crisan, R., and Nascu, I. (2015). RGA analysis and decentralized control for a wastewater treatment plant. pages 453–458.

Muntean I., Both R., Crisan R., and Nascu I. (2015). RGA analysis and decentralized control for a wastewater treatment plant. In *2015 IEEE International Conference on Industrial Technology (ICIT)*, pages 453–458.

Murphey, Y. L., Crossman, J. A., ZhiHang, C., and Cardillo, J. (2003). Automotive fault diagnosis part ii: a distributed agent diagnostic system. *IEEE Transactions on Vehicular Technology*, 52(4):1076–1098.

Mustafa, Cagdas, O., Fernando, Martin, S., and Fouad, T. (2016). Optimization of aeration profiles in the activated sludge process. *Chemical Engineering Science*, 139:1 – 14.

Na, L., Ronghu, C., and Biao, H. (2023). Data-driven set-point control for nonlinear nonaffine systems. *Information Sciences*, 625:237–254.

Nejjari, F., Benhammou, A., Dahhou, B., and Roux, G. (1997). Nonlinear multivariable control of a biological wastewater treatment process. In *1997 European Control Conference (ECC)*, pages 183–189.

Nejjari, F., Dahhou, B., Benhammou, A., and Roux, G. (1999). Non-linear multivariable adaptive control of an activated sludge wastewater treatment process. *International Journal of Adaptive Control and Signal Processing*, 13(5):347–365.

Nejjari, F. and Quevedo, J. (2004). Predictive control of a nutrient removal biological plant. volume 3, pages 2290 – 2295 vol.3.

Nelder, J. A. and Mead, R. (1965). A simplex method for function minimization. *Computer Journal*, 7(1):308–313.

NielsenJohn, J. and Liden., V. (2003). *Modeling of Growth Kinetics In: Bioreaction Engineering Principles.* Springer, Boston, MA.

Nor'Azlan, N. A., Selamat, N. A., and Yahya, N. M. (2018). Multivariable PID controller design tuning using bat algorithm for activated sludge process. *IOP Conference Series: Materials Science and Engineering*, 342:012030.

Norbert, J. and H. Johannes, P. (1996). Influence of the enhanced biological phosphorus removal on the waste activated sludge production. *Water Science and Technology*, 34(1):17 – 23.

Nordfeldt, P. and Hagglund, T. (2006). Decoupler and PID controller design of TITO systems. *Journal of Process Control*, 16(9):923–936.

Norhaliza, A. W., Reza, K., and Jonas, B. (2009). Multivariable PID control design for activated sludge process with nitrification and denitrification. *Biochemical Engineering Journal*, 45(1):239–248.

Normey, R. and Julio, E. (2007). *Control of Dead-time Processes*. Springer-Verlag London, First edition.

Novak, M. and Horvat, P. (2012). Mathematical modelling and optimisation of a wastewater treatment plant by combined oxygen electrode and biological wastewater treatment model. *Applied Mathematical Modelling*, 36(8):3813–3825.

Nuhoglu, A., Keskinler, B., and Yildiz, E. (2005). Mathematical modelling of the activated sludge process-the erzincan case. *Process Biochemistry*, 40(7):2467–2473.

O'Brien, M., Mack, J., Lennox, B., Lovett, D., and Wall, A. (2011). Model predictive control of an activated sludge process: A case study. *Control Engineering Practice*, 19(1):54 – 61.

O'Brien, M., S. E. Pinto, C., and Katebi, R. (2005). Model based predictive control for wastewater applications. *IFAC Proceedings Volumes*, 38(1):167 – 172.

Olsson, G. (2012). Ica and me–a subjective review. *Water Res.*, 46(6):1585–624.

Orhon, D., Cokgor, E. U., Insel, G., Karahan, O., and Katipoglu, T. (2009). Validity of monod kinetics at different sludge ages peptone biodegradation under aerobic conditions. *Bioresource Technology*, 100(23):5678 – 5686.

Pallavhee, T., Sundaramoorthy, S., and Sivasankaran, M. A. (2018). Optimal control of small size single tank activated sludge process with regulated aeration and external carbon addition. *Industrial & Engineering Chemistry Research*, 57(46):15811–15823.

Park, S., Kim, B. J., and Jung, S. Y. (2014). Simulation methods of a system dynamics model for efficient operations and planning of capacity expansion of activated-sludge wastewater treatment plants. *Procedia Engineering*, 70:1289 – 1295.

Parrott, Joanne, L. and Blunt, Beverley, R. (2005). Life-cycle exposure of fathead minnows (pimephales promelas) to an ethinylestradiol concentration below 1 ng/l reduces egg fertilization success and demasculinizes males. *Environmental Toxicology*, 20(2):131–141.

Patartics, B., Seiler, P., Takarics, B., and Vanek, B. (2023). Worst case uncertainty construction via multifrequency gain maximization with application to flutter control. *IEEE Transactions on Control Systems Technology*, 31(1):155–165.

Patartics, B., Seiler, P., and Vanek, B. (2020). Construction of an uncertainty to maximize the gain at multiple frequencies. In *2020 American Control Conference (ACC)*, pages 2643–2648.

Peilong, X., Hongde, Q., Jingran, M., Zhongchao, D., and Yifan, X. (2023). Data-driven model predictive control for ships with gaussian process. *Ocean Engineering*, 268:113420.

Penttinen, J. and Koivo, H. N. (1980). Multivariable tuning regulators for unknown systems. *Automatica*, 16(4):393–398.

Perkins, J. (1991). Multivariable feedback design: by j. m. maciejowski (addison-wesley, wokingham, 1989). *Journal of Process Control*, 1(1):55.

Piotrowski, R., Brdys, M. A., and Miotke, D. (2010). Centralized dissolved oxygen tracking at wastewater treatment plant: Nowy dwor gdanski case study. *IFAC Proceedings Volumes*, 43(8):292–297.

Prabhu Y., T. and Sankar, Rao, C. (2019). Design of robust PI controller with decoupler for a fluid catalytic cracking unit. *Industrial and Engineering Chemistry Research*, 58(45):20722–20733.

Qiao, J. F., Han, G. T., Han, H. G., Yang, C. L., and Li, W. (2019). Decoupling control for wastewater treatment process based on recurrent fuzzy neural network. *Asian Journal of Control*, 21(3):1270–1280.

Qin, L., Haiyan, W., Haoyan, L., and Dianhai, Y. (2015). Enhanced biological nutrient removal in modified carbon source division anaerobic anoxic oxic process with return activated sludge pre-concentration. *Chinese Journal of Chemical Engineering*, 23(6):1027 – 1034.

Qiu, J., Wang, T., Yin, S., and Gao, H. (2017). Data-based optimal control for networked double-layer industrial processes. *IEEE Transactions on Industrial Electronics*, 64(5):4179–4186.

Rajapandiyan, C. and Chidambaram, M. (2012a). control configuration selection and controller design for multivariable processes using normalized gain. *Industrial and Engineering Chemistry Research*, 51:12398–12410.

Rajapandiyan, C. and Chidambaram, M. (2012b). Controller design for MIMO processes based on simple decoupled equivalent transfer functions and simplified decoupler. *Industrial & Engineering Chemistry Research*, 51(38):12398–12410.

Raviteja, K., Purushottama, Rao, D., and A. Seshagiri, R. (2016). Improved controller design for two-input-two-output (TITO) unstable processes. *Resource-Efficient Technologies*, 2:S76 – S86.

Razali, M. C., Wahab, N. A., Balaguer, P., Rahmat, M. F., and Samsudin, S. I. (2013). Multivariable PID controllers for dynamic process. In *2013 9th Asian Control Conference (ASCC)*, pages 1–5.

Reddy, B., Chidambaram, M., and Darwish, M. K. A. G. (1997). Design of centralized controllers for a MSF desalination plant. *Desalination*, 113(1):27 – 38.

Revollar, S., Vega, P., Vilanova, R., and Francisco, M. (2017). Optimal control of wastewater treatment plants using economic-oriented model predictive dynamic strategies. *Applied Sciences*, 7:813.

Rim, Y. T., Yang, H. J., Yoon, C. H., Kim, Y. S., Seo, J. B., Ryu, J. K., and Shin, E. B. (1997). A full-scale test of a biological nutrients removal system using the sequencing batch reactor activated sludge process. *Water Science and Technology*, 35(1):241 – 247.

Ruano, M. V., Ribes, J., Sin, G., Seco, A., and Ferrer, J. (2010). A systematic approach for fine-tuning of fuzzy controllers applied to WWTPs. *Environmental Modelling and Software*, 25(5):670 – 676.

Rusul, N., Saad, A., and Lu, X. (2013). Biological nutrient removal with limited organic matter using a novel anaerobic-anoxic/oxic multi-phased activated sludge process. *Saudi Journal of Biological Sciences*, 20(1):11 – 21.

Safonov, M. and Tsao, T. C. (1997). The unfalsified control concept and learning. *IEEE Transactions on Automatic Control*, 42(6):843–847.

Sakai, Y., Kawaguchi, N., Arrieta, O., and Sato, T. (2023). Data-driven cascade control system: Response estimation and controller design. *ISA Transactions*.

Sanjith, S. A. and Chinta, Sankar, R. (2020a). Centralized proportional integral controller design for the activated sludge process. *Chemical Engineering Technology*, 45(3):467–478.

Sanjith, S. A. and Chinta, Sankar, R. (2020b). Robust decentralized proportional integral controller design for an activated sludge process. *Asia Pacific Journal of Chemical Engineering*, 18(1):e2531.

Sanjith, S. A. and Rao, Chinta, S. (2020). Robust decentralized proportional-integral controller design for an activated sludge process. *Asia Pacific Journal of Chemical Engineering*, 15(6):e2531.

Santin, I., Barbu, M., Perret, C., and Vilanova, R. (2019). Dissolved oxygen control in biological wastewater treatments with non-ideal sensors and actuators. *Industrial and Engineering Chemistry Research*, 58(45):20639–20654.

Santin, I., Pedret, C., and Vilanova, R. (2015). Fuzzy control and model predictive control configurations for effluent violations removal in wastewater treatment plants. *Industrial & Engineering Chemistry Research*, 54(10):2763–2775.

Sarma, K. and Chidambaram, M. (2013). Centralized PI/PID controllers for nonsquare systems with rhp zeros. *J. Indian Inst. Sci.*, 85(4):201–2014.

Schei, T. S. (1993). Automatic tuning of simple decouplers in multivariable control systems. *IFAC Proceedings Volumes*, 26(2, Part 4):65 – 72.

Sendin, O., Moles, C., Alonso, A., and Banga, J. (2004). Chapter D4 multi-objective integrated design and control using stochastic global optimization methods. *Computer Aided Chemical Engineering*, 17.

Sergiu, C., M. S. and Maruan, B. (2007). Predictive control of a wastewater treatment process. *International Journal of Computers, Communications and Control*, 2(132-142):8.

Seshagiri, Rao, A., Rao, V. S. R., and Chidambaram, M. (2007). Delay-compensated controllers for two-input/two-output (TITO) multivariable processes. *Asia-Pacific Journal of Chemical Engineering*, 2(6):510–516.

Shameli-Sendi, A. (2020). An efficient security data-driven approach for implementing risk assessment. *Journal of Information Security and Applications*, 54:102593.

Shannon, M. A., Paul, W. B., Menachem, E., John, G. G., Benito, J. M., and Mayes, A. M. (2008). Science and technology for water purification in the coming decades. *Nature*, 452(1):301–310.

Shen, W., Chen, X. Q., and Corriou, J.-P. (2008). Application of model predictive control to the BSM1 benchmark of wastewater treatment process. *Computers and Chemical Engineering*, 32:2849–2856.

Shen, Y., Cai, Wen, J., and Li, S. (2010a). Multivariable process control: Decentralized, decoupling, or sparse? *Industrial & Engineering Chemistry Research*, 49(2):761–771.

Shen, Y., Cai, W.-J., and Li, S. (2010b). Normalized decoupling control for high-dimensional mimo processes for application in room temperature control hvac systems. *Control Engineering Practice*, 18(6):652–664.

Shen, Y., Shaoyuan, L., Ning, L., and Cai, Wen, J. (2011). Partial decoupling control for multivariable processes. *Industrial & Engineering Chemistry Research*, 50(12):7380–7387.

Shen, Y., Sun, Y., and Xu, W. (2014). Centralized PI/PID controller design for multivariable processes. *Industrial & Engineering Chemistry Research*, 53(25):10439–10447.

Shi, Q., Zhao, L., Zhang, E., Xia, J., Li, H., Wang, K., and Jiang, K. (2023). The future capacity prediction using a hybrid data-driven approach and aging analysis of liquid metal batteries. *Journal of Energy Storage*, 67:107637.

Shimura, M. and Tabuchi, T. (1994). The effect of livestock on the concentration of nitrogen in stream water. *Water Science and Technology*, 30(7):167 – 170.

Shohreh, Azizi, A. V. and Thami, S. (2013). Development of a modified attached growth bioreactor as a decentralized approach for small communities. *The Scientific World Journal*, page 8.

Shubham, K. and Ketan, P. D. (2020). The optimal detuning approach based centralized control design for MIMO processes. *Journal of Process Control*, 96:23–36.

Sina, B., Giuseppe, C., Alberto, C., Lorenza, M., Deborah, P., Ravina, M., Vincenzo, R., Barbara, R., Gerardo, S., and Mariachiara, Z. (2019). Optimization of the wastewater treatment plant: From energy saving to environmental impact mitigation. *Science of The Total Environment*, 691:1182 – 1189.

Sivagurunathan, G., Kotteeswaran, R., M., S., and Kirthini, Godweena, A. (2021). Design of centralized controller for multivariable process using MOPSO algorithm. *Indian Journal of Science and Technology*, 14(26):2223–2237.

Smets, I. Y., Verdickt, L., and Van Impe, J. F. (2004). Towards a linear asm1 based multi-model for the activated sludge process: Validation with benchmark simulations. *IFAC Proceedings Volumes*, 37(3):177–182.

Smith, J. M. and Jones, A. B. (2012). *Book Title*. Publisher, 7th edition.

Song, H., Liu, X., and Song, M. (2023). Comparative study of data-driven and model-driven approaches in prediction of nuclear power plants operating parameters. *Applied Energy*, 341:121077.

Sorensen, J., Thornberg, D. E., and Nielsen, M. K. (1994). Optimization of a nitrogen-removing biological wastewater treatment plant using on-line measurements. *Water Environment Research*, 66(3):236–242.

Soumya, Ranjan, M., Bidyadhar, S., and Sandip, G. (2019). Design and experimental realization of a robust decentralized PI controller for a coupled tank system. *ISA Transactions*, 89:158 – 168.

Sridhar, P., Madni, A. M., and Jamshidi, M. (2008). Multi-criteria decision making in sensor networks. *IEEE Instrumentation & Measurement Magazine*, 11(1):24–29.

Steilos, R. and Patrick, L. (2002). Systematic development of optimal activated sludge process designs. *Computers and Chemical Engineering*, 26(4):585 – 597.

Su, S. W., Bao, J., and Lee, P. L. (2006). Decentralized control for multivariable processes with actuator nonlinearities. *Developments in Chemical Engineering and Mineral Processing*, 14(1):163–172.

Sudarshan, K. V. and Madhusudan, S. (2020). Optimization strategy of bio-inspired metaheuristic algorithms tuned PID controller for PMBDC actuated robotic manipulator. *Procedia Computer Science*, 171:2040 – 2049.

Sundaresan, K. R. and Krishnaswamy, P. R. (1978). Estimation of time delay time constant parameters in time, frequency, and laplace domains. *The Canadian Journal of Chemical Engineering*, 56(2):257–262.

Taiwo, O., Adeyemo, S., Bamimore, A., and King, R. (2014). Centralized robust multivariable controller design using optimization. *IFAC Proceedings Volumes*, 47(3):5746–5751.

Tanttu, J. T. and Lieslehto, J. (1991). A comparative study of some multivariable PI controller tuning methods. *IFAC Proceedings Volumes*, 24(1):357 – 362.

Teck, Kiang, L. and Min, Sen, C. (2001). Further results on expansion design of partially decentralized controllers: 2×2 plant cases. *Chemical Engineering Research and Design*, 79(1):89 – 96.

Tianming, C., Guan, L. B., Liwei, C., Cai, S., Xiao, dan, L., Zhong, l. C., and Shun, Peng, L. (2007). Enhanced biological phosphorus removal with P seudomonas putida GM6 from activated sludge.

Torres, C., Ramakrishna, S., Chiu, C., Nelson, K., Westerhoff, P., and Brown, R. K. (2011). Fate of sucralose during wastewater treatment. *Environmental Engineering Science*, 28(5):325–331.

Tran, N. H., Gan, J., Nguyen, V. T., Chen, H., You, L., Duarah, A., Zhang, L., and Gin, K. Y.-H. (2015). Sorption and biodegradation of artificial sweeteners in activated sludge processes. *Bioresource Technology*, 197:329 – 338.

Truong, Nguyen, L. V. and Moonyong, L. (2010a). Multi-loop PI controller design based on the direct synthesis for interacting multi-time delay processes. *ISA Transactions*, 49(1):79 – 86.

Truong, N. L. V. and Moonyong, L. (2010b). Independent design of multi-loop PI/PID controllers for interacting multivariable processes. *Journal of Process Control*, 20(8):922 – 933.

Turmel, V. J., David, W., and Karl, O. J. (1997). Dissolved oxygen control strategies in an activated sludge process. *IFAC Proceedings Volumes*, 30(6):1569 – 1573.

Ujjwal, Manikya, N., Chanchal, D., and Rajani, K. M. (2017). Model identification of coupled-tank system - MIMO process. *Proceedings of the 2017 2nd IEEE International Conference on Electrical, Computer and Communication Technologies, ICECCT*.

V. Dhanya, R. and Chidambaram, M. (2015). Simple method of designing centralized PI controllers for multivariable systems based on SSGM. *ISA Transactions*, 56:252 – 260.

V. Vijay, K., Rao, V. S. R., and Chidambaram, M. (2012). Centralized PI controllers for interacting multivariable processes by synthesis method. *ISA Transactions*, 51(3):400-–409.

Vega, P., Revollar, S., Francisco, M., and Martin, J. M. (2014). Integration of set point optimization techniques into nonlinear MPC for improving the operation of WWTPs. *Computers and Chemical Engineering*, 68:78 – 95.

W. Harmon, R. (1983). Multivariable process control - a survey. *Computers and Chemical Engineering*, 7(4):367–394.

Wang, Y., Zhou, D., and Gao, F. (2008). Iterative learning model predictive control for multi-phase batch processes. *Journal of Process Control*, 18(6):543–557.

Wichern, M., Obenaus, F. Wulf, P., and Rosenwinkel, K. H. (2001). Modelling of full-scale wastewater treatment plants with different treatment processes using the activated sludge model no. 3. *Water Sci Technol.*, 44(1):49=56.

Witcher, M. and McAvoy, T. J. (1977). Interacting control systems: Steady state and dynamic measurement of interaction. *ISA Trans.*, 16(1):35–41.

Witcher, M. F. (1977). Interacting control systems: steady state and dynamic measurement of interaction. *ISA Trans.*, 16:35–41.

Wu, P. (2018). Performance monitoring of MIMO control system using kullback-leibler divergence. *The Canadian Journal of Chemical Engineering*, 96(7):1559–1565.

X., L., Chen, Q., and Liu, F. (2014). Centralized PI control for high dimensional multivariable systems based on equivalent transfer function. *ISA Trans.*, 53(5):1554–61.

Xianjun, D., Wang, J., Jegatheesan, V., and Shi, G. (2018). Dissolved oxygen control in activated sludge process using a neural network-based adaptive PID algorithm. *Applied Sciences*, 8(2).

Xiong, Q., Cai, W.-J., and He, M.-J. (2007). Equivalent transfer function method for pi/pid controller design of mimo processes. *Journal of Process Control*, 17(8):665–673.

Yadav, G., Kiran, G. U., and Rao, C. S. (2020). Robust optimal centralized PI controller for a fluid catalytic cracking unit:. *Chemical Product and Process Modeling*, page 20200019.

Yao, W., Li, W., and Junfei, Q. (2010). Research on modeling and simulation of activated sludge process. In *2010 International Conference on Intelligent Computation Technology and Automation*, volume 3, pages 22–27.

Ye, S., Wang, C., Wang, Y., Lei, X., Wang, X., and Yang, G. (2023). Real-time model predictive control study of run-of-river hydropower plants with data-driven and physics-based coupled model. *Journal of Hydrology*, 617:128942.

Yiming, W., Tamas, K., Michel, V., and Fredrik, G. (2016). Data-driven robust receding horizon fault estimation. *Automatica*, 71:210–221.

Yong, Kuen, H., Farouq, S. M., and Hak, Koon, Y. (2013). Centralized vs decentralized adaptive generalized predictive control of a biodiesel reactor. *Asia-Pacific Journal of Chemical Engineering*, 8(1):137–143.

Yu, Sheng, L., Chao, Min, C., and Chung, Hsin, C. (2005). Non-overshooting PI control of variable-speed motor drives with sliding perturbation observers. *Mechatronics*, 15(9):1143–1158.

Zaeim, R. and Nekoui, M. A. (2009). Centralized and decentralized controller design for FGS using linear and nonlinear model. In *2009 Second International Conference on Computer and Electrical Engineering*, volume 1, pages 56–60.

Zahid, A. and Sharma, R. (2023). Personalized health care in a data-driven era: A post-covid-19 retrospective. *Mayo Clinic Proceedings: Digital Health*, 1(2):162–171.

Zahir, B., Derradji, C., and Saci, N. (2012). Dynamic modelling of the secondary settler of a wastewater treatment via activated sludge to low-load. *Energy Procedia*, 18:1 – 9.

Zamani, M. G., Nikoo, M. R., Rastad, D., and Nematollahi, B. (2023). A comparative study of data-driven models for runoff, sediment, and nitrate forecasting. *Journal of Environmental Management*, 341:118006.

Zhang, L. (2021). Data-driven building energy modeling with feature selection and active learning for data predictive control. *Energy and Buildings*, 252:111436.

Zhang, X. and Hoo, K. A. (2008). Controlling a coupled set of biological reactors for wastewater treatment. *Control Engineering Practice*, 16(5):553 – 568.

Zhang, X., Li, X., Zhang, Q., Peng, Q., Zhang, W., and Gao, F. (2014). New insight into the biological treatment by activated sludge: The role of adsorption process. *Bioresource Technology*, 153:160 – 164.

Zhong, Sheng, H. and Zhuo, W. (2013). From model-based control to data-driven control: Survey, classification and perspective. *Inf. Sci.*, 235:3–35.

Zhu, L.-X., Gu, L., Qi, H.-Y., Yu, F., Yu, D.-W., and Yu, D. L. (2017). Decentralised PI controller design and tuning approaches. In *2017 International Conference on Computer Systems, Electronics and Control (ICCSEC)*, pages 644–648.

Zvi, B. (1992). Application of neural networks to water and wastewater treatment plant operation. *ISA Transactions*, 31(1):25–33.